Selim Gürgen *Editor*

Shear Thickening Fluids in Protective Applications

Springer

Shear Thickening Fluids in Protective Applications

Selim Gürgen
Editors

Shear Thickening Fluids in Protective Applications

Springer

Editor
Selim Gürgen
Department of Aeronautical Engineering
Eskişehir Osmangazi University
Eskişehir, Türkiye

ISBN 978-3-031-42950-7 ISBN 978-3-031-42951-4 (eBook)
https://doi.org/10.1007/978-3-031-42951-4

This Springer imprint is published by the registered company Springer Nature Switzerland AG
The registered company address is: Gewerbestrasse 11, 6330 Cham, Switzerland

Paper in this product is recyclable.

Preface

The book *Shear Thickening Fluids in Protective Applications* is a source on shear thickening fluid (STF)-based protective applications. Engineers, researchers, and scientists will benefit from this book and understand STF in various protective systems. STF is effectively used in a wide range of protective applications. STF-based energy absorbing systems, anti-impact structures, deceleration devices, shock attenuation composites, body armor applications are presented in this book. The book will help readers understand STF usage in protective structures through literature surveys, case studies, and research.

Eskişehir, Türkiye — Selim Gürgen

Contents

1 Introduction 1
Selim Gürgen

2 Penetration Resistance of High-Performance Textiles Treated with CNT-Reinforced STF 3
Mohammad Rauf Sheikhi, Ömer Yay, and Melih Cemal Kuşhan

3 Deceleration Behavior of Shear-Thickening Fluid Impregnated Foams Under Low-Velocity Impact 17
Mohammad Rauf Sheikhi, Tarık Türkistanlı, Nasra Sonat Akşit, and Selim Gürgen

4 Shock Absorption in Shear-Thickening Fluid Included 3D-Printed Structures 27
Ömer Yay, Mohammad Rauf Sheikhi, Gökhan Kunt, and Selim Gürgen

5 Fabrication and Impact Properties of Shear-Thickening Fluid-Impregnated High-Performance Fabric Composites 39
Ehteshamul Islam and Leena Nebhani

6 High-Velocity Impact Applications with Shear-Thickening Fluid . . . 69
Prince Kumar Singh and Neelanchali Asija Bhalla

7 Blast Protection with Shear-Thickening Fluid-Integrated Composites 89
Mohammad Rauf Sheikhi and Mahdi Hasanzadeh

Index 103

About the Editor

Selim Gürgen, Ph.D., is an Associate Professor in the Department of Aeronautical Engineering at Eskişehir Osmangazi University. He is the Director of Eskişehir Vocational School. He received his B.Sc. and M.Sc. degrees in Mechanical Engineering from Gazi University and Middle East Technical University, respectively, and his Ph.D. in Mechanical Engineering from Eskişehir Osmangazi University. He was a visiting researcher at the University of Wollongong for a project on smart materials and worked as a researcher with the School of Transportation at Anadolu University for four years. Before his academic life, he worked as a manufacturing engineer in a joint venture of KMWE-Dutch Aero for three years. Dr. Gürgen has contributed to several industrial and research projects in collaboration with major organizations such as Fiat Automobiles, the Turkish Air Force, and the Scientific and Technological Research Council of Turkey (TÜBİTAK). He has many publications in refereed international journals and conferences and is co-editor of the book Materials, Structures, and Manufacturing for Aircraft (Springer, 2022). He serves as an editorial member for several international journals. His primary area of research is material science, in particular smart fluids and their applications in defense and aerospace applications. His Ph.D. studies were on shear thickening fluid (STF) and many of his projects and publications focus on STF and its applications.

Chapter 1
Introduction

Selim Gürgen

Shear-thickening fluid (STF) has recently gained significant attention as a new class of smart materials with remarkable properties, especially in the field of protective applications. This fluid exhibits a unique behavior of viscosity increase and resistance to deformation when subjected to sudden loading, making it ideal for use in various protective applications including body armor, helmets, impact pads, bumpers, sports equipment and crashworthiness applications [1–4]. Recent advances in material science and engineering have enabled the development of more efficient and effective STFs. Modifying components, including additive phases, tailoring concentrations, etc. have been extensively investigated by researchers to fabricate advanced STF for protective systems. These advancements have also led to the discovery of new applications for STF beyond its traditional use as a coating in high-performance textiles. Hence, STF has been integrated into sandwich structures, multilayer composites or advanced foams in recent protective applications [5–9].

This book aims to provide a comprehensive source of the current state of research and development in the field of STF for protective applications. The book covers the various applications of STF in protective structures including high-performance textiles, advanced foams, three-dimensional-printed composites, sandwich structures, etc. The effects of STF integration in these structures are discussed in terms of energy attenuation, deceleration behavior, shock absorbing properties, low/high velocity impact resistance, spalling behavior and blast properties.

The book includes contributions from leading experts in the field of STF and protective applications, providing a wide range of perspectives and insights into this exciting and rapidly evolving field. The book is intended for researchers, engineers, technical staff and students interested in the field of materials science and

S. Gürgen (✉)
Department of Aeronautical Engineering, Eskişehir Osmangazi University, Eskişehir, Turkey
e-mail: sgurgen@ogu.edu.tr

S. Gürgen (ed.), *Shear Thickening Fluids in Protective Applications*,
https://doi.org/10.1007/978-3-031-42951-4_1

engineering, particularly those interested in the development of shear-thickening-based protective applications.

To sum up, this book provides various cases of the latest developments and future prospects of STF in protective applications as well as highlighting STF potential to revolutionize the field of protective structures.

References

1. Zarei M, Aalaie J (2020) Application of shear thickening fluids in material development. J Mater Res Technol 9(5):10411–10433
2. Wei M, Lin K, Sun L (2022) Shear thickening fluids and their applications. Mater Des 216:110570
3. Gürgen S, Kuşhan MC, Li W (2017) Shear thickening fluids in protective applications: a review. Prog Polym Sci 75:48–72
4. Srivastava A, Majumdar A, Butola BS (2012) Improving the impact resistance of textile structures by using shear thickening fluids: a review. Crit Rev Solid State Mater Sci 37(2):115–129
5. Sheikhi MR, Gürgen S (2022) Anti-impact design of multi-layer composites enhanced by shear thickening fluid. Compos Struct 279:114797
6. Soutrenon M, Michaud V (2014) Impact properties of shear thickening fluid impregnated foams. Smart Mater Struct 23(3):035022
7. Tu H, Xu P, Yang Z, Tang F, Dong C, Chen Y et al (2023) Effect of shear thickening gel on microstructure and impact resistance of ethylene–vinyl acetate foam. Compos Struct 311:116811
8. Gürgen S, Fernandes FAO, de Sousa RJA, Kuşhan MC (2021) Development of eco-friendly shock-absorbing Cork composites enhanced by a non-Newtonian fluid. Appl Compos Mater 28(1):165–179
9. Liu H, Zhu H, Fu K, Sun G, Chen Y, Yang B et al (2022) High-impact resistant hybrid sandwich panel filled with shear thickening fluid. Compos Struct 284:115208

Chapter 2
Penetration Resistance of High-Performance Textiles Treated with CNT-Reinforced STF

Mohammad Rauf Sheikhi, Ömer Yay, and Melih Cemal Kuşhan

2.1 Introduction

Personal protection against various threats such as ballistic, impact, stabbing, and blast injuries is a critical issue for many individuals and professionals. Body armor is a type of protective clothing that aims to provide protection. However, due to the strict regulation of firearms, non-ballistic threats such as knives and other sharp objects have become more prevalent as weapons of assault, posing serious risks to personal safety. Moreover, some occupations, such as law enforcement officers and medical personnel, require enhanced personal protection in their work environments. To effectively mitigate aggressive attacks, the efficacy of body protective systems can be enhanced through the utilization of soft composite structures that maintain optimal flexibility. While the defense industry predominantly employs such structures, other sectors such as forestry, logistics, and manufacturing can also employ soft composite structures to safeguard their personnel from puncture injuries. Consequently, researchers have dedicated their efforts to exploring the stab and puncture resistance of composite materials in order to enhance the protective capabilities of garments.

Shear-thickening fluid (STF) is a type of liquid that exhibits a non-Newtonian behavior, meaning that its viscosity changes depending on the applied shear stress. A Newtonian fluid, such as water, has a constant viscosity regardless of the shear

M. R. Sheikhi
Key Laboratory of Traffic Safety on Track of Ministry of Education, School of Traffic & Transportation Engineering, Central South University, Changsha, Hunan, China

Ö. Yay (✉)
Department of Aeronautical Engineering, Gebze Technical University, Gebze, Turkey
e-mail: omeryay@gtu.edu.tr

M. C. Kuşhan
Department of Aeronautical Engineering, Eskişehir Osmangazi University, Eskişehir, Turkey

S. Gürgen (ed.), *Shear Thickening Fluids in Protective Applications*,
https://doi.org/10.1007/978-3-031-42951-4_2

stress. On the other hand, a non-Newtonian fluid, such as STF, can have a variable viscosity depending on the shear stress. In particular, STF becomes more viscous, or thicker, when subjected to higher shear stress. This means that STF behaves like a liquid under resting conditions but turns into a solid-like material when exposed to a sudden or violent force [1, 2].

STF-treated fabrics are fabrics that are impregnated with STF to enhance their mechanical properties and resistance to penetration. STF can be applied to the fabric by various methods, such as dipping, spraying, coating, or printing. STF can also be mixed with other additives, such as nanoparticles, polymers, or fibers, to improve its performance and stability. STF-treated fabrics can be made of different materials, such as Kevlar, Nylon, cotton, or silk. They can also have different structures, such as woven, knitted, or nonwoven [1, 3, 4]. They have been shown to have improved stab resistance over neat fabrics of the same material and weight. This is because the STF acts as a filler that reduces the gap between the fabric fibers and increases the friction between them. When a stabbing force is applied, the STF undergoes a rapid transition from a liquid-like state to a solid-like state, creating a rigid barrier that impedes the penetration of the blade. STF also absorbs some of the kinetic energy of the impact and distributes it over a larger area, reducing the local stress on the fabric. The stab resistance of STF-treated fabrics can be measured by various methods, such as using standard test methods (e.g., ASTM F1790 or ISO 13998), using custom-made devices (e.g., drop-weight or ballistic pendulum), or using numerical simulations (e.g., finite element analysis or discrete element method).

The stab resistance of STF-treated fabrics depends on several factors, such as the type and concentration of STF, the type and structure of fabric, the thickness and shape of blade, and the velocity and angle of impact. Some studies have found that STF-treated Kevlar fabrics have higher stab resistance than STF-treated Nylon fabrics [4], while others have found that STF-treated Nylon fabrics have higher stab resistance than STF-treated Kevlar fabrics [5]. Conditions are a key factor in the protective properties of STF-treated fabrics. Some studies have also found that increasing the concentration of STF improves the stab resistance of STF-treated fabrics [4], while others have found that there is an optimal concentration of STF that maximizes the stab resistance of STF-treated fabrics [6]. Some studies have also found that using different shapes of blades (e.g., single-edged or double-edged) or different angles of impact (e.g., 0° or 45°) affects the stab resistance of STF-treated fabrics [7]. The optimal combination of these factors may vary depending on the specific application and threat scenario.

Initial investigations involved the utilization of high-performance fabrics as a protective material against impact-related damages, with a particular emphasis on examining the impact of different weaving methods on fabric performance. It was widely acknowledged that the structural composition of the fabric played a significant role in determining its protective capabilities, as the failure of fabrics was directly associated with the interactions between individual yarns, which could be manipulated through various weaving techniques. Numerous publications have explored the variation of fiber orientation within composite laminates, highlighting

the crucial influence of reinforcement material directly on the mechanical properties of these structures. Additionally, researchers have examined the properties of base materials utilized in composites as another key factor. High-performance fabrics, composed of diverse materials such as aramid, ultrahigh molecular weight polyethylene, and carbon fibers, exhibit distinct performance characteristics when subjected to stab or impact conditions. In a study conducted by Simeoli et al. [8], glass fiber fabrics were employed in different polypropylene matrices, with a specific focus on investigating the interfacial strength of these laminates subsequent to low-velocity impacts. Taraghi et al. [9] conducted a study investigating the effects of incorporating multi-walled carbon nanotubes (MWCNTs) into Kevlar/epoxy composites on their response to impacts. Tehrani et al. [10] investigated the assessment of impact damage in carbon fiber fabric–reinforced carbon nanotube (CNT)/epoxy composites. In recent studies, surface treatments have been widely employed to enhance the protective properties of structures against penetration [11–13]. Among these treatments, there has been considerable interest in utilizing STF over the past decade [14–20]. Researchers extensively employed STF as an impregnation agent in fabric-based composite structures with high-performance requirements, providing protection against impacts at both low and high velocities [21–24]. Additionally, although to a lesser extent, STFs in bulk form have been used in impacted containers and between sandwich layers to investigate the response of this intelligent fluid in protective applications [25, 26]. Moreover, Galindo-Rosales et al. [27] developed a novel eco-friendly composite by filling engraved cavities in micro-agglomerated cork layers with STF, creating lightweight energy-absorbing materials. This composite was suggested as a safety padding material suitable for motorcycle or bike helmets. Furthermore, Dawson [28] proposed the use of flexible and reticulated foams filled with STF to enhance impact protection in vehicles.

2.2 Penetration Resistance of High-Performance Textiles Enhanced with CNT-Reinforced STF

2.2.1 Shear-Thickening Mechanism

The mechanism of shear thickening in STF is not fully understood, but several theories have been proposed to explain it. One of the most widely accepted theories is the hydrodynamic cluster model [29, 30], which suggests that STF consists of colloidal particles suspended in a carrier liquid. Under low shear stress, the particles are randomly distributed and separated by a thin layer of fluid. The viscosity of the STF is mainly determined by the viscosity of the carrier fluid. Under high shear stress, however, the particles collide and form clusters due to hydrodynamic interactions. The clusters increase the effective volume fraction and reduce the interstitial fluid layer between the particles. The viscosity of the STF is then determined by the friction and lubrication between the particles and clusters. The formation and

breakage of clusters are reversible and dynamic, depending on the magnitude and duration of the shear stress.

Another theory that has been proposed to explain the shear thickening in STF is the order–disorder transition model [31], which suggests that STF consists of rod-like or plate-like particles suspended in a carrier liquid. Under low shear stress, the particles are randomly oriented and form an isotropic suspension. The viscosity of the STF is mainly determined by the Brownian motion and thermal fluctuations of the particles. Under high shear stress, however, the particles align along the flow direction and form an anisotropic suspension. The alignment reduces the entropy and increases the free energy of the system. The viscosity of the STF is then determined by the elastic resistance and interparticle interactions of the aligned particles. The alignment and disordering of particles are reversible and dynamic, depending on the magnitude and duration of the shear stress.

A third theory that has been proposed to explain shear thickening in STF is the jamming transition model [32], which suggests that STF consists of hard spheres suspended in a carrier liquid. Under low shear stress, the spheres are loosely packed and can move freely within their cages formed by their neighbors. The viscosity of the STF is mainly determined by the diffusion and rearrangement of the spheres. Under high shear stress, however, the spheres are densely packed and cannot move within their cages due to geometric constraints. The system undergoes a transition from a liquid-like state to a solid-like state, similar to a granular material under compression. The viscosity of the STF is then determined by the contact forces and friction between the spheres. The jamming and unjamming of spheres are reversible and dynamic, depending on the magnitude and duration of the shear stress.

2.2.2 CNT-Reinforced STF

CNTs are cylindrical nanostructures composed of carbon atoms arranged in a hexagonal lattice. CNTs have remarkable mechanical, electrical, thermal, and optical properties, making them attractive for various applications [33, 34]. CNTs can be added to STF to enhance its performance and stability. The changes in STF when CNTs are added are mainly related to the rheological, mechanical, and functional properties of the composite system. The rheological properties refer to the flow behavior and viscosity of the STF under different shear rates and stresses. The mechanical properties refer to the strength, stiffness, toughness, and durability of the STF-treated fabrics under different loading conditions and environments. The functional properties refer to the electrical, thermal, optical, and antibacterial properties of STF-treated fabrics that can provide additional benefits for various applications [35].

The rheological properties of STF can be improved by adding CNTs in several ways. First, CNTs can increase the viscosity and yield stress of STF due to their high aspect ratio and surface area, which enhance the hydrodynamic interactions between the particles and the fluid [35, 36]. Second, CNTs can increase the

shear-thickening effect of the STF due to their ability to form networks or clusters under high shear stress, which increase the effective volume fraction and reduce the interstitial fluid layer between the particles [37]. Third, CNTs can stabilize the STF against sedimentation or aggregation due to their electrostatic or steric repulsion, which prevents the particles from settling or sticking together. Mechanical properties can also be enhanced with CNT fillers. CNTs increase the tensile strength and modulus of the fabrics due to their high intrinsic strength and stiffness [38]. Moreover, CNTs increase the impact resistance and energy absorption of the fabrics due to their high strain to failure and toughness, which dissipate the kinetic energy of the impact [39]. On the other hand, the durability and washability of the fabrics are enhanced by using CNT fillers due to the high chemical stability and adhesion of CNT [40]. Functional properties of STF-treated fabrics are also related to CNT fillers. CNTs increase the electrical conductivity [35, 41] and capacitance of the fabrics due to their high charge carrier mobility and density, which enable the fabrics to act as sensors or actuators. CNTs increase the thermal conductivity and stability of the fabrics [42] due to their high phonon transport and heat resistance, which enable the fabrics to act as heaters or coolers. Furthermore, the optical reflectance and transmittance of the fabrics are improved with CNT addition [43] because CNTs provide advanced light absorption and scattering behavior, which enables the fabrics to act as color changers or filters [44]. CNT fillers are also beneficial to the antibacterial properties of the fabrics due to their high surface reactivity and biocompatibility, which enable the fabrics to act as disinfectants or wound dressings [45, 46].

The amount of CNTs that should be added to STF depends on several factors, such as the type and size of CNTs, the type and concentration of STF particles, the type and structure of fabric fibers, and the desired properties and applications of STF-treated fabrics. There is no universal optimal amount of CNTs that can suit all cases, but rather a trade-off between benefits and drawbacks that need to be considered. For example, adding an excessive amount of CNT increases the viscosity and shear-thickening effect of STF, making it difficult to apply to or remove from fabrics [36, 47]. It may also increase the cost and environmental impact of STF production and disposal. Therefore, finding an optimal amount of CNT that can balance between performance enhancement and practical feasibility is a challenging task that requires careful experimentation and optimization.

2.2.3 Stab and Penetration Resistance in Fabrics Treated with CNT-Added STF

CNT-added STF applications provide enhanced stab resistance in protective fabrics in comparison to only STF applications. CNTs increase the viscosity and yield stress of the STF due to their high aspect ratio and surface area, which enhance the hydrodynamic interactions between the particles and the fluid. This means that the

STF can form a more rigid and resistant barrier against the stabbing under high shear stress. Moreover, CNTs increase the inter-yarn friction in the fabrics due to their high adhesion and alignment with the fabric fibers. This means that the fabrics prevent the relative motion of yarns and distribute the impact energy over a larger area. Additionally, CNTs increase the tensile strength and modulus of the fabrics due to their high strength and stiffness, which reinforce the fibers. The fabrics resist the cutting or tearing action of the blade in this way [6, 48].

2.3 A Case Study: Penetration Resistance in High-Performance Fabrics Treated with CNT-Added STF

2.3.1 Preparation of STF

STF was produced through the dispersion of fumed silica particles with a size ranging from 15 to 25 nm in a medium of polyethylene glycol (PEG) with a molecular weight of 400 g/mol. The fabrication process involved the gradual addition of fumed silica to the PEG medium while homogenizing the mixture using a high-speed homogenizer. The proportion of fumed silica in the STF suspension was maintained at 40% by weight, following the recommendation by Caglayan et al. [13] for achieving an optimal thickening mechanism. Once the STF was fabricated, CNTs were incorporated into the suspension at a concentration of 1% by weight and stirred with a homogenizer for 30 min. The resulting suspension, which contained CNTs, was left to settle overnight at room temperature to allow any trapped air bubbles to escape.

2.3.2 Preparation of High-Performance Fabrics Treated with CNT-Added STF

Composite targets were constructed using Twaron layers, 80 mm × 80 mm in size. The STF and CNT-added STF application processes to the textile layers was about immersing the layers in the suspensions and then applying pressure with a roller until the gaps within the layers were fully infused. To enhance the treatment of the fabrics with the suspensions, ethanol was added to the mixtures at a volumetric ratio of 1:3. The fabrics were submerged in the diluted mixtures for 1 min, and excess liquid was removed from the fabrics using a mangle. Subsequently, the fabrics were dried in an oven at a temperature of 79 °C for 30 min to remove the ethanol. Figure 2.1 shows a schematic representation of the target configurations.

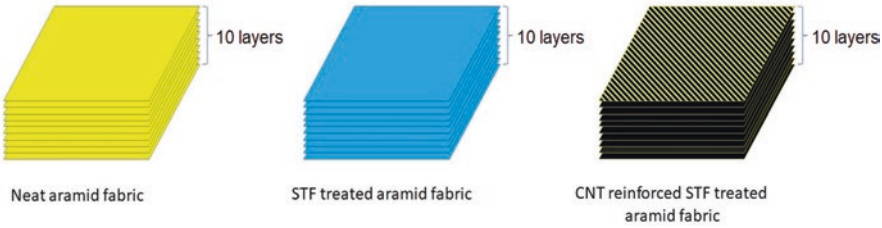

Fig. 2.1 Target configurations

2.3.3 Rheological Measurements and Stab Tests

The rheological properties of STFs were investigated by using an MCR 302 Anton Paar stress-controlled rheometer equipped with a parallel plate apparatus. The distance between the plates was maintained at 1 mm, and the shear rate was increased from 0 to 1000 s^{-1} during the measurements. All measurements were conducted at a constant temperature of 20 °C.

During the drop tower testing, the National Institute of Justice (NIJ) Standard 0115.00 was followed, wherein an intentionally designed object referred to as an "engineered spike" was dropped onto the targets from the heights of 0.5, 1, and 1.5 m. To determine the impact energy, the drop heights were measured for each impact, and the "impactor" (the engineered spike) was securely attached to a crosshead with a combined mass of 1 kg. The targets were positioned on a single layer of foam made from extruded polystyrene (XPS). This choice of material was made because the brittle nature of XPS allows for clear penetration of the impactor. Figure 2.2 shows an illustration of the experimental setup used in the stab tests. For each level of impact energy, the targets were subjected to three repeated strikes to ensure consistency. To measure the depth of penetration by the impactor, the distance between the XPS foam and the crosshead was measured using a digital caliper after each impact. The measured distance was then subtracted from the total length of the impactor, resulting in the penetration depth (PD). Energy absorbed by the targets (EA_T) was found using Eq. 2.1.

$$EA_T = mgh ? EA_{XPS} \tag{2.1}$$

where m is the mass of the impactor, g is the gravitational acceleration, h is the impacting height, and EA_{XPS} is the energy absorbed by the XPS. EA_{XPS} is found stabbing an XPS layer from various impacting heights and then measuring the depth of penetrations. From this stage, EA_{XPS} is provided as a function of penetration depth (PD) as given in Eq. 2.2.

$$EA_{XPS} = 0.0475\,PD + 0.1951 \tag{2.2}$$

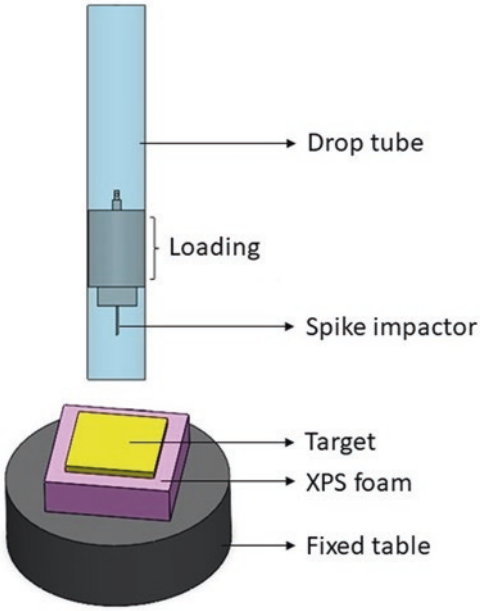

Fig. 2.2 Stab testing setup

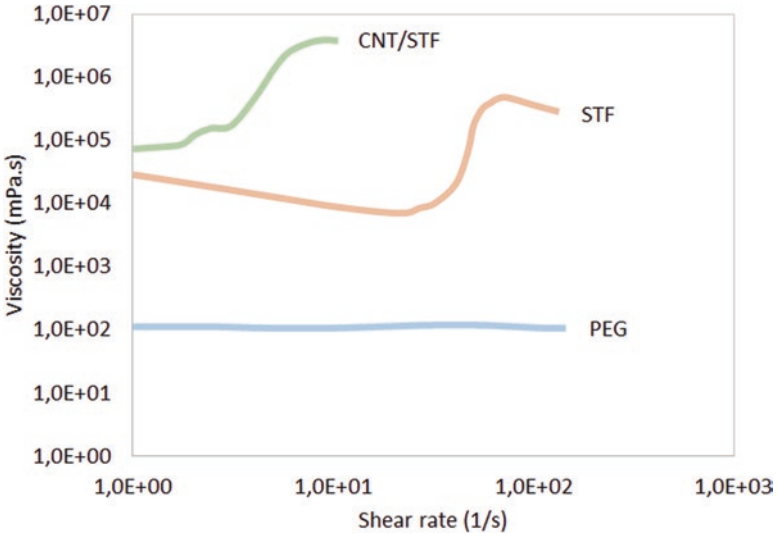

Fig. 2.3 Rheological behavior of the suspensions

2.3.4 Rheological Behavior of the Suspensions

Figure 2.3 shows the rheological behavior of the suspensions. It can be clearly seen that PEG shows almost no viscosity change with respect to shear rate. This rheology is known as Newtonian behavior. However, rheological characteristics are changed

to non-Newtonian behavior as silica particles are included in PEG, as shown in STF. STF shows a slight reduction in viscosity up to a critical point and then shows a sudden jump, which is called shear thickening. This behavior stems from the interaction between the silica particles in the carrier liquid. According to previous studies [49–52], silica particles are randomly distributed in the liquid medium, and the particles show a self-lubricating effect at low shear rates. This behavior is due to the layered orientation of the particles, which facilitates flowability and consequently reduces the viscosity. As particles are introduced to higher shear rates, hydrodynamic forces acting on the particles get stronger. For this reason, particles come closer to each other and begin to develop large particle groups in the flow field. These particle groups gradually get enlarged as shear rate increases and finally stop the fluid from flowing. Because of this microstructural change, viscosity shows a drastic increase, and shear-thickening rheology is observed in the suspension. On the other hand, CNT inclusion heavily changes the STF rheology. Because the solid volume fraction increases in the suspension, CNT-integrated STF shows higher viscosity at zero shear rate. In addition, CNT enhances the particle-to-particle interactions in the silica phase. For this reason, the onset of silica groups is observed at lower shear rates, and therefore, shear-thickening behavior begins at early stages. It is possible to state that CNT addition to the STF enhances the shear-thickening rheology, thereby enabling it to reach higher viscosity levels.

2.3.5 Penetration Resistance of the Targets

Figure 2.4 shows the energy absorbed by the targets for each impacting height. It is clear that energy-absorbing capacities in the targets show the same manner for each impact height. STF treatment increases the energy-absorbing capability of the fabrics. Moreover, CNT addition in the STF provides a further increase in energy absorption. Neat textiles have generally low surface and inter-yarn frictions in comparison to STF-treated textiles [2]. Because of low frictional interactions in the textiles, fibers within the yarns are easily separated upon impact by a sharp object. This phenomenon is also called windowing effect related to textile-based protective structures. For this reason, penetration depth is increased, thereby leading to a low grade of energy absorbed by the target. Targets with low frictional interactions show lower penetration resistance. On the other hand, STF application provides higher energy-absorbing capacity in textiles. This is due to the increased frictional interactions in fibers. Due to the sticky nature of STF, fiber separation is hindered, thereby windowing effect is mostly avoided in the yarns. The yarns are strained as if they are impacted by a blunt object without showing an opening for the sharp point of the impactor. Hence, the penetration resistance is increased by STF treatment in the textile. Furthermore, impact energy is distributed over a larger area on the fabric due to the straining yarns. Far-field yarns contribute to the energy-absorbing process during stabbing. STF acts as a continuous matrix on fibers. Therefore, an increased coupling effect is achieved in the fibers and yarns. This mechanism provides an

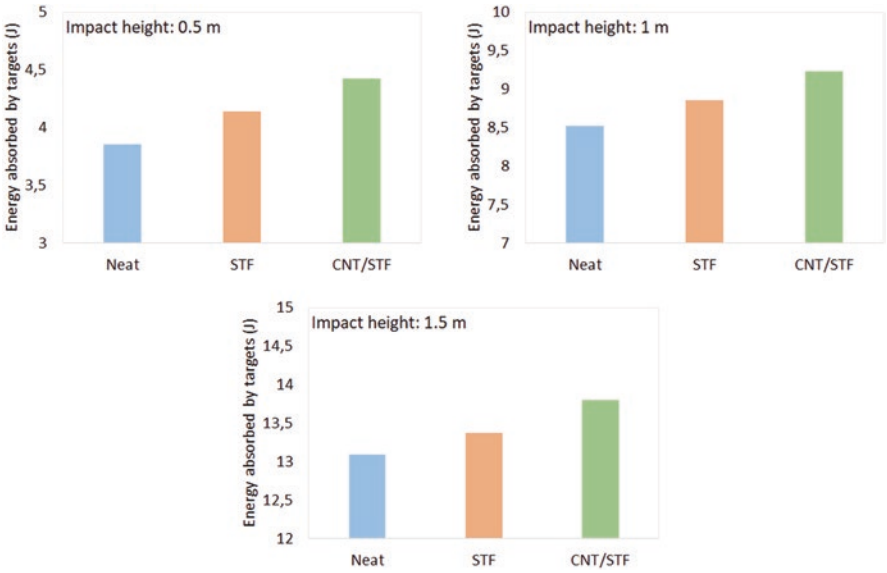

Fig. 2.4 Energy absorbed by the targets for each impact height

Table 2.1 Percentage increase in energy absorption of the treated targets in comparison to the neat target

	Treatment	
Impact height (m)	STF	CNT/STF
0.5	7.4%	14.8%
1	3.9%	8.4%
1.5	2.2%	5.4%

additional energy attenuation process for textiles. It is also clear that CNT integration into STF exhibits a further development in the energy-absorbing capability of textiles. CNT fillers enhance the viscosity magnitude of the STF. In addition, CNT provides advanced mechanical properties for textiles [53]. According to Cao et al. [54], CNT-integrated STF treatments in Kevlar fabrics show friction coefficients up to 0.80, while it is only about 0.50 in STF-treated ones. From this point of view, it is obvious that frictional interactions between the fibers greatly increase with the addition of CNT in the STF treatment, thereby leading to an additional energy-absorbing mechanism in textiles. For this reason, the penetration resistance of textiles is enhanced by the contribution of CNT fillers in STF treatment.

Table 2.1 gives the percentage increase in the energy absorption of the treated targets in comparison to the neat target. From the results, percentage increases are about twofold in CNT/STF-treated textiles with respect to the STF-treated ones. Hence, it is possible to mention that CNT-integrated STF in textile treatment provides higher energy-absorbing capabilities than only STF. Another important point is that the effect of STF or CNT/STF treatment reduces as impact height increases.

This is associated with impact velocity, which increases by dropping the impactor from higher heights. According to previous studies [20], STF has a larger protection performance at low-velocity impact conditions. Shear rate in the stabbing point increases with increasing impact velocity so that shear-thickening phenomenon is disrupted at shear rates beyond the peak viscosity levels. This is due to the structural breakdown of aggregated silica particles in STF. At excessive shear rates, developed stresses in STF reach such a high level that the silica groups in the suspension cannot withstand. For this reason, shear-thickening behavior fades away at that level.

2.4 Conclusions

In this study, the effect of STF treatment on the penetration resistance of high-performance textiles is investigated. To enhance the shear-thickening behavior, CNT fillers are integrated into STF. Rheological changes due to the CNT additives are discussed. Only STF and CNT-added STF are applied to high-performance fabrics with the impregnating method. The structures are subjected to stab tests for different impact energy levels. According to the results, STF application to the fabrics provides higher energy-absorbing capabilities and also penetration resistance. Furthermore, an additional performance gain is obtained by distributed CNT additives in STF treatment. STF provides higher frictional interactions between the fibers within fabrics. Fiber coupling and yarn-to-yarn interactions are pronounced in this way. This leads to an increased energy dissipation mechanism over the fabrics upon impact so that penetration resistance is enhanced in the structures. CNT fillers have a further contribution to the friction increase in textiles, and therefore, CNT-integrated STF exhibits an additional gain of performance in fabrics.

References

1. Wei M, Lin K, Sun L (2022) Shear thickening fluids and their applications. Mater Des 216:110570. https://doi.org/10.1016/j.matdes.2022.110570
2. Gürgen S, Kuşhan MC, Li W (2017) Shear thickening fluids in protective applications: a review. Prog Polym Sci 75:48–72. https://doi.org/10.1016/j.progpolymsci.2017.07.003
3. Ahn HC, Na WJ, Han SJ et al (2014) Characterizations of STF-treated aramid fabrics using picture frame test. Key Eng Mater 611–612:344–348. https://doi.org/10.4028/www.scientific.net/KEM.611-612.344
4. Decker MJ, Halbach CJ, Nam CH et al (2007) Stab resistance of shear thickening fluid (STF)-treated fabrics. Compos Sci Technol 67:565–578. https://doi.org/10.1016/j.compscitech.2006.08.007
5. Wang L, Du Z, Fu W, Wang P (2021) Study of mechanical property of shear thickening fluid (STF) for soft body-armor. Mater Res Express 8:045021. https://doi.org/10.1088/2053-1591/abf76a
6. Egres RG, Decker MJ, Halbach CJ et al (2006) Stab resistance of shear thickening fluid (STF)–Kevlar composites for body armor applications. In: Transformational Science and Technology for the Current and Future Force. WORLD SCIENTIFIC, pp 264–271

7. Gürgen S (2019) An investigation on composite laminates including shear thickening fluid under stab condition. J Compos Mater 53:1111–1122. https://doi.org/10.1177/0021998318796158
8. Simeoli G, Acierno D, Meola C et al (2014) The role of interface strength on the low velocity impact behaviour of PP/glass fibre laminates. Compos Part B Eng 62:88–96. https://doi.org/10.1016/j.compositesb.2014.02.018
9. Taraghi I, Fereidoon A, Taheri-Behrooz F (2014) Low-velocity impact response of woven Kevlar/epoxy laminated composites reinforced with multi-walled carbon nanotubes at ambient and low temperatures. Mater Des 53:152–158. https://doi.org/10.1016/j.matdes.2013.06.051
10. Tehrani M, Boroujeni AY, Hartman TB et al (2013) Mechanical characterization and impact damage assessment of a woven carbon fiber reinforced carbon nanotube–epoxy composite. Compos Sci Technol 75:42–48. https://doi.org/10.1016/j.compscitech.2012.12.005
11. Wang P, Sun B, Gu B (2012) Comparison of stab behaviors of uncoated and coated woven fabrics from experimental and finite element analyses. Text Res J 82:1337–1354. https://doi.org/10.1177/0040517511418560
12. LaBarre ED, Calderon-Colon X, Morris M et al (2015) Effect of a carbon nanotube coating on friction and impact performance of Kevlar. J Mater Sci 50:5431–5442. https://doi.org/10.1007/s10853-015-9088-8
13. Roy R, Laha A, Awasthi N et al (2018) Multi layered natural rubber coated woven *P* -aramid and UHMWPE fabric composites for soft body armor application. Polym Compos 39:3636–3644. https://doi.org/10.1002/pc.24391
14. Lomakin EV, Mossakovsky PA, Bragov AM et al (2011) Investigation of impact resistance of multilayered woven composite barrier impregnated with the shear thickening fluid. Arch Appl Mech 81:2007–2020. https://doi.org/10.1007/s00419-011-0533-0
15. Gürgen S, Kuşhan MC (2017) The effect of silicon carbide additives on the stab resistance of shear thickening fluid treated fabrics. Mech Adv Mater Struct 24:1381–1390. https://doi.org/10.1080/15376494.2016.1231355
16. Gürgen S, Kuşhan MC (2017) The stab resistance of fabrics impregnated with shear thickening fluids including various particle size of additives. Compos Part A Appl Sci Manuf 94:50–60. https://doi.org/10.1016/j.compositesa.2016.12.019
17. Hasanzadeh M, Mottaghitalab V, Babaei H, Rezaei M (2016) The influence of carbon nanotubes on quasi-static puncture resistance and yarn pull-out behavior of shear-thickening fluids (STFs) impregnated woven fabrics. Compos Part A Appl Sci Manuf 88:263–271. https://doi.org/10.1016/j.compositesa.2016.06.006
18. Majumdar A, Butola BS, Srivastava A (2013) An analysis of deformation and energy absorption modes of shear thickening fluid treated Kevlar fabrics as soft body armour materials. Mater Des 51:148–153. https://doi.org/10.1016/j.matdes.2013.04.016
19. Majumdar A, Butola BS, Srivastava A (2014) Development of soft composite materials with improved impact resistance using Kevlar fabric and nano-silica based shear thickening fluid. Mater Des (1980–2015) 54:295–300. https://doi.org/10.1016/j.matdes.2013.07.086
20. Gürgen S, Kuşhan MC (2017) The ballistic performance of aramid based fabrics impregnated with multi-phase shear thickening fluids. Polym Test 64:296–306. https://doi.org/10.1016/j.polymertesting.2017.11.003
21. Park JL, B IL Y, Paik JG, Kang TJ (2012) Ballistic performance of *p* -aramid fabrics impregnated with shear thickening fluid; Part I – Effect of laminating sequence. Text Res J 82:527–541. https://doi.org/10.1177/0040517511420753
22. Park JL, IL YB, Paik JG, Kang TJ (2012) Ballistic performance of *p* -aramid fabrics impregnated with shear thickening fluid; Part II – Effect of fabric count and shot location. Text Res J 82:542–557. https://doi.org/10.1177/0040517511420765
23. Srivastava A, Majumdar A, Butola BS (2011) Improving the impact resistance performance of Kevlar fabrics using silica based shear thickening fluid. Mater Sci Eng A 529:224–229. https://doi.org/10.1016/j.msea.2011.09.021
24. Tan VBC, Tay TE, Teo WK (2005) Strengthening fabric armour with silica colloidal suspensions. Int J Solids Struct 42:1561–1576. https://doi.org/10.1016/j.ijsolstr.2004.08.013

25. Petel OE, Ouellet S, Loiseau J et al (2015) A comparison of the ballistic performance of shear thickening fluids based on particle strength and volume fraction. Int J Impact Eng 85:83–96. https://doi.org/10.1016/j.ijimpeng.2015.06.004
26. Petel OE, Ouellet S, Loiseau J et al (2013) The effect of particle strength on the ballistic resistance of shear thickening fluids. Appl Phys Lett 102. https://doi.org/10.1063/1.4791785
27. Galindo-Rosales FJ, Martínez-Aranda S, Campo-Deaño L (2015) CorkSTFμfluidics – a novel concept for the development of eco-friendly light-weight energy absorbing composites. Mater Des 82:326–334. https://doi.org/10.1016/j.matdes.2014.12.025
28. Dawson MA (2009) Composite plates with a layer of fluid-filled, reticulated foam for blast protection of infrastructure. Int J Impact Eng 36:1288–1295. https://doi.org/10.1016/j.ijimpeng.2009.03.008
29. Liu H, Fu K, Cui X et al (2023) Shear thickening fluid and its application in impact protection: a review. Polymers (Basel) 15:2238. https://doi.org/10.3390/polym15102238
30. Zhao P, Chen Q, Gao X, Wu Z (2020) Mechanical properties and cushioning mechanism of shear thickening fluid. J Mech Sci Technol 34:4575–4588. https://doi.org/10.1007/s12206-020-0904-y
31. Liu M, Jian W, Wang S et al (2018) Shear thickening fluid with tunable structural colors. Smart Mater Struct 27:095012. https://doi.org/10.1088/1361-665X/aad587
32. Fall A, Huang N, Bertrand F et al (2008) Shear thickening of cornstarch suspensions as a reentrant jamming transition. Phys Rev Lett 100:018301. https://doi.org/10.1103/PhysRevLett.100.018301
33. Bellucci S (2005) Carbon nanotubes: physics and applications. Physica Status Solidi (c) 2:34–47. https://doi.org/10.1002/pssc.200460105
34. Kukovecz Á, Kozma G, Kónya Z (2013) Multi-walled carbon nanotubes. In: Springer handbook of nanomaterials. Springer, Berlin/Heidelberg/Berlin/Heidelberg, pp 147–188
35. Sheikhi MR, Hasanzadeh M, Gürgen S (2023) The role of conductive fillers on the rheological behavior and electrical conductivity of multi-functional shear thickening fluids (M-STFs). Adv Powder Technol 34:104086. https://doi.org/10.1016/j.apt.2023.104086
36. Nakonieczna P, Wierzbicki Ł, Wróblewski R et al (2019) The influence of carbon nanotube addition on the properties of shear thickening fluid. Bull Mater Sci 42:162. https://doi.org/10.1007/s12034-019-1860-y
37. Wei M, Lv Y, Sun L, Sun H (2020) Rheological properties of multi-walled carbon nanotubes/silica shear thickening fluid suspensions. Colloid Polym Sci 298:243–250. https://doi.org/10.1007/s00396-020-04599-3
38. Yao Z, Wang C, Wang Y et al (2019) Tensile properties of CNTs-grown carbon fiber fabrics prepared using Fe–Co bimetallic catalysts at low temperature. J Mater Sci 54:11841–11847. https://doi.org/10.1007/s10853-019-03741-z
39. Siegfried M, Tola C, Claes M et al (2014) Impact and residual after impact properties of carbon fiber/epoxy composites modified with carbon nanotubes. Compos Struct 111:488–496. https://doi.org/10.1016/j.compstruct.2014.01.035
40. Singh BP (2018) Carbon nanotubes in protective fabrics: a short review. Trends Textile Eng Fashion Technol 3. https://doi.org/10.31031/TTEFT.2018.03.000562
41. Chen Q, Liu M, Xuan S et al (2017) Shear dependent electrical property of conductive shear thickening fluid. Mater Des 121:92–100. https://doi.org/10.1016/j.matdes.2017.02.056
42. Jang J, Park HC, Lee HS et al (2018) Electrically and thermally conductive carbon fibre fabric reinforced polymer composites based on nanocarbons and an in-situ polymerizable cyclic oligoester. Sci Rep 8:7659. https://doi.org/10.1038/s41598-018-25965-w
43. Sa'aya NSN, Demon SZN, Abdullah N et al (2019) Optical and morphological studies of multiwalled carbon nanotube-incorporated poly(3-hexylthiophene-2,5-diyl) nanocomposites. Sens Mater 31:2997. https://doi.org/10.18494/SAM.2019.2513
44. Norizan MN, Moklis MH, Ngah Demon SZ et al (2020) Carbon nanotubes: functionalisation and their application in chemical sensors. RSC Adv 10:43704–43732. https://doi.org/10.1039/D0RA09438B

45. Teixeira-Santos R, Gomes M, Gomes LC, Mergulhão FJ (2021) Antimicrobial and anti-adhesive properties of carbon nanotube-based surfaces for medical applications: a systematic review. iScience 24:102001. https://doi.org/10.1016/j.isci.2020.102001
46. Schifano E, Cavoto G, Pandolfi F et al (2023) Plasma-etched vertically aligned CNTs with enhanced antibacterial power. Nano 13:1081. https://doi.org/10.3390/nano13061081
47. Shoukat R, Khan MI (2021) Carbon nanotubes: a review on properties, synthesis methods and applications in micro and nanotechnology. Microsyst Technol 27:4183–4192. https://doi.org/10.1007/s00542-021-05211-6
48. Li D, Wang R, Guan F et al (2022) Enhancement of the quasi-static stab resistance of Kevlar fabrics impregnated with shear thickening fluid. J Mater Res Technol 18:3673–3683. https://doi.org/10.1016/j.jmrt.2022.04.052
49. Gürgen S (2019) Tuning the rheology of nano-sized silica suspensions with silicon nitride particles. J Nano Res 56:63–70. https://www.scientific.net/JNanoR.56.63
50. Gürgen S, Sofuoğlu MA, Kuşhan MC (2019) Rheological compatibility of multi-phase shear thickening fluid with a phenomenological model. Smart Mater Struct 28:035027. https://iopscience.iop.org/article/10.1088/1361-665X/ab018c
51. Gürgen S, Sofuoğlu MA, Kuşhan MC (2020) Rheological modeling of multi-phase shear thickening fluid using an intelligent methodology. J Braz Soc Mech Sci Eng 42:1–7. https://link.springer.com/article/10.1007/s40430-020-02681-z
52. Gürgen S, de Sousa RJA (2020) Rheological and deformation behavior of natural smart suspensions exhibiting shear thickening properties. Arch Civil Mech Eng 20:1–8. https://link.springer.com/article/10.1007/s43452-020-00111-4
53. Jeddi M, Yazdani M (2021) Dynamic compressive response of 3D GFRP composites with shear thickening fluid (STF) matrix as cushioning materials. J Compos Mater 55:2151–2164. https://journals.sagepub.com/doi/pdf/10.1177/0021998320984247
54. Cao S, Pang H, Zhao C, Xuan S, Gong X (2020) The CNT/PSt-EA/Kevlar composite with excellent ballistic performance. Compos B Eng 185:107793. https://doi.org/10.1016/j.compositesb.2020.107793

Chapter 3
Deceleration Behavior of Shear-Thickening Fluid Impregnated Foams Under Low-Velocity Impact

Mohammad Rauf Sheikhi, Tarık Türkistanlı, Nasra Sonat Akşit, and Selim Gürgen

3.1 Introduction

The acceleration or deceleration concept is a critical issue in many applications including sports, automotive, aerospace and military and industrial fields. In these applications, energy must be dissipated to prevent injuries or damages to the surrounding environment. Various materials and devices have been developed to avoid sudden acceleration or deceleration including foams, gels and polymers. However, these materials may not always provide sufficient protection or may be too bulky to be practical in certain applications.

Shear-thickening fluids (STFs) are a promising alternative for these kinds of applications due to their unique properties. STFs are suspensions of solid particles in an inert liquid medium that exhibits a quick increase in viscosity under high shear rates. This unique property allows STFs to dissipate energy rapidly when subjected to sudden acceleration, deceleration, impact or shock loading. The development of STFs for protective applications has gained significant attention in recent years. Researchers have explored various types of particles and liquids to fabricate STFs with optimal properties for enhanced protection. One recent development in STF is the use of additive fillers in the suspensions. Fillers are made of any kind of advanced materials with different properties such as size, shape or surface chemistry. By controlling the composition of fillers, researchers can create multi-phase STFs with

M. R. Sheikhi (✉)
Key Laboratory of Traffic Safety on Track of Ministry of Education, School of Traffic & Transportation Engineering, Central South University, Changsha, Hunan, China
e-mail: mohammadraufsheikhi@csu.edu.cn

T. Türkistanlı · N. S. Akşit
Turkish Aerospace Industries Inc., Ankara, Turkey

S. Gürgen
Department of Aeronautical Engineering, Eskişehir Osmangazi University, Eskişehir, Turkey

S. Gürgen (ed.), *Shear Thickening Fluids in Protective Applications*,
https://doi.org/10.1007/978-3-031-42951-4_3

tailored properties. In recent works [1–5], multi-phase STFs were fabricated by using various particle fillers. It was stated that rheological properties could be altered by changing the parameters related to the fillers. Moreover, multi-phase STF was also integrated into high-performance textiles to enhance the protective properties [6–8]. According to the results, fillers in STF provided an additional energy-absorbing mechanism during the impact process. STFs have been investigated for various protective applications including protective clothing, impact-resistant structures and shock-absorbing devices. These smart materials have been used to create protective clothing that can attenuate impact energy. A recent study conducted by Bajya et al. [9] demonstrated that STF-impregnated fabrics could provide superior protection against ballistic impact compared to conventional fabrics. STFs have also been used to create impact-resistant materials such as composites and coatings. Sun et al. [10] demonstrated that STF-impregnated carbon fiber–reinforced composites exhibited superior impact resistance in comparison to conventional composites. STF was also used as a filler in sandwich structures to enhance the impact resistance [11–13]. Based on the results, promising achievements were made to design anti-impact systems. In another study [14], polyester foams were impregnated with STF, and a multilayered composite was fabricated with foams and warp-knitted spacer fabrics. According to the impact test results, STF integration into the composites greatly helped in enhancing energy-absorbing capacities. Shock-absorbing devices such as helmet liners and vehicle bumpers have also benefitted from the protective performance of STFs. Serra et al. [15] showed that STF-filled helmets provided superior protection against impact compared to conventional helmets. In another work [16], cork layers were intercalated with STF to enhance the shock-absorbing capabilities for crashworthiness applications. STF inclusion provides significant reduction in peak forces to prove its protective performance. Another concept related to protection is deceleration behavior that is of importance for many engineering applications. Deceleration concept is about protecting humans or devices from sudden g-forces in case of impacts or crashes. For this purpose, various protective designs have been developed in recent years. Sheikhi et al. [17] developed a protective design by including STF in cork panels for sensitive systems such as electronic devices, robotic structures and unmanned aerial vehicles to avoid sudden acceleration or decelerations.

In this study, STF-impregnated polyurethane foams are used for a smooth deceleration process under impact, crash or sudden braking conditions. Two different STF formulations are used in the impregnation stage. The first STF is based on silica and polyethylene glycol, which is known as a single-phase STF. On the other hand, the second one includes carbon nanotube (CNT) fillers in the single-phase STF called the multi-phase STF. The composites are tested in a drop tower system by placing them under a dropping mass. An accelerometer is attached to the dropping mass, and the deceleration of the dropping mass is recorded during the impact process. According to the results, STF impregnation provides significant reduction in the peak deceleration values in the foams. CNT fillers lead to a further performance improvement in the deceleration behavior.

3.2 Experimental Details

The single-phase STF used in this study was based on a 20-nm-fumed silica (from Evonik) and 400-g/mol polyethylene glycol (from Sigma-Aldrich). In the fabrication process, silica was gradually added in the polyethylene glycol pool and distributed by a high-speed homogenizer for 1 h. An excessive amount of ethanol was used to facilitate the blending process. After completing the homogenization, the suspension was rested to remove the ethanol from the mixture. The silica concentration was 60 wt% in the final single-phase STF. An 8–10-nm CNT (from Nanografi) was included in the single-phase STF to produce the multi-phase STF. The CNT amount was kept at 1 wt% in the suspension. Polyurethane foams (from Espol) were sized into 40 mm × 40 mm × 40 mm before STF impregnation. Then, the foams were immersed into an ethanol-diluted STF pool. Upon ensuring that the foams were fully impregnated with the suspension, they were rested for 3 days to remove the ethanol from the structures. Figure 3.1 shows the specimen photos. Table 3.1 gives the specimen details in this study.

As suggested in an earlier study [18], a drop tower system was used in the deceleration tests as shown in Fig. 3.2. A 15-mm diameter hemispherical impact head was loaded with 1 kg, and it was dropped from three different heights: 50, 100 and 150 mm. Deceleration of the dropping head was collected by an accelerometer attached on the head.

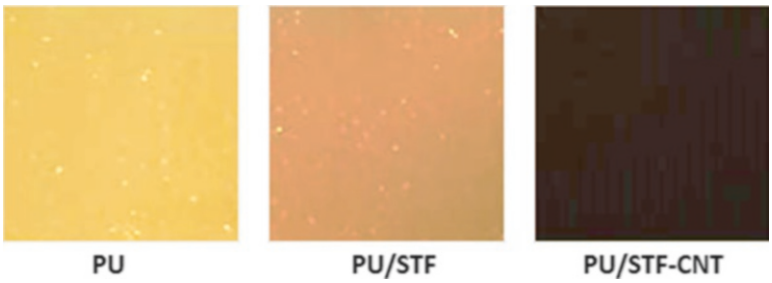

Fig. 3.1 Specimens before and after STF treatments

Table 3.1 Specimens in the deceleration tests

Specimen	Content
PU	Pristine polyurethane foam
PU/STF	Single-phase STF-impregnated polyurethane foam
PU/STF-CNT	Multi-phase STF-impregnated polyurethane foam

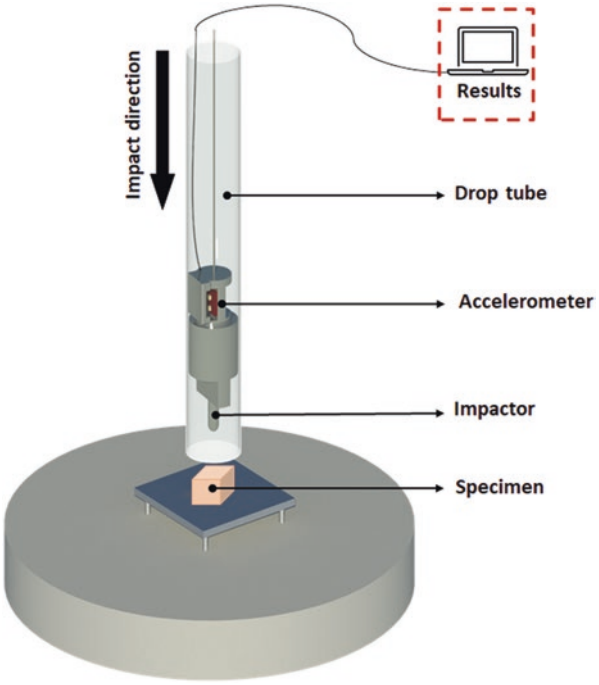

Fig. 3.2 Drop tower system in deceleration testing

3.3 Results and Discussion

Figure 3.3 shows the deceleration curves for the specimens subjected to drop tests from 50 mm. From these charts, peak deceleration values for the specimens PU, PU/STF and PU/STF-CNT are 77.8, 37.4 and 22.2 g, respectively. It is clear that there is a decreasing trend in the peak decelerations by treating the polyurethane foam with single-phase and multi-phase STFs. Single-phase STF leads to the peak value that is almost half of that by the pristine polyurethane foam. Moreover, multi-phase STF provides a further decrease in the peak deceleration, thereby producing about one-third of that obtained by the pristine polyurethane foam. The reductions in the peak values are significant due to the effect of STF impregnation. Another important point is about the time interval of the loadings on the dropping mass. As shown in the graphs, the dropping mass is loaded in a very short time period upon impacting the pristine polyurethane foam, which produces a drastically sharp deceleration. On the other hand, the time spans during the dropping mass loading are extended by using single-phase and multi-phase STFs in the polyurethane foams. Comparing the single-phase and multi-phase STF-impregnated cases, it is obvious that multi-phase STF provides an extended impact loading on the dropping mass. From these findings, it is possible to state that STF impregnation especially the multi-phase one leads to a smoother deceleration on the dropping mass in

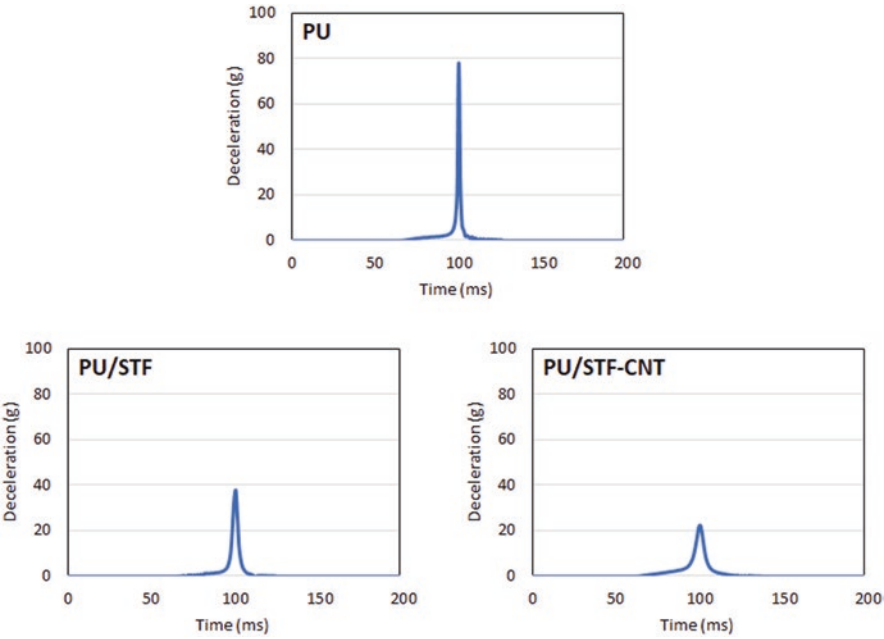

Fig. 3.3 Deceleration curves for the specimens

comparison to the pristine polyurethane foam. Hence, the detrimental effect of deceleration is lowered by the contribution of STF impregnation in the polyurethane foam [19–21]. The extended time period during the loading process in the STF cases can be associated with the shear-thickening behavior. When the STF is introduced to a sudden loading, shear-thickening mechanism is triggered, thereby increasing the suspension viscosity [22]. The suspension behaves stiffer due to this quick change in the viscosity. Since the polyurethane foam is impregnated with this fluid, the viscosity increase is spread from the impact point to the far fields over the foam. For this reason, the polyurethane foam exhibits stiffer characteristics during the loading process. The rheological phenomenon in the STF provides an enhanced dissipation characteristic for the polyurethane foams impregnated with this smart fluid. Because the STF acts as a continuous matrix in the polyurethane foam, thickening behavior predominates over the whole structure beginning from the impact point. Thus, stiffened matrix within the polyurethane foam leads to a whole-body response to the loading instead of a local response at the impact point. For this reason, loading process is delayed over an extended time period while suppressing the sharp increase in deceleration. Regarding the multi-phase STF, it is possible to mention that CNT fillerscontribute to this process consequently providing more extended time span as well as having suppressed deceleration. Due to the advanced strength of CNT fillers, the texture in the multi-phase STF gets much stiffer during shear thickening. Furthermore, CNT fillers increase the solid particle amount in the

suspension, thereby leading to an increase in the overall viscosity profile. This is also associated with the enhanced stiffness in the system.

Figure 3.4 shows the peak decelerations on the dropping mass for different drop heights. As shown in the chart, peak values of the deceleration increase by increasing the drop height. On the other hand, STF impregnation provides a lowering effect in the peak decelerations for each drop height. Although single-phase STF is significant in lowering the peak decelerations, multi-phase STF provides an increased performance in this process. Table 3.2 shows the reductions in the peak deceleration by the single-phase and multi-phase STFs with respect to the pristine polyurethane foam. From the results, STF effect diminishes in intensity by increasing the drop height. This can be associated with the increasing impact velocity that produces higher shear rates in the specimens. In previous works [23–26], it is stated that the STF effect is pronounced at low-velocity impact conditions rather than the higher velocities. The solid particles in STF establish a chain-like force networks during the shear-thickening process. These particle networks bear the developed forces during thickening phenomenon in the suspension. However, the particle clusters cannot keep their integrity at higher shear rates, and therefore, a microstructural breakdown is observed in the particle networks. For this reason, shear thickening is suggested for low-velocity impact conditions for an enhanced protective performance. Otherwise, STF performance gradually reduces as shear rate increases. From this fact, our results show a good match with the literature. It can also be mentioned that the developed stresses show a reduction after the maximum viscosity point in the suspensions, thereby leading to a lower stress-bearing capacity beyond this point. For this reason, shear rates during the impact process should be in the vicinity of that point to have the maximum viscosity jump, thereby properly

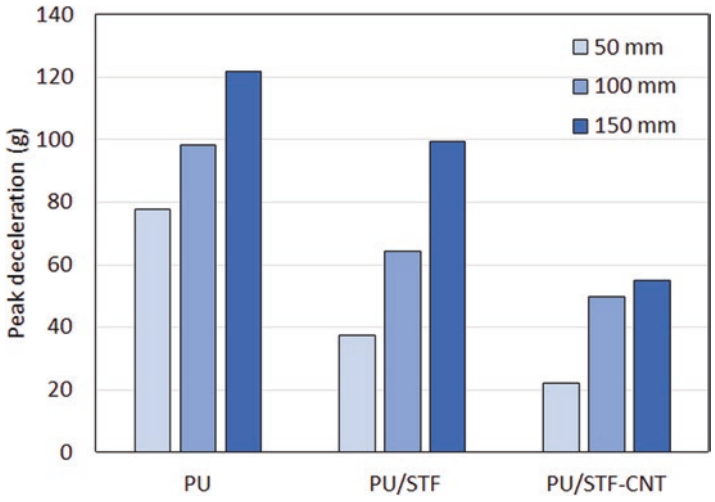

Fig. 3.4 Peak decelerations for the specimens

Table 3.2 Reductions in peak deceleration with respect to pristine polyurethane foam

	Drop heights		
Specimen	50 mm	100 mm	150 mm
PU/STF	52%	35%	18%
PU/STF-CNT	71%	49%	55%

benefitting from the shear-thickening behavior. According to previous studies [27–31], shear rates in the range of 100–500 s^{-1} generally correspond to the maximum viscosity points for the STFs based on silica and polyethylene glycol.

3.4 Conclusions

STFs are a promising alternative for protective applications due to their unique properties. Recent developments in STFs such as multi-phase systems have expanded their potential application in suppressing deceleration. STFs have been explored for various protective applications including protective textiles, impact-resistant structures and shock absorbing systems. While the development of STFs for protective applications is still in its early stages, the potential benefits are significant. STFs have a great potential to provide lightweight solutions in protective systems especially for low-velocity conditions. However, there are still challenges to be addressed such as tailoring the microstructural properties, controlling the rheology and preventing the degradation under various ambient exposures. Deceleration concept is one of the promising fields for STFs. Sensitive devices such as electronic units, robotic structures and unmanned aerial vehicles as well as humans suffer from sudden acceleration or deceleration in many different conditions such as crashworthiness applications and sharp maneuvers. In this study, a silica and polyethylene glycol–based STF was used as an impregnation agent for polyurethane foams. Moreover, the STF was filled with 1 wt% of CNT fillers to have a multi-phase system. The deceleration behavior of polyurethane foams was tested in a drop tower setup. An accelerometer was attached to a dropping mass, which was dropped on the polyurethane foam specimens from three different heights. Deceleration curves of the dropping mass were obtained during the impact processes, and therefore, the STF effect was discussed. According to the results, STF impregnation provides a significant reduction in the peak deceleration compared to the pristine polyurethane foam. Moreover, CNT inclusion in the STF led to an additional performance increase by further lowering the peak decelerations. Although the STF treatments provide a considerable reduction in the peak decelerations, shear-thickening effect had a loss of performance at high-velocity conditions. STF-impregnated polyurethane foams are promising structures in protective applications; however, the rheological properties of STF and the structural design of the foams have to be precisely tailored to take advantage of smart behavior in these systems.

Acknowledgments This study is funded by the Turkish Aerospace Industries Inc.

References

1. Gürgen S, Sofuoğlu MA, Kuşhan MC (2019) Rheological compatibility of multi-phase shear thickening fluid with a phenomenological model. Smart Mater Struct 28(3):035027
2. Mawkhlieng U, Majumdar A, Bhattacharjee D (2021) Graphene reinforced multiphase shear thickening fluid for augmenting low velocity ballistic resistance. Fibers Polym 22(1):213–221
3. Gürgen S, Sofuoğlu MA, Kuşhan MC (2020) Rheological modeling of multi-phase shear thickening fluid using an intelligent methodology. J Braz Soc Mech Sci Eng 42(11):605
4. Gürgen S (2019) Tuning the rheology of nano-sized silica suspensions with silicon nitride particles. J Nano Res 56:63–70
5. Liu L, Cai M, Luo G, Zhao Z, Chen W (2021) Macroscopic numerical simulation method of multi-phase STF-impregnated Kevlar fabrics. Part 2: Material model and numerical simulation. Compos Struct 262:113662
6. Hasanzadeh M, Mottaghitalab V, Babaei H, Rezaei M (2016) The influence of carbon nanotubes on quasi-static puncture resistance and yarn pull-out behavior of shear-thickening fluids (STFs) impregnated woven fabrics. Compos Part Appl Sci Manuf 88:263–271
7. Gürgen S (2020) Numerical modeling of fabrics treated with multi-phase shear thickening fluids under high velocity impacts. Thin-Walled Struct 148:106573
8. Gürgen S, Kuşhan MC (2022) Improvement of spall liner performance with smart fluid applications. Thin-Walled Struct 180:109854
9. Bajya M, Majumdar A, Butola BS, Verma SK, Bhattacharjee D (2020) Design strategy for optimising weight and ballistic performance of soft body armour reinforced with shear thickening fluid. Compos Part B Eng 183:107721
10. Sun L, Wei M, Zhu J (2021) Low velocity impact performance of fiber-reinforced polymer impregnated with shear thickening fluid. Polym Test 96:107095
11. Wu L, Wang J, Jiang Q, Lu Z, Wang W, Lin JH (2020) Low-velocity impact behavior of flexible sandwich composite with polyurethane grid sealing shear thickening fluid core. J Sandw Struct Mater 22(4):1274–1291
12. Warren J, Cole M, Offenberger S, Kota KR, Lacy TE, Toghiani H et al (2021) Hypervelocity impacts on honeycomb core sandwich panels filled with shear thickening fluid. Int J Impact Eng 150:103803
13. Liu H, Zhu H, Fu K, Sun G, Chen Y, Yang B et al (2022) High-impact resistant hybrid sandwich panel filled with shear thickening fluid. Compos Struct 284:115208
14. Sheikhi MR, Gürgen S (2022) Anti-impact design of multi-layer composites enhanced by shear thickening fluid. Compos Struct 279:114797
15. Ferreira Serra G, Fernandes FAO, de Sousa RJA, Noronha E, Ptak M (2022) New hybrid cork-STF (Shear thickening fluid) polymeric composites to enhance head safety in micro-mobility accidents. Compos Struct 301:116138
16. Gürgen S, Fernandes FAO, de Sousa RJA, Kuşhan MC (2021) Development of eco-friendly shock-absorbing cork composites enhanced by a non-Newtonian fluid. Appl Compos Mater 28(1):165–179
17. Sheikhi MR, Gürgen S (2022) Deceleration behavior of multi-layer cork composites intercalated with a non-Newtonian material. Arch Civ Mech Eng 23(1):2
18. Shamsadinlo B, Sheikhi MR, Unver O, Yildirim B (2020) Numerical and empirical modeling of peak deceleration and stress analysis of polyurethane elastomer under impact loading test. Polym Test 89:106594
19. Liu X, Huo J, Li TT, Wang H, Wu L, Lin JH et al (2020) Mechanical properties of a STF capsule filled flexible polyurethane composite foam. Mater Lett 269:127580
20. Soutrenon M, Michaud V (2014) Impact properties of shear thickening fluid impregnated foams. Smart Mater Struct 23(3):035022
21. Zhao F, Wu L, Lu Z, Lin JH, Jiang Q (2022) Design of shear thickening fluid/polyurethane foam skeleton sandwich composite based on non-Newtonian fluid solid interaction under low-velocity impact. Mater Des 213:110375

22. Li TT, Ling L, Wang X, Jiang Q, Liu B, Lin JH et al (2019) Mechanical, acoustic, and thermal performances of shear thickening fluid-filled rigid polyurethane foam composites: effects of content of shear thickening fluid and particle size of silica. J Appl Polym Sci 136(18):47359
23. Gürgen S, Kuşhan MC (2017) The ballistic performance of aramid based fabrics impregnated with multi-phase shear thickening fluids. Polym Test 64:296–306
24. Haris A, Lee HP, Tay TE, Tan VBC (2015) Shear thickening fluid impregnated ballistic fabric composites for shock wave mitigation. Int J Impact Eng. 80:143–151
25. Lee YS, Wetzel ED, Wagner NJ (2003) The ballistic impact characteristics of Kevlar® woven fabrics impregnated with a colloidal shear thickening fluid. J Mater Sci 38(13):2825–2833
26. Petel OE, Ouellet S, Loiseau J, Marr BJ, Frost DL, Higgins AJ (2013) The effect of particle strength on the ballistic resistance of shear thickening fluids. Appl Phys Lett 102(6):064103
27. Gürgen S, Kuşhan MC, Li W (2017) Shear thickening fluids in protective applications: a review. Prog Polym Sci 75:48–72
28. Gürgen S, Kuşhan MC, Li W (2016) The effect of carbide particle additives on rheology of shear thickening fluids. Korea-Aust Rheol J 28(2):121–128
29. Gürgen S, Li W, Kuşhan MC (2016) The rheology of shear thickening fluids with various ceramic particle additives. Mater Des 104:312–319
30. Jeddi M, Yazdani M, Hasan-nezhad H (2021) Energy absorption characteristics of aluminum sandwich panels with Shear Thickening Fluid (STF) filled 3D fabric cores under dynamic loading conditions. Thin-Walled Struct 168:108254
31. Liu L, Cai M, Liu X, Zhao Z, Chen W (2020 Dec) Ballistic impact performance of multi-phase STF-impregnated Kevlar fabrics in aero-engine containment. Thin-Walled Struct 157:107103

Chapter 4
Shock Absorption in Shear-Thickening Fluid Included 3D-Printed Structures

Ömer Yay, Mohammad Rauf Sheikhi, Gökhan Kunt, and Selim Gürgen

4.1 Introduction

Shear-thickening fluids (STFs) have gained significant attention in recent years due to their unique mechanical properties, particularly their ability to transition from a liquid-like state to a solid-like state under the application of high shear rates. This property, known as shear thickening, makes them promising candidates for various engineering applications, including impact protection and shock absorption. One emerging area of interest is the integration of STFs within three-dimensional (3D)-printed structures to enhance their shock-absorbing capabilities.

Traditional shock-absorbing materials, such as foams or elastomers, have some limitations in terms of their tunability and overall performance. On the other hand, STFs offer a potential solution by harnessing the unique behavior of suspensions of particles in a liquid matrix. When subjected to rapid deformation, the particles in the fluid aggregate and form a network structure, resulting in an increased viscosity and the ability to dissipate large amounts of energy. This phenomenon enables STFs to exhibit exceptional impact resistance and energy absorption properties.

In recent years, 3D-printing technologies have advanced rapidly, enabling the fabrication of complex structures with precise control over geometry and material

Ö. Yay (✉)
Department of Aeronautical Engineering, Gebze Technical University, Gebze, Turkey
e-mail: omeryay@gtu.edu.tr

M. R. Sheikhi
Key Laboratory of Traffic Safety on Track of Ministry of Education, School of Traffic & Transportation Engineering, Central South University, Changsha, Hunan, China

G. Kunt
Turkish Aerospace Industries Inc., Ankara, Turkey

S. Gürgen
Department of Aeronautical Engineering, Eskişehir Osmangazi University, Eskişehir, Turkey

S. Gürgen (ed.), *Shear Thickening Fluids in Protective Applications*,
https://doi.org/10.1007/978-3-031-42951-4_4

distribution. By incorporating STFs into 3D-printed structures, it is possible to design and manufacture customized shock-absorbing materials with tailored properties. This opens up new possibilities for applications in areas such as protective wear, automotive components, aerospace systems, and sports equipment. The combination of STFs and 3D printing presents several research challenges that need to be addressed to fully exploit their potential. Understanding the complex interplay between material properties, geometry, and printing parameters is crucial for optimizing the shock-absorbing performance of these composite structures. Parameters such as the type and concentration of shear-thickening particles, rheological behavior of the fluid, and printing parameters (e.g., layer thickness, infill density) influence the resulting mechanical properties and shock absorption capabilities of the 3D-printed structures. Moreover, it is essential to investigate the stability, durability, and long-term performance of STF-based composites. Factors such as the effects of repeated loading, temperature variations, and exposure to environmental conditions (e.g., humidity, ultraviolet radiation) can influence the rheological properties and structural integrity of the 3D-printed structures over time. The long-term reliability and practicality of these composites need to be thoroughly evaluated to ensure their suitability for real-world applications.

Liu et al. [1] made up an anti-impact system bringing an STF and a 3D-printed structure together. The STF was fabricated by dispersing nano-size silica particles in a polyethylene glycol having a molecular weight of 400. The particle concentration was 58.8% in the STF. The 3D structure was printed with a fine layer height to ensure good printing quality. The infill density was set as 37%. Honeycomb design was used in the printing, and a wall thickness of 1 mm was used to highlight the STF effect in the tests. The lower and upper sides of the honeycomb structures were covered with facesheets. An acrylate-based adhesive was used to join these components. The STF was filled the cavities inside the honeycombs. These specimens were subjected to low-velocity impact tests in a drop tower machine. A hemispherical impact head with a diameter of 12.7 mm was used in the impact tests. The impact head was dropped on the specimens with a velocity of 4 m/s, which corresponds to an impact energy of 17 J. According to the results, the STF-filled specimens lead to lower damage on the impact surface in comparison to the specimens with no STF. Impact damage is mostly seen as crack formation and delamination on the specimens. In the pristine honeycomb structures, the impact head shows excessive penetration into the material, thereby leading to an excessive deformation extending to the bottom surface. With the existence of STF in the honeycomb structures, shear-thickening behavior contributes to the rigidity of the structures, thereby increasing the structural stability. A big part of impact energy is absorbed in the shear-thickening phenomenon, and therefore, anti-impact resistance is enhanced by the contribution of STF in the structures. Despite these advantages, particle sedimentation in STF is a problem for long-term usage. To overcome this struggle, STF needs a stirring process at certain intervals. A similar study was conducted by Wu et al. [2]. In this study, an STF was synthesized by dispersing hydrophilic silica particles in polyethylene glycol pool. The silica loading was 20% in the STF. The STF was filled the cavities in a polyurethane layer, which was designed with a grid

pattern for sealing the STF. The polyurethane layer with STF filling was covered with nonwoven nylon fabrics. The STF volume fraction in the polyurethane layers was varied as 30%, 50%, and 70% depending on the grid sizes in the structures. In the shock-absorbing tests, the structures were impacted by a circular flat head having a diameter of 80 mm. The impact heights were varied from 150 to 350 mm to observe the effect of impact energy. In the impact load versus displacement curves, specimens without STF show a long plateau followed by a sharp peak. On the other hand, STF-included specimens has no plateau in this graph. These specimens show an increasing loading curve with respect to the displacement, which means that the structure absorbs more and more energy during the impact process, thereby withstanding impact loading with a greater stiffness. The impact loading leads to the onset of shear-thickening mechanism in the STF. For this reason, the polyurethane layer gains stiffer characteristics during the impact. According to the impact force charts, peak force is greatly lowered in the STF-included structures. For the impact head dropping from a height of 250 mm, the specimen without STF shows about 4.1 kN, while the STF-integrated specimens shows about 2.3 kN. When the STF volume is increased in the specimens, the energy-absorbing capacity is enhanced in the structures. More importantly, STF integration in the structures provides an improvement not only in energy absorption capacity but also specific energy absorption. Thus, STF contributes to the design of lightweight protective structures.

Gürgen et al. [3] integrated STF with an eco-friendly material, i.e., cork, to have enhanced shock-absorbing properties. Because cork is a natural material, it provides eco-friendly and sustainable properties. In addition, cork is widely used in anti-impact systems due to its high impact resistance, good damping behavior, and low density. The STF was fabricated with nano-size silica and polyethylene glycol. Various types of multi-layer designs were studied in this work. The STF was intercalated with cork layers, and the final structures were subjected to impact testing. A hemispherical impact head was used in the tests, and a load cell was used to collect the forces behind the specimens during the impact process. Compared to the pristine cork layers, STF inclusion greatly lowers the shock-absorbing properties in the specimens. The peak reaction forces are reduced to about 36% by the effect of STF intercalation. Hence, STF and cork-based composites are suggested for a wide range of applications such as damping, shock absorption, and crashworthiness. Gu et al. [4] designed lattice truss structures filled with STF. These structures were proposed to anti-impact and shock-absorbing applications. The STF used in this study was synthesized with spherical silica particles and polyethylene glycol. The dynamic compressive behavior of the structures was investigated in high-velocity impact testing. Furthermore, numerical simulations were carried out to observe the high strain rate behavior of these structures. In the numerical work, a hydrodynamic-constitutive model was created to simulate the STF behavior. According to the results, STF provides higher stiffness for the lattice truss structure. The viscosity increase during the shear-thickening phase contributes to the coupling effect between the lattice structures and STF, and therefore, the deformation mode is heavily changed. Consequently, energy-absorbing capacity of the structures is greatly enhanced by the STF integration into the lattice truss structures. Sheikhi et al. [5]

investigated the anti-impact properties of multi-layer composites including STF. They fabricated an STF based on fumed nano-size silica and polyethylene glycol. Then, the STF was injected into a polyester foam layer to contain the STF. In their work, various types of multi-layer composites were designed by using cork layers, polyester foams, and warp-knitted spacer fabrics. A drop tower system was used in the impact testing. A 15-mm diameter hemispherical impactor was dropped on the specimens from different drop heights. Reaction forces in the impact process were investigated by the researchers. Furthermore, energy absorbing and energy absorbing per unit mass were calculated in this study. According to the results, STF integration into the composites suppresses the reaction forces on the structures. Moreover, energy-absorbing capabilities are enhanced by the contribution of STF. Upon impacting the structures, STF shows a sudden viscosity increase at the impact point, thereby increasing the stiffness at that point. The shear-thickening behavior is originated from the impact point to the far fields. For this reason, impact energy is spread over a larger area on the structures. Increasing viscosity acts as an additional energy-consuming mechanism in the system. Hence, a part of impact energy fades away during the shear-thickening process. In addition to the beneficial results in energy absorption, the structures can be designed in a lighter manner with STF because the STF-included composites provide higher energy-absorbing rates per unit mass.

STF and 3D-printed structures were also brought together in different systems such as brake applications. Due to the shear-thickening rheology, STF provides a smooth deceleration while eliminating the shock loadings in the brakes. Tian et al. [6] designed a 3D-printed rotational brake by using STF inside the structure. The STF used in this system was fabricated with silica and ethylene glycol. The structure consisted of two main components: a rotator and an STF holder. The STF holder is a cup filled with STF, while the rotator has blades rotating in the STF medium. Based on the designers, STF shows shear-thickening behavior during the rotation of the blades, thereby decelerating the rotator in the braking phase. A smooth deceleration is obtained due to the gradual viscosity increase in the STF. Since the STF is a self-induced material, there is no external stimulation in the system to activate the shear-thickening behavior. Compared to the magnetorheological systems, there are some benefits with this design. One of the advantages is that there is no need for a power supply unit in the system because the torque change is based upon the inherent rheological properties of the STF. Another advantage over the magnetorheological systems is the simpler structure. Magnetorheological devices require a magnetic unit along with a controller system. However, STF-based system is not dependent on an external unit for running. This also leads to an economical solution that greatly reduces the installation cost in the applications. Last but not least, the STF-based system provides higher stability in the process.

In this study, we aim to explore the potential of STF inclusion within 3D-printed structures for shock absorption. For this purpose, an STF was prepared by distributing nano-size silica particles in the polyethylene glycol medium. In addition, the

STF was reinforced with carbon nanotubes (CNTs) to enhance the stiffness in this smart material. The shear-thickening rheology of the samples was verified in the rheological tests. In the 3D printing stage, a honeycomb design was used to encapsulate the STF. The bottom and top surface of the honeycomb structures were covered with AA2024 sheets. The specimens were subjected to impact testing with a hemispherical impactor to observe the shock-absorbing properties. Various impact energies were used in the study. Impact loads were collected by a load cell, and the results were evaluated. Based on the results, STF application reduces the peak forces developed during the impacting process. A further reduction in the peak forces is achieved by using carbon nanotubes in the STF. It can be stated that STF especially with carbon nanotubes enhances the shock-absorbing properties of the 3D-printed structures. The findings of this research could have significant implications for the design and fabrication of next generation shock-absorbing materials. By combining the advantages of STF and 3D printing, we can potentially develop highly efficient and customized structures capable of dissipating impact loading in a tailored way. This can lead to improved safety, enhanced protection, and increased durability in various applications, including personal protective equipment, automotive crash structures, aerospace components, and sports equipment.

4.2 Materials and Method

In this study, STF was fabricated by distributing 20-nm fumed silica particles (from Evonik) in polyethylene glycol with a molar mass of 200 g/mol (from Sigma-Aldrich). The silica concentration was kept at 40 wt% in the mixture. A high-speed homogenizer was used to have a well-dispersed suspension. In addition, another suspension was fabricated by including 1 wt% carbon nanotubes (CNT) in the STF. The rheological measurements were carried out in an MCR302 rheometer within the shear rate range of 1 to 1000 s^{-1}. A pre-shear procedure was applied before the measurements so that the samples were sheared by 1 s^{-1} for 60 s to eliminate the loading effects.

STF and CNT-included STF mixtures were contained in a 3D-printed structure. Polylactic acid (PLA)-based 3D-printed structures were produced in an Ender-5 Plus 3D printer. The geometrical details with the structures are given in Fig. 4.1. The gaps in the honeycombs were filled with the suspensions, and the bottom and top surfaces were covered with AA2024 sheets with 0.5 mm thickness. Table 4.1 gives three different specimen configurations used in the impact testing. A drop tower system was used in the impact testing. The specimens were impacted by a hemispherical impactor having a diameter of 15 mm. Each specimen was impacted by three different impact energies; 3.5, 7, and 10.5 J. Impact loads were collected by a load cell (Kistler) under the specimens. Figure 4.2 shows the drop tower system used in the impact tests.

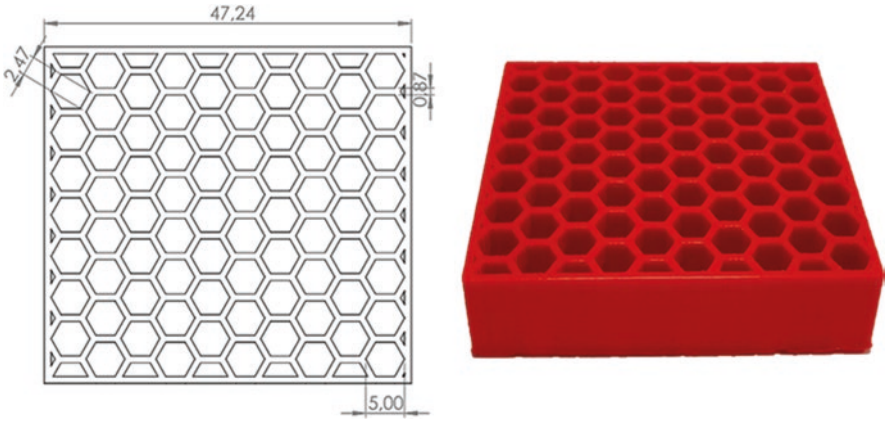

Fig. 4.1 Geometrical details of the 3D-printed structures

Table 4.1 Design of the specimens

Specimen	Content
3D	3D-printed structure without any filler in the honeycombs
3D/STF	3D-printed structure with STF in the honeycombs
3D/STF–CNT	3D-printed structure with STF–CNT in the honeycombs

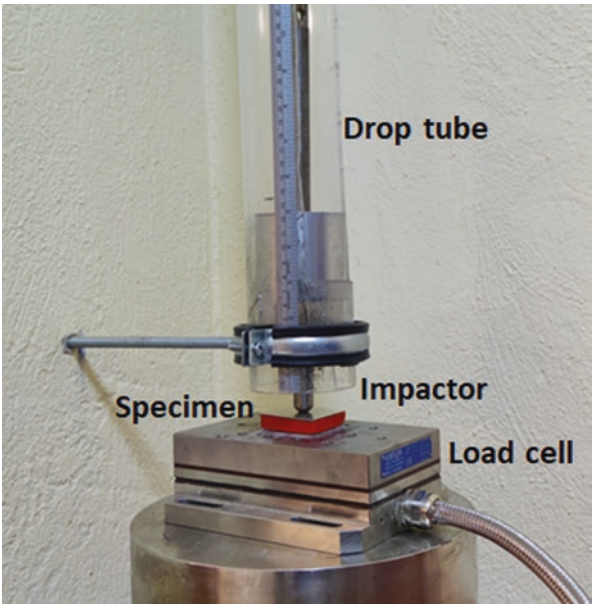

Fig. 4.2 Drop tower system

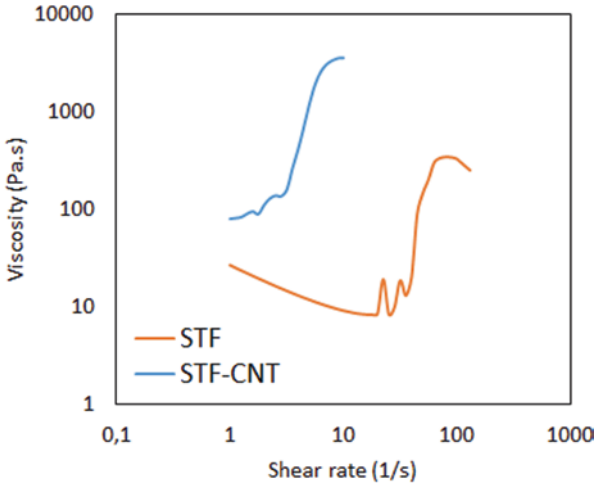

Fig. 4.3 Rheological flow curves for the suspensions

4.3 Results and Discussion

Figure 4.3 shows the rheological flow curves for the suspensions. As shown in the curves, STF has a slight shear-thinning behavior up to the critical shear rate of 20 s^{-1}. Beyond this point, there are some instabilities and a sharp jump in the suspension viscosity. After reaching out the peak viscosity point, the suspension shows one more shear thinning. This curve shows a regular STF behavior, which can be explained by the hydro-clustering theory and contact rheology model [7–11]. At zero shear state, the particles in the suspension attract each other, and therefore, the mixture has a relatively high initial viscosity [12]. The particles get motion, while the particle interactions are interrupted by increasing shear rate in the suspension. The particles form self-lubricating layers in the suspension, thereby facilitating the flowing. Consequently, suspension viscosity shows a slight decrease at low shear rates [13]. At the critical shear rate, hydrodynamic forces acting on the particles grow stronger. For this reason, the flow introduces to some difficulties where the particles come closer to each other by the effect of hydrodynamic interactions. Beyond the critical shear rate, aggregated particle groups, namely hydro-clusters get bigger, thereby extending in the suspension. These particle units hinder the fluid to flow by increasing the suspension viscosity [14, 15]. This phenomenon is called shear thickening. After the maximum viscosity point, hydro-clusters cannot bear the developed forces in the suspension. The extending particle chains in the mixture are broken into smaller parts. The flowability of the suspension is increased again similar to the first shear-thinning phase occurring between zero shear rate and critical shear rate.

CNT-included STF shows similar rheological behavior with the pristine STF. However, critical shear point reduces to lower rates so that the shear-thickening onset is observed very quickly in the suspension. Moreover, this suspension does not show a shear-thinning regime due to the CNT fillers disturbing the layered

orientation of the silica particles. For this reason, self-lubricating effect fades away for the shearing range from zero to critical shear rate. The reduction in the critical shear rate is associated with the CNT contribution to the shear-thickening rheology. The CNT fillers lead to entanglements in the microstructure, thereby facilitating the hydro-clustering formation in the suspension. For this reason, the extension of the silica particle groups occurs at lower shear rates. On the other hand, peak viscosity is increased by the CNT inclusion in the pristine STF. The silica particles by the contribution of CNT entanglement withstand higher forces developed in the mixture. CNT fillers cover the hydro-clusters during the shear-thickening process, and the force-bearing capabilities are enhanced. For this reason, higher peak viscosity can be reached in the CNT-included STF [16]. In addition, solid volume content is enhanced by adding CNT fillers in the mixture, and therefore, the suspension viscosity gets higher values. Hence, overall viscosity increases in the CNT-integrated STF. It is possible to mention that CNT fillers support the shear-thickening mechanism in the suspensions [17]. This can be observed by calculating the thickening ratios in the mixtures. Thickening ratio is one of the indicators regarding the shear-thickening behavior. This metric is calculated dividing the peak viscosity by the viscosity at critical shear rate [18]. Based on the rheological measurements, thickening ratios are 40.2 and 44.4 for the pristine and CNT added STFs, respectively. According to these results, CNT increases the thickening ratio in the suspensions, which means that shear-thickening rheology is enhanced by the CNT fillers.

Figure 4.4 shows the impact-loading peaks for the specimens. As shown in the charts, the first force peaks show the main impact reactions by the specimens upon impact. In addition, there are one or more successive peaks after the first peaks, which are produced due to the rebounding of the impactor just after the main impact. It is clear that the specimens are loaded by quite heavy forces in very small time periods upon impact. For ease of comparison, peak forces are extracted from these charts and presented in Fig. 4.5. According to the peak force results, STF integration suppresses the peak force values in the 3D structures for each impact energy level. There are some more reductions by using the CNT-included STF in the specimens; however, this effect is not at a significant level. Table 4.2 gives the reduction in the peak forces with respect to the 3D specimen. From these results, STF integration contributes to the force suppression in the range of 7.7–11.2% for all the impact energy levels. The peak force suppressions are about 10.7% and 12% when the structures are filled with CNT-included STF. Comparing these results, the force reductions are quite close to each other. Yet, it is possible to state that STF with CNT fillers provides higher shock-absorbing capabilities than the pristine STF.

The suppression in the peak forces is simply associated with the shear-thickening mechanism that is activated by the impacts [19]. To calculate the shear rates in the impact tests, impact velocity is divided by the diameter of the impactor. According to this calculation, shear rates are found to be 160, 230, and 280 s^{-1} for the impact energy levels. Recalling the rheological flow curves in Fig. 4.3, critical shear rates are much below the shear rates obtained in the impact tests. Hence, it is possible to state that the impacts are sufficiently strong for the onset of shear-thickening rheology. To support this issue, previous studies [20, 21] state that the shear-thickening

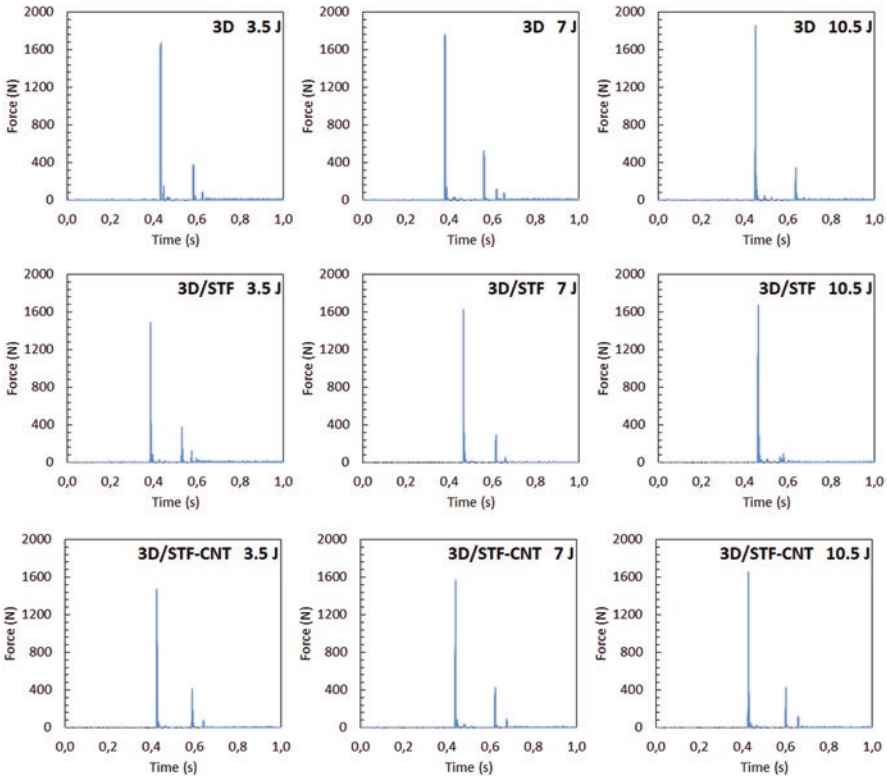

Fig. 4.4 Impact-loading peaks for the specimens

mechanism is even triggered under quasi-static loadings. In this context, we can point out the viscosity jump in the suspensions, thereby providing a shock-absorbing behavior for the structures.

Shear thickening is developed in the suspensions that were filled into the impacted honeycombs. Far-field honeycombs are not much affected by the impacts so that the suspensions in these parts do not show a strong shear-thickening rheology. Silica particles quickly come closer to each other, and a drastic viscosity increase is observed at the impact area. For this reason, the honeycombs at the impacted area are supported by stiff fillers inside the cells, and consequently, impact damage is lowered in the structure. Moreover, the suspensions in the honeycombs act as a continuous matrix in the structure. Hence, the impact loading is transferred to the adjacent cells, thereby fading away the shock loading. The accumulation of the impact loading is avoided by this way. The neighbor cells also contribute to the shock attenuation because the impact loading is distributed over a larger area on the structure. The structure benefits from the far-field honeycombs in the shock-absorbing process.

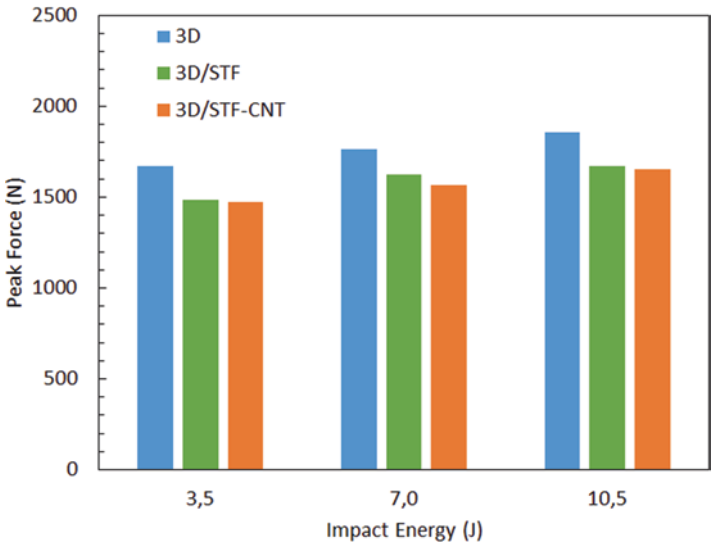

Fig. 4.5 Peak forces for the specimens

Table 4.2 Reduction in the peak forces with respect to the 3D specimen

	Impact energy		
Specimen	3.5 J	7 J	10.5 J
3D/STF	11.2%	7.7%	9.8%
3D/STF–CNT	12.0%	11.2%	10.7%

It is obvious that STF with CNT additives provides high-absorbing capabilities comparing the pristine and CNT-included suspensions. This is simply related to the contribution of CNT fillers to the shear-thickening behavior. Since the CNT fillers have entangling effect in the suspensions, silica-based hydro-clusters are easily formed without breaking into small parts under high-level loadings. Upon impact, the CNT-included STF provides stiffer characteristics in the honeycombs, thereby withstanding higher loadings.

4.4 Conclusions

In this study, 3D-printed structures are investigated under impact conditions. To enhance the shock-absorbing properties of these structures, STF is used as a filler material in the honeycombs. In addition to the pristine STF, a multi-phase system is also fabricated by including CNT in the suspension. According to the rheological measurements, pristine STF shows obvious shear-thickening behavior under increasing shear rate. Shear-thickening properties are greatly enhanced by the CNT

fillers in the suspension. The 3D-printed structures benefit from the STF reinforcement in the impact tests. STF application reduces the peak forces developed during the impacting process. A further reduction in the peak forces is achieved by using CNT fillers in the STF reinforcements. It can be stated that STF especially with CNT fillers enhances the shock-absorbing properties of the 3D-printed structures.

References

1. Liu H, Fu K, Zhu H, Yang B (2022) The acoustic property and impact behaviour of 3D printed structures filled with shear thickening fluids. Smart Mater Struct 31(1):015026
2. Wu L, Wang J, Jiang Q, Lu Z, Wang W, Lin JH (2020) Low-velocity impact behavior of flexible sandwich composite with polyurethane grid sealing shear thickening fluid core. J Sandw Struct Mater 22(4):1274–1291
3. Gürgen S, Fernandes FAO, De Sousa RJA, Kuşhan MC (2021 Feb) Development of eco-friendly shock-absorbing cork composites enhanced by a non-Newtonian fluid. Appl Compos Mater 28(1):165–179
4. Gu ZP, Wu XQ, Li QM, Yin QY, Huang CG (2020) Dynamic compressive behaviour of sandwich panels with lattice truss core filled by shear thickening fluid. Int J Impact Eng 143:103616
5. Sheikhi MR, Gürgen S (2022) Anti-impact design of multi-layer composites enhanced by shear thickening fluid. Compos Struct 279:114797
6. Tian T, Nakano M (2017) Design and testing of a rotational brake with shear thickening fluids. Smart Mater Struct 26(3):035038
7. Mari R, Seto R, Morris JF, Denn MM (2014) Shear thickening, frictionless and frictional rheologies in non-Brownian suspensions. J Rheol 58(6):1693–1724
8. Seto R, Mari R, Morris JF, Denn MM (2013) Discontinuous shear thickening of frictional hard-sphere suspensions. Phys Rev Lett 111(21):218301
9. Lin NYC, Guy BM, Hermes M, Ness C, Sun J, Poon WCK et al (2015) Hydrodynamic and contact contributions to continuous shear thickening in colloidal suspensions. Phys Rev Lett 115(22):228304
10. Gürgen S, Kuşhan MC, Li W (2016) The effect of carbide particle additives on rheology of shear thickening fluids. Korea-Aust Rheol J 28(2):121–128
11. Peters IR, Majumdar S, Jaeger HM (2016) Direct observation of dynamic shear jamming in dense suspensions. Nature 532(7598):214–217
12. Gürgen S (2019) Tuning the rheology of nano-sized silica suspensions with silicon nitride particles. J Nano Res 56:63–70
13. Gürgen S, Sofuoğlu MA, Kuşhan MC (2019) Rheological compatibility of multi-phase shear thickening fluid with a phenomenological model. Smart Mater Struct 28(3):035027
14. Maranzano BJ, Wagner NJ (2002) Flow-small angle neutron scattering measurements of colloidal dispersion microstructure evolution through the shear thickening transition. J Chem Phys 117(22):10291–10302
15. Wagner NJ, Brady JF (2009) Shear thickening in colloidal dispersions. Phys Today 62(10):27–32
16. Sheikhi MR, Hasanzadeh M, Gürgen S (2023) The role of conductive fillers on the rheological behavior and electrical conductivity of multi-functional shear thickening fluids (M-STFs). Adv Powder Technol 34(8):104086
17. Chen Q, Liu M, Xuan S, Jiang W, Cao S, Gong X (2017) Shear dependent electrical property of conductive shear thickening fluid. Mater Des 121:92–100
18. Gürgen S, Li W, Kuşhan MC (2016) The rheology of shear thickening fluids with various ceramic particle additives. Mater Des 104:312–319

19. Sheikhi MR, Gürgen S (2022) Deceleration behavior of multi-layer cork composites intercalated with a non-Newtonian material. Arch Civ Mech Eng 23(1):2
20. Decker MJ, Halbach CJ, Nam CH, Wagner NJ, Wetzel ED (2007) Stab resistance of shear thickening fluid (STF)-treated fabrics. Compos Sci Technol 67(3–4):565–578
21. Gürgen S, Kuşhan MC, Li W (2017) Shear thickening fluids in protective applications: a review. Prog Polym Sci 75:48–72

Chapter 5
Fabrication and Impact Properties of Shear-Thickening Fluid-Impregnated High-Performance Fabric Composites

Ehteshamul Islam and Leena Nebhani

5.1 Introduction

Shear thickening is a phenomenon in which a sudden increase in viscosity is usually observed when subjected to a high shear or impact (Fig. 5.1). It is commonly observed in concentrated colloidal dispersions. Shear-thickening fluid (STF) has attracted considerable amount of interest in potentially low velocity and ballistic impact applications due to its unique behavior [1–4]. STF is commonly prepared by dispersing sub-micron particles into a dispersing medium. The most critical factor for the applicability of STF is its ability to revert to its initial state after the removal of the externally applied force, thereby absorbing significant amount of energy during the cycle. This unique property of STF arises due to the shear-driven structural reorganization of the dispersed particles in a dispersing medium. Due to its solid-like behavior at higher shear rates, STF can be effectively utilized for the fabrication of protective clothing in anti-impact applications [4, 5]. The basic idea behind the STF usage for impregnating high-performance fabrics is to make more flexible and lighter protective structures with higher impact resistance [6–17].

The shear-thickening behavior of concentrated dispersions is extensively studied by researchers, and various models have been proposed to explain the underlying mechanisms behind such behavior. In an early attempt, Hoffman demonstrated that hexagonally ordered layers are the precondition for the shear-thickening transition. At lower shear rates, these layers move across each other leading to shear thinning followed by the disruption of these layers and becoming disordered at higher shear rates, resulting in an increase in the viscosity [18]. However, it was confirmed by Bossis et al. that the ordering of particles before shear thickening is not a necessary

E. Islam · L. Nebhani (✉)
Department of Materials Science and Engineering, Indian Institute of Technology Delhi, New Delhi, India
e-mail: Leena.Nebhani@mse.iitd.ac.in

S. Gürgen (ed.), *Shear Thickening Fluids in Protective Applications*,
https://doi.org/10.1007/978-3-031-42951-4_5

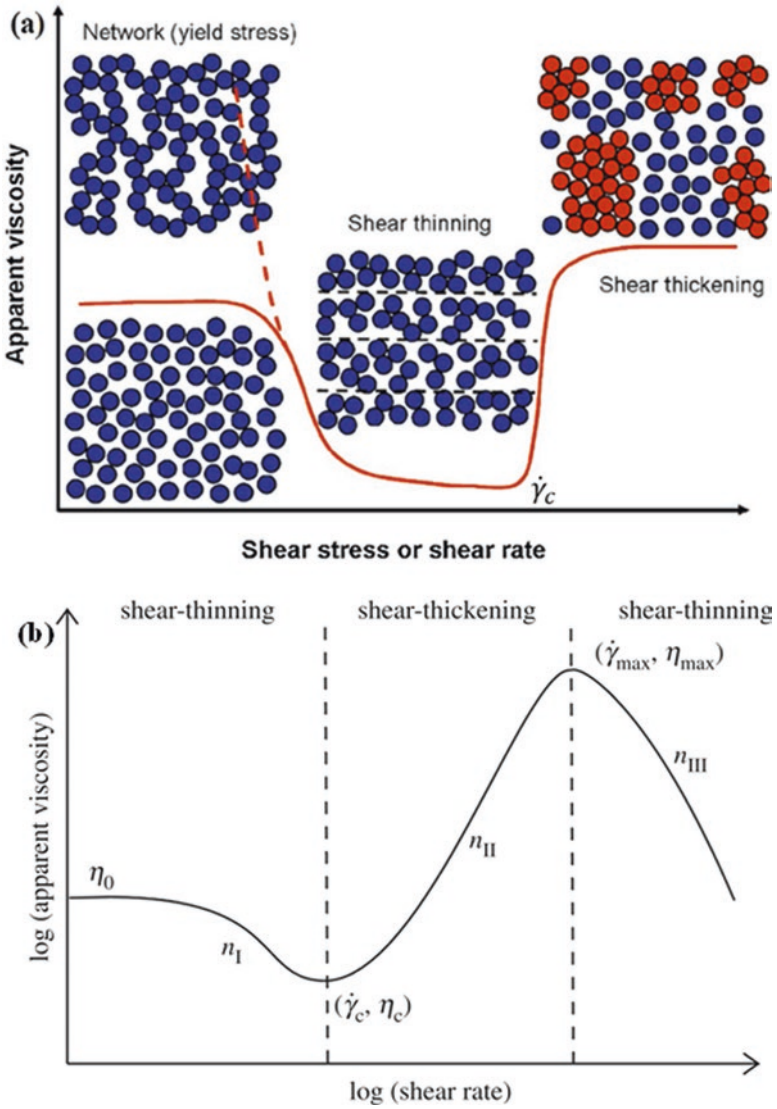

Fig. 5.1 (**a**) Schematic of shear-thickening mechanism by hydrocluster formation [26] and (**b**) typical shear-thickening curve [27]

criterion to occur [19]. The results of various simulation studies showed that the formation of hydroclusters is due to the hydrodynamic lubrication interactions between the particles during the shear-driven flow [20–22]. Later, small-angle neutron scattering (SANS) and small-angle light scattering (SALS) studies of the colloidal suspensions have shown that shear thickening occurs due to the formation of

hydroclusters at higher shear rates when hydrodynamic forces between the particles are prevalent over the electrostatic forces [23–25].

Moreover, Cheng et al. have used a high-resolution confocal microscope, which is combined with a rheometer to observe the microstructure of the submicron silica particles under shear. Their findings suggest that the lowering of entropic contribution to the initial viscosity and the formation of hydroclusters is due to the presence of lubrication stresses, which are responsible for shear-induced thickening in the colloidal suspension [28]. In recent years, frictional contact theory was explored to differentiate continuous shear thickening (CST) from the discontinuous shear-thickening (DST) behavior in concentrated suspensions [29, 30]. In relatively dense suspensions, frictional contact forces are the dominating factor, which results in the generation of large shear stresses. The magnitude of frictional forces generated in a dense suspension is due to the contribution of applied shear forces along with the lubrication forces. Mari et al. have concluded in their contact rheology model that at a higher volume fraction, the normal force deviates toward positive values, where the friction forces are the key factor for shear thickening [31]. Lin et al. observed in their shear reversal study that the contact forces play a major role in both the DST and the CST in a colloidal suspension, and this confirms the origin of contact forces developed between the particles due to inter-particle friction [32]. Peters et al. have also observed that in a dense suspension contact, force networks develop when shear rate increases, and the resultant shear thickening is predominantly driven by the contact forces [33]. In many recent studies, it is also found that the inter-particle friction is responsible for shear thickening in concentrated suspensions [34–39]. Figure 5.2 shows the contribution of frictional interactions in shear-thickening mechanism.

In this chapter, fabrication techniques for improved STF/high-performance fabric composites have been discussed. Moreover, various compositions for the preparation of STF/fabric composites have been reviewed. This study also gives an idea about the impact properties and major application areas of STF.

5.2 Dispersed Phase and Dispersing Medium

It has been observed that shear thickening is dependent on various factors of the dispersed phase such as volume fraction, surface properties, particle size, size distribution, and particle shape. The dispersed particles can be broadly classified into two categories, namely inorganic particles and organic/polymeric particles. In the class of inorganic particles, silica has been extensively studied as a dispersed phase for the preparation of shear-thickening dispersions. In an earlier study, Eastman and Barnes have shown a qualitative agreement to the shear-thickening phenomena in a micron-sized starch suspension dispersed in different ratios of glycerin/water mixture. Later, Frith et al. have given a more

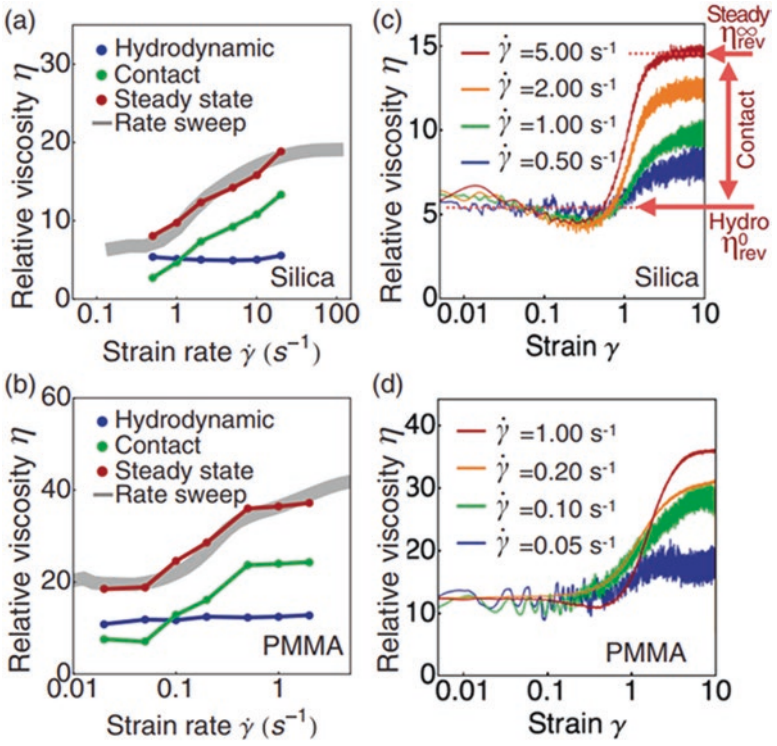

Fig. 5.2 Relative viscosity plotted with respect to strain rate for (**a**) silica and (**b**) Poly(methyl methacrylate) (PMMA) suspensions. Rate-sweep plots of silica and PMMA suspensions are shown in grey line, steady-state relative viscosities after the flow reversal test (red), hydrodynamic (blue), and contact (green) contribute to the relative viscosity. A sharp rise in the relative viscosity after shear reversal rheology of the (**c**) silica and (**d**) PMMA suspensions [32]

quantitative account of the shear-thickening behavior of cornstarch particle suspension in water and ethylene glycol. Boersma et al. have utilized monodispersed micron-sized silica particles to produce a shear-thickening dispersion in glycerol/water (86.1/13.9 w/w) mixture. They observed that the silica dispersion has shown shear-thickening behavior at a volume fraction of 52.4% [40]. Raghavan et al. have carried out both steady and oscillatory shear experiments with fumed silica suspensions in a polar organic media, polypropylene glycol (PPG). They have introduced a correlation between strain thickening and shear thickening using a modified Cox-Merz rule [41]. Yang et al. observed shear-thickening behavior in a titanium oxide (TiO_2)/water suspension at a narrow range of the Peclet (Pe) number, i.e., $10 < Pe < 100$ at a temperature of 50–70 °C [42]. Maranzano et al. have used charged stabilized silica sub-micron-sized particles ranging between 75 and 650 nm and studied the effect of particle size on the reversibility of the shear-thickening effect in a concentrated colloidal suspension. In order to prepare the suspension, they have partially neutralized the

silica surface by 3-(trimethoxysilyl)propyl methacrylate (TPM) and dispersed it in tetrahydrofurfuryl alcohol (THFFA) [43].

Apart from the steady shear rheology, White et al. have studied the rate of extension on the development of extensional viscosity in a dense cornstarch/water suspension [44]. Lim et al. have explored the transient response of concentrated colloidal silica suspension under different compression strain rates using the split Hopkinson pressure bar (SHPB). They have observed that the time for transition to reach the shear-thickening state decreases logarithmically at a very narrow compressive strain window [45]. Liu et al. have shown that gelation can be induced in a fumed silica suspension at a critical volume fraction or by selecting a high-molecular weight dispersing medium [46]. Gürgen et al. have used fumed silica–based STF to reduce the chatter vibrations in cutting tools. It was observed that calcium carbonate is another promising material for the preparation of STF [47]. Chen et al. have noted that the calcium carbonate suspension (CCS) in glycerin has shown excellent reversible shear-thickening behavior. Moreover, the calcium carbonate suspension has shown a discontinuous rise in viscosity above a critical volume fraction of 41% [48]. Surface properties of dispersed phase in STFs can be an extremely critical factor for tuning shear-thickening behavior. It has been found that the atomic level interactions between the particles such as hydrogen bonding, electrostatic interactions, and π-π stacking in a colloidal suspension can be crucial for determining the critical volume fraction of the dispersed phase [49]. Gürgen et al. have developed sandwich structures by integrating a fumed silica–based STF and studied the vibration attenuating scope of these intelligent composites. According to their results, they have suggested that STF can be used in structures for vibration damping purposes [50].

In addition to the inorganic particles, polymeric particles have been extensively used for the preparation of shear-thickening suspensions with different aims. Due to the molecular attributes and surface properties of polymer particles, they are extensively used for the preparation of STFs. It was observed that the pH of the STF suspension can also alter the shear-thickening behavior. When the zeta potential of a polystyrene-ethyl acrylate (PStEA) copolymer suspension was near its isoelectric point, shear thickening appears at a lower critical shear rate [51]. It is also possible to control the critical shear rate by simply varying the concentration of the glycerin/water ratio. It was observed that the critical shear rate decreases with the increase in the glycerin/water ratio for the polymethylmethacrylate (PMMA) particle suspensions. Chang et al. have studied the steady shear as well as dynamic shear rheology of the polystyrene (PS)/acrylate particle–based STF suspensions (Fig. 5.3). They have concluded that the particle agglomeration and deagglomeration are presumably artifacts of the gap between the plates of the rheometer. As a result, the particles agglomerated at a relatively smaller gap between the plates and have shown shear thinning at low shear rate. However, at larger gaps, the particles behave as a stable sol, which lead to stronger shear-thickening effect [28]. Comtet et al. have studied the frictional interactions between a pair of particles and correlated the frictional response to the rheological properties of poly(vinyl chloride) (PVC) suspension in 1,2-cyclohexane

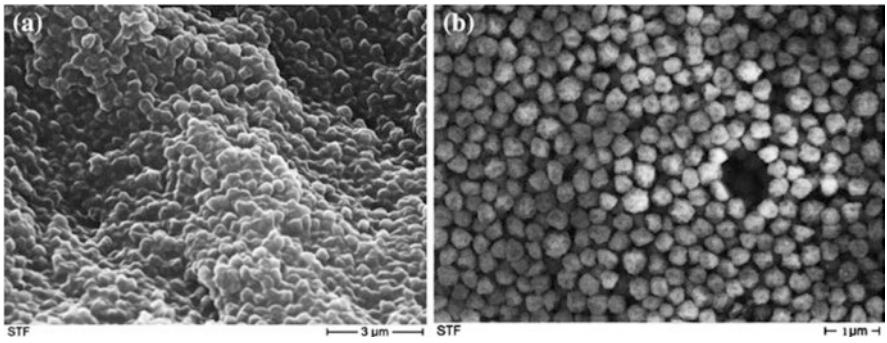

Fig. 5.3 (**a**) STF with polystyrene/acrylate particles in ethylene glycol and (**b**) polystyrene/acrylate particles after washing with water [28]

dicarboxylic acid di-isononyl ester [52]. They have observed that the reason for discontinuous shear thickening in PVC suspension is the breakdown of lubrication forces and the formation of contact networks. Son et al. have suggested that the polystyrene–poly(2-hydroxyethyl methacrylate) (PSt–PHEMA) particles with higher 2-hydroxyethyl methacrylate (HEMA) content can be an adaptive approach to improve the shear-thickening behavior by exploiting strong inter-particle hydrogen bonding.

In the past few years, the use of multiphase particles as a dispersing phase has been adopted to tailor the shear-thickening behavior of particle suspensions. Hasanzadeh et al. have demonstrated the effect of the addition of the multiwalled carbon nanotube (MWCNT) on the rheological properties of fumed silica suspensions. They have concluded that MWCNT has a suppressive effect on the viscosity of the suspension, while the onset of shear thickening can be delayed to a higher shear rate [53]. Gürgen et al. have prepared an STF and used different kinds of ceramic particles such as silicon carbide (SiC), aluminum oxide (Al_2O_3), and boron carbide (B_4C) in a fumed silica suspension. They have found that these particles have a detrimental effect on the shear-thickening behavior at higher volume fractions owing to their inability to extend the hydrocluster formation [54]. Islam et al. have compared the effect of micron-sized cellulose beads on a shear-thickening suspension based on silica and polyethylene glycol (PEG). They have observed that cellulose beads have shown improved interactions with PEG through hydrogen bonding [55]. Wei et al. have added cerium oxide (CeO_2) as secondary particles in a fumed silica suspension. They observed a significant increase in the apparent viscosity of the suspension [56]. In a recent study, a multiphase STF system has been designed containing graphene oxide (GO) and carbon nanotube (CNT) fillers in a silica suspension. It was observed that the onset of the shear thickening in the multiphase (GO and CNT) STF systems has reduced to a lower critical shear rate, thereby resulting in a lower thickening ratio owing to their higher aspect ratios [57]. The types of particles and dispersing media are given in Table 5.1.

Table 5.1 Dispersed phase and dispersing medium in STFs

Phase of particles	Type of particles	Dispersing medium	Year	Reference
Single phase	Cornstarch (5–20 μm) Cornstarch (~19 μm)	Glycerin/water Ethylene glycol	1974 1995	[58] [59]
	Silica (1.92 μm)	Glycerol/water	1990	[40]
	Fumed silica (12 nm)	PPG (725 g/Mol)	1997	[41]
	TiO_2 (237 nm)	Water	2000	[42]
	Colloidal silica (75–650 nm)	THFFA	2001	[2]
	Modified fumed silica (12 nm)	PPG (400 and 2000 g/Mol)	2008	[60]
	Cornstarch (5–50 μm)	Water	2010	[44]
	Colloidal silica (~520 nm)	PEG (200 g/Mol)	2010	[45]
	Fumed silica (12 nm)	PEG (200 g/Mol and 400 g/Mol)	2015	[46]
	Precipitated calcium carbonate (30–200 nm)	Glycerin	2015	[48]
	Colloidal silica (220 nm)	PEG (400 g/Mol)	2017	[49]
	Fumed silica (20 nm)	PEG (400 g/Mol)	2020	[50]
	PMMA	Glycerin/water	2010	[61]
	PS/acrylate (300 nm)	Ethylene glycol	2011	[28]
	PSt–EA copolymer (370 nm)	Ethylene glycol	2014	[51]
	PVC (1 μm)	Dinch/mineral oil	2017	[52]
	PSt-PHEMA (500 nm)	Ethylene glycol	2018	[62]
Multiphase	Fumed silica/MWCNT	PEG (200 g/Mol)	2016	[53]
	Fumed silica/SiC, Al_2O_3, B_4C	PEG (400 g/Mol)	2016	[54]
	Colloidal silica/cellulose bead	PEG (200 g/Mol)	2018	[55]
	Fumed silica/CeO_2	PEG (200 g/Mol)	2019	[56]
	Styrene acrylate/CNT	PEG	2020	[63]
	Colloidal silica/GO/CNT	PEG (200 g/Mol)	2020	[57]

5.3 Methods for the Preparation of STF

The preparation of STF is quite a simple yet very tedious process. A number of different techniques have been used by researchers to prepare homogenous STF dispersions. STFs are usually prepared by means of solvent exchange, mechanical mixing, ultrasonic vibration, homogenizer, paint shaker, centrifugal mixing, and ball milling. In the solvent exchange method, an aqueous colloidal silica suspension is used, and the amount of water present in the suspension is gradually exchanged with the organic dispersing medium at a certain temperature. Since silica is in a colloidal suspension, mechanical agitation is a precondition during the evaporation stage to avoid the agglomeration of particles in the final STFs [64, 65]. The effectiveness of a mechanical stirrer for dispersing particles in a dispersing medium is relatively low. Many researchers have prepared STF by using simple mechanical blenders and have used it for different applications, where the bulk property of the

STF was a critical factor [66, 67]. Sun et al. have mechanically mixed the silica powder into the dispersing medium using a vortex hybrid mixer to prepare the STF [68]. Tryznowski et al. used a 250-ml reactor equipped with a stainless steel propeller geometry and mixed the dispersion at a low mixing rate for 14 days to prepare the STF [69]. Ultrasonic vibration is the widely accepted method over mechanical mixing for achieving a uniform dispersion [70–72]. The ultrasonication method utilizes ultrasonic cavitation into a solvent with low viscosity, which generates high-pressure jet between the particles. This high-pressure jet helps to deagglomerate the particles and helps to get a uniform dispersion. Figure 5.4 shows the ultrasonication method for STF preparation. Rheological properties show significant variations depending upon the dispersion of particles in low-molecular weight dispersing media [11, 64, 73].

High-speed homogenization is also one of the commonly used techniques for the initial mixing of two phases in an STF suspension [74]. This method exploits the high-pressure-driven cavities or bubbles, which release energy when they implode directly on the surface of the particles. As a result, the particles break down and, in this way, it helps in producing a uniform suspension. Mostly, homogenization of the dispersed phase in an organic medium is followed by ultrasonication for a stable suspension [75, 76].

Otsubu et al. have reported a unique method using paint shaker to prepare shear-thickening suspensions by dispersing carbon nanofibers and spherical carbon black in an aqueous solution of poly(vinyl alcohol) [77]. Yang et al. have used a centrifugal mixer to disperse silica nanoparticles in PEG. The centrifugal mixer uses the centrifugal force at a required rotational speed to mix the components. In the last stage, a vacuum chamber is used to remove the volatiles generated during the mixing [78]. In several studies, a high-speed ball grinding method has been used to prepare STF. Ball milling can be used in dry or wet conditions to grind the agglomerates into fine particles. Mostly, the wet grinding method is used where nanoparticles along with dispersing medium are charged into the mill, mixing them thoroughly for several hours and grinding the suspension uniformly to obtain the final STF compositions [79–82].

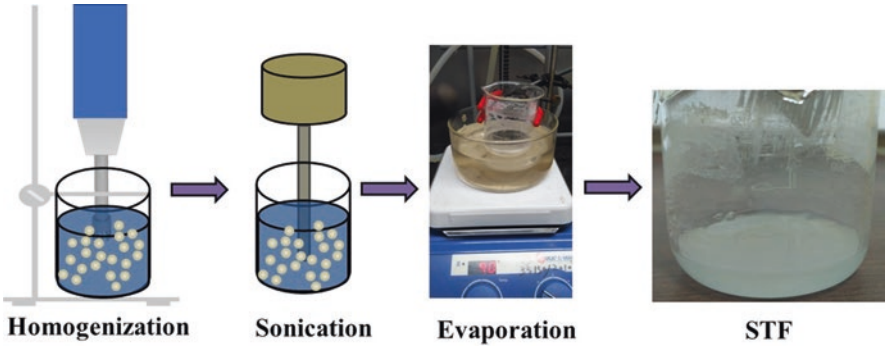

Fig. 5.4 Schematic for the preparation of STF using ultrasonication method

5.4 High-Performance Fabrics

In STF-impregnated fiber-reinforced composites, high-performance fabrics such as aramid, ultrahigh-molecular weight polyethylene (UHMWPE) fibers, and p-phenylene-2,6-benzobisoxazole (PBO) are commonly used. Generally, these high-performance fabrics have been employed for ballistic application, owing to their high strength-to-weight ratio, modulus, and flexibility. There are several criteria that must be considered for improving the impact performance of a ballistic structure. Among them, the easiest way to improve the impact property of a ballistic material is to increase the number of layers of the fabrics [83, 84]. However, this can improve the ballistic property of the final fabric structure but at the cost of the weight and flexibility of the product. A comparative overview of the mechanical properties of high-performance fibers with reference to their tenacity and modulus is given in Fig. 5.5.

5.4.1 Aramid Fibers

In the 1960s, the development of aramid fibers based on Kevlar by DuPont paved the way for the development of modern high-performance anti-ballistics protection systems including soft-body armors. Many researchers have exploited Kevlar's high modulus and high tenacity for the development of bullet-proof soft-body armor [86–89]. Similar to Kevlar, other aramids are available under the trade names of Twaron and Technora developed by Teijin. All forms of Kevlar fibers were found to

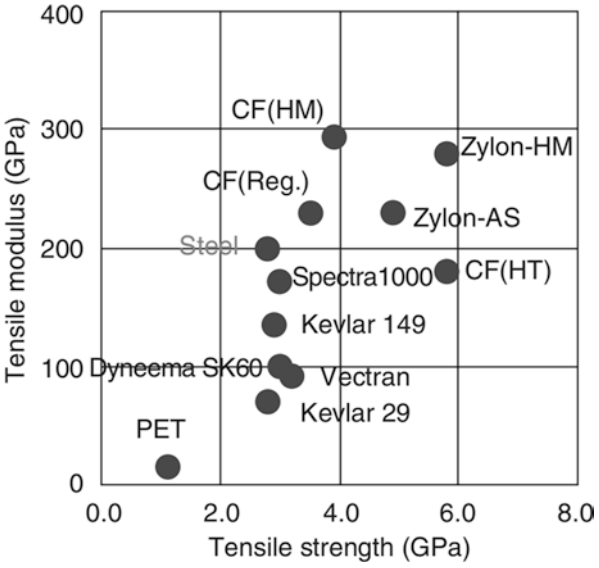

Fig. 5.5 Schematic overview of high-performance fibers in terms of tensile strength and modulus [85]

Table 5.2 Mechanical properties of different grades of ballistic fabrics

Fiber grade	Density (g/cm^3)	Tensile modulus (GPa)	Tensile strength (GPa)	Tensile elongation (%)	Reference
Kevlar 29	1.44	70.5	2.92	3.6	[91]
Kevlar 49	1.44	112.4	3.0	2.4	[91]
Kevlar 149	1.47	179	3.4	2.0	[91]
Dyneema	0.97	110	3.6	3.5	[92]
Spectra	0.97	117	3.4	2.7–3.6	[92]
PBO	1.54–1.56	180–270	5.8	2.5–3.5	[93]

be flexible and have five times higher tensile strength than steel. They also show excellent cut and wear resistance while sustaining higher velocity ballistic impacts. A series of Kevlar fibers have been developed, e.g., Kevlar 29, Kevlar 49, and Kevlar 149, based on the molecular orientation and crystallinity of the fibers, which leads to higher modulus and strength (Table 5.2). Moreover, highly oriented polymer chains can bring higher anisotropy to the fiber in the axial direction including a negative coefficient of expansion in the direction of the fiber axis [90]. Moreover, aramid fibers display excellent thermal stability over a wide range of temperatures and begin to carbonize above 420 °C. Some of the drawbacks associated with the p-aramid fibers are their low compressive strength and susceptibility to hydrolytic degradation due to their higher moisture absorption.

5.4.2 Ultrahigh-Molecular Weight Polyethylene (UHMWPE) Fibers

Ultrahigh-molecular weight polyethylene fibers are well known for their high strength, lightweight, and flexibility. Owing to these properties, it is widely used for enhancing high-velocity ballistic resistance, which makes UHMWPE fibers highly suitable for the fabrication of body armor jackets [94]. When the molecular weight of polyethylene reaches or exceeds 1 million Da, the polymer is referred to as ultrahigh-molecular weight polyethylene. The processing of UHMWPE fibers is very difficult due to their inherent higher molecular entanglements leading to very high viscosity and lower draw ratio. Therefore, commercially UHMWPE fibers are produced by gel-spinning process. In this process, UHMWPE is solvated in a solvent that helps in reducing the number of polymer chain entanglements, thereby allowing to achieve high draw ratio leading to high molecular orientation; as a result, UHMWPE fibers with high tensile strength and high modulus are manufactured. UHMWPE fiber–reinforced polymer composites are usually recommended for ballistic applications than their woven fiber counterparts. Due to the low coefficient of friction of UHMWPE spun fibers, only a few filaments get engaged in energy absorption during a high-velocity impact and allow the projectile to pass through the fabric [95].

UHMWPE fabrics are available with the trade name Dyneema manufactured by DSM and Spectra by Honeywell. These fibers are available with different deniers for a much wider range of applications. For ballistic applications, UHMWPE fibers are unidirectionally (UD) arranged in $[0/90°]_n$ nomenclature and reinforced with a thermoplastic polymer, where n varies between 1 and 3 depending on the end application. The ballistic panels are composed of ceramic plates bonded with UHMWPE sheets as a backing material to arrest the deformation of the ceramic plates as well as the fragments generated during the impact. UHMWPE fabrics also have excellent wear [96, 97], cut [98], and stab resistance [99], which makes them suitable for the manufacture of bulletproof jackets for law enforcement personals [100].

5.4.3 p-Phenylene-2,6-Benzobisoxazole (PBO) Fibers

Poly(p-phenylene benzobisoxazole) (PBO) is a rod-type heterocyclic polymer, which was commercialized by Toyobo Co. (Osaka, Japan) under the trade name Zylon in 1998. It shows lyotropic liquid crystalline behavior in solution. PBO is soluble in protic acids such as polyphosphoric acid and commercially used in dry jet wet spinning method to prepare high-performance fibers. Generally, 10–15 wt.% of PBO polymer is used for the preparation of spinning solution at a temperature range between 100 and 170 °C. PBO also has a higher decomposition temperature (650 °C) than Kevlar fibers. It was found that the PBO armor vest has shown superior ballistic performance than Kevlar KM2 and Kevlar 29 when tested against 2-grain and 64-grain projectiles [101]. PBO high-performance fibers have the capability to replace Kevlar fibers for ballistic applications, due to their ability to absorb impact energy twice as compared to Kevlar and UHMWPE, but at a higher cost. However, PBO fibers are extremely sensitive to hydrothermal aging conditions and can undergo benzoxazole ring opening and get converted to amide linkages, which can further hydrolyze to carboxylic acid and aminophenol moieties. This hydrolytic aging results in an approximately 40% decrease in the tensile strength of the PBO fibers within a period of 5 months [102]. However, a similar effect on the reduction in tensile strength can be achieved after more rapid aging with saturated steam at 180 °C [93].

5.5 Fabrication of STF-Impregnated Fabric Composites

A number of methods have been tried to enhance the ballistic performance of the high-performance fabrics such as Kevlar, UHMWPE, Twaron, PBO, and carbon fibers [103–109]. Although these methods can be extremely helpful in enhancing the ballistic performance of the composite structures, they lack many aspects such as overall weight, toxicity of fillers, lack in flexibility, and processing difficulties for the overall development of fiber-reinforced composites and their further use. A

unique method has been proposed by Lee et al. where they have used a shear-thickening colloidal suspension of silica to impregnate Kevlar fabrics for the improvement of the ballistic performance of the Kevlar fabric without compromising the flexibility and aerial density of the fabric [110]. They diluted the highly viscous STF with ethanol to reduce the viscosity and utilized a simple dipping method to impregnate the fabrics.

In the fabrication process of STF/high-performance fabric composites, the particles are dispersed into a dispersing phase by means of different mechanical or ultrasonication methods, which has been discussed in detail in the previous section. The viscous STF suspension is diluted in alcohol at a constant volume with respect to the STF. The dilution of STF with alcohol decreases the viscosity of the STF and helps in reaching the interstitial spaces between the yarns of the fabrics resulting in a uniform coating of the STF onto the fabrics. In several studies, different methods for impregnating STF have been discussed. Finally, the fabric is soaked into the STF for a definite time limit to attain a constant add-on percentage of the dispersed phase into the fabrics, and then the fabrics are dried in an oven at a constant temperature to remove the remaining alcohol in the fabrics.

The dipping and drying processes have been discussed in several studies. Kalman et al. impregnated Kevlar fabric by dipping them for 1 min in a diluted alcohol–STF solution followed by the removal of alcohol by passing through rubber rollers. The impregnated fabrics were first dried in air at room temperature for 10 min followed by oven drying at 60 °C for 30 min to remove the final traces of alcohol [8]. Hasan et al. have used a STF/ethanol (60:40 vol/vol) solution to impregnate Kevlar or Nylon fabric by dipping process for 1 min followed by the removal of excess ethanol by using 11.3 kg steel cylinder and drying at room temperature for 48 hours to remove the rest of the solvent [9]. In many studies, the dipping time of fabric has increased from minutes to hours to improve the penetration of STF solution into the filaments of the fabrics. Park et al. kept the Kevlar targets for 1 h in an ethanol-diluted colloidal silica solution. Afterward, excess ethanol was removed by using rubber rollers and drying at 80 °C [111]. Haris et al. used 300 mm × 120 mm Twaron fabrics and used a dipping method to impregnate the fabric with the STF solution. Here, they have not used any secondary process to remove the excess solvent from the fabric [112]. Wang et al. diluted the multiphase STF-containing graphene nanoplatelets with the help of ethanol at a ratio of 1:1 (vol/vol) and further sonicated for 1 hour. Afterward, polyethylene terephthalate (PET) fabric was impregnated by dipping into the dilute solution for 15 min, then the STF-infused fabric was passed through the vertically aligned padding rollers to remove the excess solvent [113]. Similar methods have been widely used by many researchers working on the related field [114–119]. A schematic of different methods for impregnating fabrics with STF is shown in Fig. 5.6.

Majumdar et al. optimized the padding pressure and optimal add-on % of STF in the Kevlar fabric for improved impact energy absorption. They have utilized a horizontal padding mangle where they have varied the STF to solvent ratio between 3:1 and 5:1 at different roller pressures of 1, 2, and 3 bar. It was found that the higher add-on % of silica and higher padding pressure are critical for high-impact energy absorption in STF-impregnated Kevlar fabric [120]. In an earlier study, Srivastava

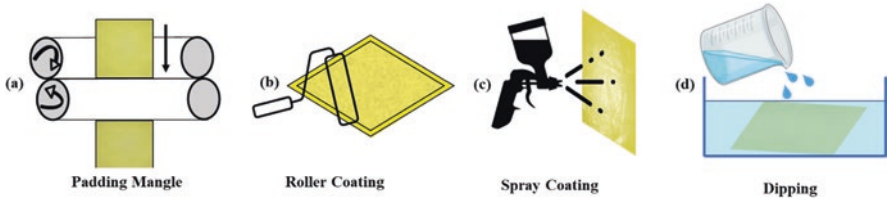

Fig. 5.6 Schematic for the fabrication processes for the manufacturing of STF-impregnated fabrics

et al. have shown that the lower padding pressure for the impregnation of Kevlar fabric leads to a higher add-on % of the silica particles. Higher add-on % of silica particles increases the inter-yarn friction of the STF-impregnated fabric as a result a higher yarn pull-out force is required to overcome the resistance at the cross-over point of adjacent yarns [121]. Sahoo et al. have diluted the STF by ethanol at a ratio of 1:4 vol/vol (STF:ethanol) and passed the Kevlar fabric through the horizontal padding machine through the STF solution bank created at the nip between the two rollers. The padding pressure was optimized to a constant pressure of 2 bar and at a rolling speed of 2 m/min to get the optimum add-on of STF [8].

5.6 Impact Absorption of STF/Fabric Composites

The treatment of high-performance fabric with the STF is of significance in impact protection systems. The impact properties of the STF/fabric composites are influenced by many factors. It can be divided into fabric-related and STF-related factors. Fabric-related factors such as the aerial density of fabric and fabric structure play a critical role in the impact energy absorption. While impregnating high-performance fabric with STF, the key parameters that must be considered are particle size, particle volume fraction, and surface functionalization of particles. It has been found that the internal friction between the yarns during an impact scenario plays a decisive role in the high-energy absorption mechanism in STF-impregnated fabric composite system. The impact absorption properties of STF/fabric composite can be categorized under three sub-headings: (i) Quasi-static yarn pull-out test of STF/fabric composites, (ii) low-velocity stab and spike resistance of STF/fabric composites, and (iii) high-velocity impact properties of STF/fabric composites.

5.6.1 Dynamic Yarn Pull-Out Test of STF-Impregnated Fabric Composites

The inter-yarn frictional force can be quantified by yarn pull-out test, where a single yarn from the fabric is pulled out at a constant velocity by a moveable grip of a universal testing machine. The maximum force required to pull a single yarn from

the fabric at a constant pulling rate is termed as the "yarn pull-out force." Three distinctive regions were identified and explained by Neelkantan et al. in a typical load displacement curve (Fig. 5.7c) during a yarn pull-out test of an uncoated Kevlar fabric. In region I or the loading region, the applied load starts increasing as the pulling yarn moves toward the direction of the applied force. The pulling yarn movement is restrained by friction generated by the transverse yarns at every cross-over point along the fabric width. In region II, the yarn starts sliding, as a result, the loading force decreases rapidly and attains a constant force plateau, which is termed as "dynamic load." The last region III is the slipping region, where the pulled yarn is completely removed and can move freely due to less number of contacting cross-over points (Fig. 5.7). After this point, the loading force starts to decline almost linearly due to less restriction experienced by the pulled yarn [88].

Lee et al. have found that STF can be helpful in increasing the peak force required to pull a yarn of Kevlar fabric at a high strain rate [5]. Feng et al. have studied the effect of STF on the yarn pull-out force of the STF-impregnated fabric. They have found that the energy absorption properties of the fabric are significantly improved due to the higher viscosity of the STF. In addition, the digital image correlation study correlated the mode of shearing to the friction generated due to the incorporation of STF into the fabric. Indeed, the STF has increased the friction between the yarns of the fabric without affecting its flexibility [122]. Tan et al. have found that the graphene/silica based STF have shown higher shear thickening efficiancy and as a result the yarn pull-out force of graphene based STF coated fabrics has shown a 500% increase in yarn pull-out force than the fabric without STF. Gong et al. studied the effect of pull-out speed on the pull-out force for yarn displacement in STF/Kevlar fabric. According to their results, the increase in the yarn pull-out force of the STF/Kevlar fabric is due to the shear-thickening effect of STF at the higher pull-out speed, which restricts the movement of the yarn and increases the inter-yarn friction [10]. Alikarami et al. have identified the opposite trend in the yarn pull-out test of the STF-treated fabrics. They have found that the peak force for yarn pull-out decreases for the STF-treated fabrics at maximum yarn pull-out speed

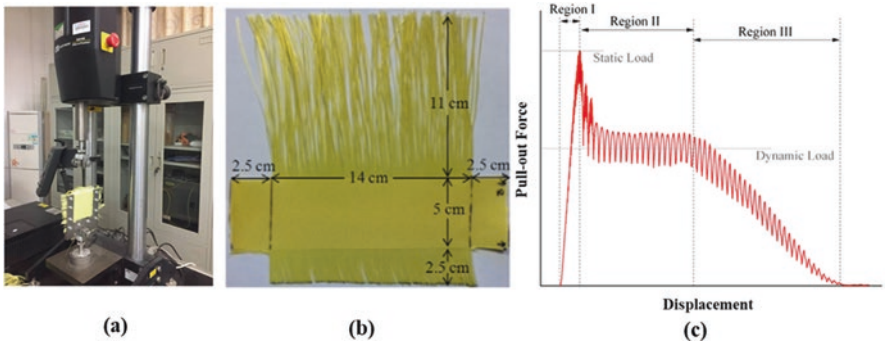

Fig. 5.7 (**a**) Yarn pull-out test setup, (**b**) fabric sample for test, and (**c**) typical load–displacement curve obtained in a yarn pull-out test [122]

[123]. While the findings of Bai et al. have been found to be in good agreement with the previous studies, they have correlated the increase in yarn pull-out force to the energy dissipation due to increased friction between the yarns of STF-impregnated plain woven Kevlar 29 fabric [124]. Similar results were also obtained by others, where they corroborated that the increased yarn pull-out force is due to the improved friction between the yarns of STF-infused fabrics [125–128].

5.6.2 Low-Velocity Stab and Spike Resistance of STF/Fabric Composites

High-energy dissipation related to the higher force required to pull-out a single yarn is the most promising attribute of STF/fabric composites in high-energy absorption. This suggests that more frictional cross-over points come under impact loading to resist any form of impact, thereby contributing to energy absorption. In most of the studies on low-velocity impact properties of ballistic fabrics, energy absorption was enhanced by the STF [129–131]. Low-velocity impact properties of STF/fabric composites are assessed either by a sharp knife stab (cut) or by a spike penetration (puncture) test using a drop tower impact testing machine. These tests have been studied according to the National Institute of Justice (NIJ) standards developed for stab resistance for soft-body armor fabrics [132].

Decker et al. have realized that there is a need for the development of high-performance soft-body armor for protection from cut (knife threat) and puncture threats. It was observed that the STF-treated Kevlar and Nylon fabric have shown significant improvements in cut resistance at different velocities, while marginal improvements were also seen in the puncture resistance test [129]. Kang et al. have treated the Kevlar fabric with fumed silica–based STF and measured their quasi-static spike puncture resistance as per the NIJ standard 0115.00. It was observed that the shear-thickening property of the STF does play a role in reducing the damage of the STF-impregnated fabric and also increased the frictional resistance between the spike and fabric [114]. Laha et al. investigated the combined effect of silica and halloysite nanotube–based STF on the quasi-static puncture resistance of STF-impregnated fabric as per the ASTM D3763 method. A hemispherical impactor of 13 mm diameter was used, which freely falls at the fabric at a velocity of 5.5 m/s. The silica-based STF has significantly improved the impact energy absorption of the Kevlar fabric. They have also found that the optimum level of the halloysite tube for the improvement of impact absorption depends on the type of Kevlar fabric used [133]. Hasanzadeh et al. have performed a quasi-static puncture test of the CNT/fumed silica–based STF composite of high-modulus polypropylene (HMPP) fabric as per the ASTM F1342. They have utilized a rounded tip penetrator at a velocity of 50 mm/min for dynamic stab test. It was observed that the STF-impregnated high-modulus polypropylene (HMPP) fabric–containing CNT has shown inferior stab resistance than the neat STF-treated fabric, due to the weaker

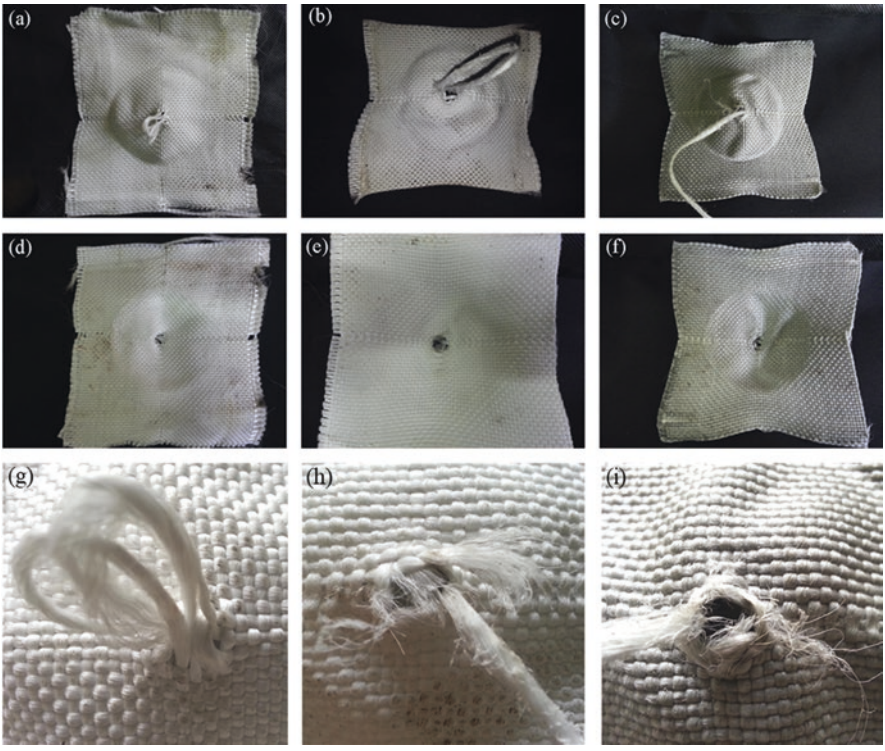

Fig. 5.8 Fabric failure views after the quasi-static tests: (**a**, **d**) untreated HMPP fabric, (**b**, **e**) STF-impregnated HMPP fabric, (**c**, **f**) STF–MWCNT-impregnated HMPP fabric composite, puncture behavior of (**g**) untreated HMPP fabric, (**h**) STF-impregnated HMPP fabric and (**i**) STF–MWCNT-impregnated HMPP fabric composite [134]

shear-thickening effect of CNT-based STF. They have also pointed out that yarn breakage was the mode of failure of fabric treated with CNT-based STF, while in the case of untreated fabric, yarn pull-out and windowing were observed as the primary mode of failure as shown in Fig. 5.8 [134].

Gürgen et al. have shown that STF treatment is more helpful in spike test, where the inter-yarn friction is more crucial than the spike test. It was also observed that the stab resistance of the STF/Kevlar fabric improved with STF containing higher concentration of bigger particles [13]. Gong et al. examined the effect of STF with different dispersed particles having different physical characteristics on resistance to knife and puncture in STF/fabric composites. They demonstrated that the hardness of the particles is the critical factor for improved knife resistance of the STF-impregnated fabric. However, in case of puncture enhancement of the STF/fabric composites, it was mainly attributed to the improved inter-yarn friction [10]. Xu et al. have studied the effect of different particle sizes and concentration of the particles on STF-treated fabric composites. They have selected a knife stabbing test with a 22.5 J impactor. They have observed that STF impregnation improved the

impact absorption of a 12-layered STF/fabric composite by 58% as compared to the 24-layered fabric composite panel [116]. Li et al. have explored the dynamic stab resistance characteristics of STF-impregnated UHMWPE fabric under both knife and spike impactor. The additive effect of polyethylene glycol with higher molecular weight has improved the penetration resistance against both the knife and the spike impactor. The reason for such improvement is due to the increased areal density of the composite, and the silica particles get restricted and confined by the high-molecular weight additive whose chain length is much longer than the dispersing medium [99]. Qin et al. have suggested an optimum STF weight fraction of 34.89% to improve the mechanical properties and obtain a better stab resistance of the STF-treated Kevlar fabric composite. They have also found that higher add-on % leads to enhanced stab resistance of STF-impregnated Kevlar fabric composite [128]. Santos et al. impregnated the Kevlar fabric with modified silica-based STF and evaluated its stab resistance using a knife threat. It was observed that at 25 wt.% silica concentration, the STF-impregnated Kevlar fabric has shown better stab resistance [135]. Gürgen et al. have performed a drop tower test using an engineered spike to test the puncture resistance of the STF and shear-stiffening gel (SSG) treated and untreated aramid fabric. They observed that the penetration depth of the STF-impregnated fabric was lower than that of the SSG-impregnated fabric. This is due to comparatively higher yarn restrictions imparted by SSG-treated fabric than the STF-treated fabric. It was also noted that the individual use of treated fabric is recommended for higher specific energy absorption. However, their synergistic effect was found to be detrimental to improving the energy absorption of the treated fabrics [136].

5.6.3 High-Velocity Impact Properties of STF/Fabric Composites

Bullet-proof armor material made from high-performance fibers such as aramid, UHMWPE, and PBO have been utilized to stop high-velocity projectiles by absorbing their kinetic energy. The kinetic energy of high-velocity impact is usually dissipated by a combination of different mechanisms, such as the tension in primary yarns, deformation of fabric, frictional slips (yarn/yarn and projectile/yarn), yarn breakage, and yarn pull-out force [137, 138]. In particular, the ballistic performance of bulletproof fibers depends on various factor such as yarns properties [139, 140], friction between yarns [141–143], projectile shape [144–147], and fabric boundary conditions [148, 149]. In several studies, it was concluded that the higher impact energy absorption is directly related to the higher inter-yarn friction of the ballistic fabrics [150–153].

STF impregnation has been found to be a unique and commonly used method to increase the ballistic performance of the STF/fabric composites. Many studies have revealed that the STF can significantly increase the inter-yarn friction of high-performance fabrics in a situation of impact. The impact energy dissipation can be

increased when a ballistic fabric is impregnated with the STF owing to increased friction between primary and secondary yarns of the fabric. Numerous studies have reported that the incorporation of STF has increased the ballistic performance of the treated fabrics [6, 7, 154]. Park et al. investigated the effect of STF impregnation on the ballistic resistance of Kevlar fabric against a 9-mm bullet at a velocity of 436 m/s. They observed that the laminating sequence of STF-treated fabric influences the back face signature (BFS) of the multilayer panel. The enhanced ballistic performance of STF-treated fabric was increased by placing treated fabric at the backside of the laminate. The better performance of the STF-impregnated fabric was believed to be due to the elongation of the yarns during the impact [155]. However, Afeshejani et al. have found that the STF has a reasonable influence on the improvement of ballistic resistance of the STF-treated fabric [156]. Na et al. have prepared STF-impregnated fabric for the development of soft-armor jackets. They have concluded that the STF impregnation increases the shear rigidity and sensitivity of the STF/fabric. The improved resistance to ballistic and stab impact of the STF-impregnated fabric was attributed to the higher rate–sensitive shear stiffness of the laminate [157]. Haris et al. have studied the shock wave and ballistic resistance of STF-impregnated Twaron fabric composite. They have found that STF impregnation is an effective way to improve the ballistic resistance of the fabric composite [112]. Fahool et al. have used gas gun for high-velocity assessment of STF-impregnated Kevlar fabric by measuring the back face signature on the simulating clay. They obtained a 30% reduction in the BFS after treating the Kevlar fabric with silica-based STF [158]. Haro and co-workers added nano-sized and micron-sized fillers into a silica STF-dispersing medium and studied their effect on ballistic resistance. They have observed that neat fabric shows less resistance to the perforation as compared to the STF-impregnated fabric [159]. Gürgen et al. prepared a multiphase hybrid STF to impregnate the Kevlar fabric and analyzed their ballistic performance. It was found that STF treatment effectively reduces the BFS and effectively dissipates the impact energy due to the increased inter-yarn friction. Particularly, a higher concentration of carbide particles increased the capacity of the STF/fabric for energy absorption. They have also concluded that the fabric with multiphase STFs has shown better protection against ballistic impact [160].

Avila et al. evaluated the influence of a multiphase STF using silica and $CaCO_3$ on the ballistic performance of the STF to impregnate Kevlar fabric. The impact test was performed with two different projectiles, 9-mm full-metal jacket (FMJ) and 357 magnum-jacketed soft point (JSP). It was found that the trauma behind the composite was significantly reduced, which was mainly attributed to the inter-yarn friction. However, the more intense deformation of composite laminated leads to more numbers of fiber breakage. The STF/Kevlar composite of 19 layers has shown comparable ballistic performance when tested with STF/Kevlar composite with 32 fabric layers [162]. Wang et al. impregnated the Kevlar fabric with polyurethane (PU) and compared the ballistic resistance of the STF/Kevlar composite. It was observed that the PU/Kevlar panels at 10% loading of PU show comparable ballistic resistance with that of STF/Kevlar at 40% loading. The enhanced energy absorption of PU/Kevlar fabric has been attributed to the strength of adhesion lower than the breaking strength of the yarn, which leads to yarn pull-out and absorption of impact

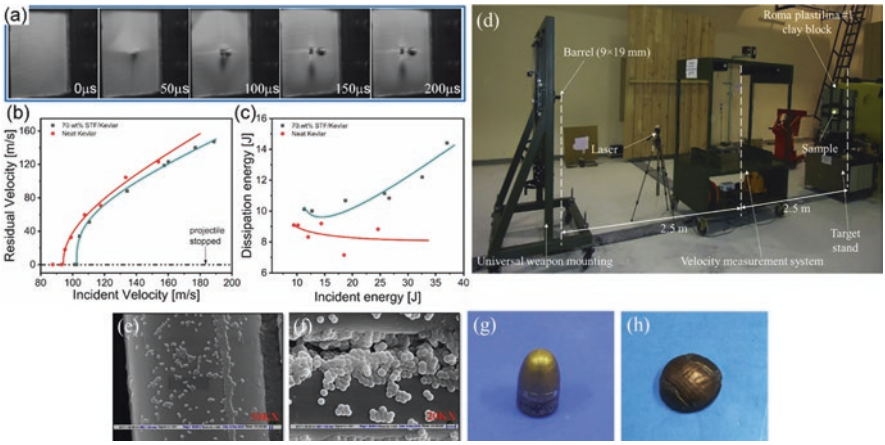

Fig. 5.9 (**a**) High-velocity impact of neat Kevlar at an incident velocity of 144 m/s captured by high-speed camera, (**b**) the results of residual velocity of STF/Kevlar and neat Kevlar after impact, (**c**) impact energy dissipation results of the STF-impregnated Kevlar and untreated Kevlar fabric during impact, (**d**) ballistic test set up, (**e**) and (**f**) scanning electron micrographs of STF-impregnated Kevlar fabric, (**g**) an undeformed 9-mm bullet before test, and (**h**) a deformed 9-mm bullet after the ballistic test [127, 161]

energy. However, when Kevlar fabric was coated with a higher mass content of PU, the mode of energy absorption changed to yarn breakage. Moreover, the STF/PU/Kevlar composite panels have shown excellent impact energy absorption owing to improved restriction in yarn mobility [163]. Zhang et al. have investigated the ballistic resistance of STF-impregnated single-layer Kevlar fabric at a very high concentration of silica (70 wt.%) (Fig. 5.9). In an event of impact, the yarns get deformed instantaneously and fail within 100 μs. As compared to the neat Kevlar, the STF/Kevlar has shown higher energy dissipation. This higher energy absorption of STF/Kevlar composite was related to the interfacial yarn sliding triggered at a higher velocity, where the rate of yarn sliding exceeds the critical shear rate of the STF, and as a result, shear thickening occurred that results in higher energy absorption [161]. Chang et al. developed polyurea-impregnated Kevlar fabric including a honeycomb spacer impregnated with silica-based STF. It was observed that the polyurea/Kevlar has shown an excellent ballistic performance than the neat Kevlar structure. Moreover, the addition of a 2-mm spacer layer of STF-impregnated honeycomb structure between the Kevlar layers has reduced a total of 10 layers with superior ballistic resistance [164].

5.7 Miscellaneous Applications of STF/Fabric Composites

In view of the unique property of the STF-impregnated high-performance composites, these composites can be employed in various applications such as sports products, medical use, and space technologies. Protective athletic gear including sleeves,

socks, and tapes was developed by Holt et al. using STF-impregnated fabric. Particles with a broad distribution of particle size were used for the preparation of STF/fabric composites. A sealing layer was attached to the surface of the substrate to contain STF. Athletic sleeves and socks were developed by dipping into STF suspension followed by drying at 80 °C for 60 min. In a bounce and recoil test, a 30% reduction in bounce was observed that serves the purpose of their use in wearer protection and injury prevention [165]. Shephard et al. have incorporated the STF preferably into Kevlar fabric and developed STF composite ribbon to cover the golf head. The shear-thickening effect might help in reducing the side spin of the golf ball when it is impacted with the golf head, thus reducing the slicing and hooking for the shot. Moreover, Shepherd and coworkers also suggested that STF can be used for the athlete shoe covers to enhance the performance in various games such as football and rugby. When an athlete takes a shot at the contact point of ball and shoe cover, the STF undergoes solid transition and becomes rigid under high stress condition. This allows the wearer to be able to transfer more energy from the kick to the ball, and this helps to depart the ball with higher velocity [166]. Hayes et al. have developed STF-impregnated garments for hip guards to prevent bone fracture in humans and animals. The STF/fabric composite can help in absorbing the impact force, thereby reducing the chance of damage to the soft tissues of the wearer [167]. Cwalina et al. have developed new extra-vehicular activity space suits for astronauts by incorporating STF/Kevlar composite fabric. This suit was designed to protect the astronauts from hyper-velocity micrometeoroid and orbital debris during space exploration [168]. Cwalina et al. have improved the cut and puncture resistance of thermal micrometeoroid garment by incorporating STF-impregnated Kevlar composite [169].

5.8 Conclusions

This chapter provides a comprehensive review of fabrication methods and impact properties of the STF-impregnated high-performance fabrics for soft-body armor application. After the latest developments in the field of STF-impregnated fabrics in the early years of 2000s, many researchers have started working on the development of high-performance fabrics for improved ballistic performance. In this chapter, the theoretical background behind the shear-thickening behavior, and the mechanism has been briefly discussed. Further to this, the constituting elements required for the preparation of STF have been discussed in detail. Silica particles in combination with polyethylene glycol have been utilized for the preparation of STF in many cases. Apart from this, hybrid STF suspensions have been reported, where SiC, Al_2O_3, CNT, GO, $CaCO_3$, cellulose beads, and ceria have been considered as an additive to improve the shear-thickening properties. These findings suggest that there is a need to look into the use of new materials for the development of high-performance impact-resistant materials in the near future.

An extensive review of the quasistatic stab and ballistic performance of the STF-impregnated high-performance composites has been presented. The fabrics treated with STFs have shown superior stab and ballistic impact as compared to untreated fabrics without compromising their flexibility. Moreover, the enhanced ballistic performance was attributed to the yarn friction due to the shear-thickening effect at higher shear force. Although a significant amount of work has been done so far in which the use of STF has been suggested to develop high performance and adaptable body armors for protection against several threats, there is still a need to develop a better understanding of the energy absorption mechanism of STF-impregnated fabric composites.

References

1. Barnes HA (1989) Shear-thickening ("dilatancy") in suspensions of nonaggregating solid particles dispersed in Newtonian liquids. J Rheol (N Y N Y) [Internet] 33(2):329–366. Available from: http://sor.scitation.org/doi/10.1122/1.550017
2. Maranzano BJ, Wagner NJ (2001) The effects of particle size on reversible shear thickening of concentrated colloidal dispersions. J Chem Phys 114(23):10514
3. Lee Y, Wagner N (2003) Dynamic properties of shear thickening colloidal suspensions. Rheol Acta [Internet] 42:199–208. Available from: http://www.springerlink.com/index/eq1j4096934j7v17.pdf
4. Wagner NJ, Brady JF (2009) Shear thickening in colloidal dispersions. Phys Today 62(10):27–32
5. Lee BW, Kim IJ, Kim CG (2009) The influence of the particle size of silica on the ballistic performance of fabrics impregnated with silica colloidal suspension. J Compos Mater 43(23):2679–2698
6. Wetzel ED (2004) The effect of rheological parameters on the ballistic properties of shear thickening fluid (STF)-Kevlar composites. AIP Conf Proc [Internet] 712(May 2013):288–293. Available from: http://link.aip.org/link/?APC/712/288/1&Agg=doi
7. Tan VBC, Tay TE, Teo WK (2005) Strengthening fabric armour with silica colloidal suspensions. Int J Solids Struct 42(5–6):1561–1576
8. Sahoo SK, Mishra S, Islam E, Nebhani L (2020) Tuning shear thickening behavior via synthesis of organically modified silica to improve impact resistance of Kevlar fabric. Mater Today Commun [Internet]. 23(August 2019):100892. Available from: https://doi.org/10.1016/j.mtcomm.2020.100892
9. Liu H, Zhu H, Fu K, Sun G, Chen Y, Yang B, et al (2022) High-impact resistant hybrid sandwich panel filled with shear thickening fluid. Compos Struct [Internet] 284(November 2021):115208. Available from: https://doi.org/10.1016/j.compstruct.2022.115208
10. Kalman DP, Merrill RL, Wagner NJ, Wetzel ED (2009) Effect of particle hardness on the penetration behavior of fabrics intercalated with dry particles and concentrated particle-fluid suspensions. ACS Appl Mater Interfaces 1(11):2602–2612
11. Hassan TA, Rangari VK, Jeelani S (2010) Synthesis, processing and characterization of shear thickening fluid (STF) impregnated fabric composites. Mater Sci Eng A [Internet]. 527(12):2892–2899. Available from: https://doi.org/10.1016/j.msea.2010.01.018
12. Gong X, Xu Y, Zhu W, Xuan S, Jiang W, Jiang W (2014) Study of the knife stab and puncture-resistant performance for shear thickening fluid enhanced fabric. J Compos Mater 48(6):641–657

13. Li W, Xiong D, Zhao X, Sun L, Liu J (2016) Dynamic stab resistance of ultra-high molecular weight polyethylene fabric impregnated with shear thickening fluid. Mater Des [Internet]. 102:162–167. Available from: https://doi.org/10.1016/j.matdes.2016.04.006
14. Majumdar A, Laha A, Bhattacharjee D, Biswas I (2017) Tuning the structure of 3D woven aramid fabrics reinforced with shear thickening fluid for developing soft body armour. Compos Struct [Internet] 178:415–425. Available from: https://doi.org/10.1016/j.compstruct.2017.07.018
15. Gürgen S, Kuşhan MC (2017) The stab resistance of fabrics impregnated with shear thickening fluids including various particle size of additives. Compos Part A Appl Sci Manuf 94:50–60
16. Haris A, Lee HP, Tan VBC (2018) An experimental study on shock wave mitigation capability of polyurea and shear thickening fluid based suspension pads. Def Technol [Internet]. 14(1):12–18. Available from: https://doi.org/10.1016/j.dt.2017.08.004
17. Zhang X, Li TT, Peng HK, Wang Z, Huo J, Lou CW et al (2020) Effects of bi-particle-sized shear thickening fluid on rheological behaviors and stab resistance of Kevlar fabrics. J Ind Text 51:3014S–3029S
18. Hoffman RL (1974) Discontinuous and dilatant viscosity behavior in concentrated suspensions. II. Theory and experimental tests. J Colloid Interface Sci 46(3):491–506
19. Bossis G, Brady JF (1989) The rheology of Brownian suspensions. J Chem Phys [Internet] 91(3):1866. Available from: http://link.aip.org/link/JCPSA6/v91/i3/p1866/s1&Agg=doi
20. Phung TN, Brady JF, Bossis G (1996) Stokesian dynamics simulation of Brownian suspensions. J Fluid Mech [Internet] 313:181–207. Available from: http://journals.cambridge.org/article_S0022112096002170%5Cn http://journals.cambridge.org/action/displayAbstract?fromPage=online&aid=378786
21. Foss DR, Brady JF (2000) Brownian dynamics simulation of hard-sphere colloidal dispersions. J Rheol (N Y N Y) 44(3):629–651
22. Melrose JR, Ball RC (2004) Continuous shear thickening transitions in model concentrated colloids—the role of interparticle forces. J Rheol (N Y N Y) [Internet] 48(5):937–960. Available from: http://sor.scitation.org/doi/10.1122/1.1784783
23. Kalman DP, Wagner NJ (2009) Microstructure of shear-thickening concentrated suspensions determined by flow-USANS. Rheol Acta 48(8):897–908
24. Crawford NC, Williams SKR, Boldridge D, Liberatore MW (2013) Shear-induced structures and thickening in fumed silica slurries. Langmuir 29(42):12915–12923
25. Gurnon AK, Wagner NJ (2015) Microstructure and rheology relationships for shear thickening colloidal dispersions. J Fluid Mech 769:242–276
26. Taylor SE (2013) Rheology and structure of cornstarch suspensions in water-poly(propylene glycol) mixtures. J Dispers Sci Technol 34(7):887–897
27. Ionescu CM, Birs IR, Copot D, Muresan CI, Caponetto R (2020) Mathematical modelling with experimental validation of viscoelastic properties in non-Newtonian fluids. Philos Trans R Soc A Math Phys Eng Sci 378(2172):20190284
28. Chang L, Friedrich K, Schlarb AK, Tanner R, Ye L (2011) Shear-thickening behaviour of concentrated polymer dispersions under steady and oscillatory shear. J Mater Sci 46(2):339–346
29. Seto R, Mari R, Morris JF, Denn MM (2013) Discontinuous shear thickening of frictional hard-sphere suspensions. Phys Rev Lett 111(21):1–5
30. Mari R, Seto R, Morris JF, Denn MM (2014) Shear thickening, frictionless and frictional rheologies in non-Brownian suspensions. J Rheol (N Y N Y) [Internet] 58(6):1693–1724. Available from: https://doi.org/10.1122/1.4890747
31. Mari R, Seto R, Morris JF, Denn MM (2015) Discontinuous shear thickening in Brownian suspensions by dynamic simulation. Proc Natl Acad Sci U S A 112(50):15326–15330
32. Lin NYC, Guy BM, Hermes M, Ness C, Sun J, Poon WCK et al (2015) Hydrodynamic and contact contributions to continuous shear thickening in colloidal suspensions. Phys Rev Lett 115(22):1–5

33. Peters IR, Majumdar S, Jaeger HM (2016) Direct observation of dynamic shear jamming in dense suspensions. Nature 532(7598):214–217
34. Fernandez N, Mani R, Rinaldi D, Kadau D, Mosquet M, Lombois-Burger H, et al (2013) Microscopic mechanism for shear thickening of non-Brownian suspensions. Phys Rev Lett [Internet]. 2013 Sep 3 [cited 2019 Aug 10];111(10):108301. Available from: https://link.aps.org/doi/10.1103/PhysRevLett.111.108301
35. Heussinger C (2013) Shear thickening in granular suspensions: Interparticle friction and dynamically correlated clusters. Phys Rev E – Stat Nonlinear, Soft Matter Phys 88(5):22–24
36. Boromand A, Jamali S, Grove B, Maia JM (2018) A generalized frictional and hydrodynamic model of the dynamics and structure of dense colloidal suspensions. J Rheol (N Y N Y). 62(4):905–918
37. Park N, Rathee V, Blair DL, Conrad JC (2019) Contact networks enhance shear thickening in attractive colloid-polymer mixtures. Phys Rev Lett [Internet] 122(22):228003. Available from: https://doi.org/10.1103/PhysRevLett.122.228003
38. Sedes O, Singh A, Morris JF (2020) Fluctuations at the onset of discontinuous shear thickening in a suspension. J Rheol (N Y N Y) 64(2):309–319
39. Singh A, Ness C, Seto R, De Pablo JJ, Jaeger HM (2020) Shear thickening and jamming of dense suspensions: the "roll" of friction. Phys Rev Lett [Internet]. 124(24):248005. Available from: https://doi.org/10.1103/PhysRevLett.124.248005
40. Boersma WH, Laven J, Stein HN (1990) Shear thickening(dilatancy) in concentrated dispersions. AIChE J [Internet]. 1990 Mar [cited 2016 Aug 4];36(3):321–32. Available from: http://doi.wiley.com/10.1002/aic.690360302
41. Raghavan S, Khan S (1997) Shear-thickening response of fumed silica suspensions under steady and oscillatory shear. J Colloid Interface Sci [Internet] 185(1):57–67. Available from: http://www.ncbi.nlm.nih.gov/pubmed/9056301
42. Yang H-G, Li C-Z, Gu H-C, Fang T-N (2001) Rheological behavior of titanium dioxide suspensions. J Colloid Interface Sci [Internet]. 2001 [cited 2016 Aug 3];236:96–103. Available from: http://www.idealibrary.com
43. Maranzano BJ, Wagner NJ (2001) The effects of interparticle interactions and particle size on reversible shear thickening: Hard-sphere colloidal dispersions. J Rheol 45:1205
44. White EEB, Chellamuthu M, Rothstein JP (2010) Extensional rheology of a shear-thickening cornstarch and water suspension. Rheol Acta 49(2):119–129
45. Lim AS, Lopatnikov SL, Wagner NJ, Gillespie JW (2010) An experimental investigation into the kinematics of a concentrated hard-sphere colloidal suspension during Hopkinson bar evaluation at high stresses. J Nonnewton Fluid Mech [Internet]. 165(19–20):1342–1350. Available from: https://doi.org/10.1016/j.jnnfm.2010.06.015
46. Liu X-Q, Bao R-Y, Wu X-J, Yang W, Xie B-H, Yang M-B (2015) Temperature induced gelation transition of a fumed silica/PEG shear thickening fluid. RSC Adv 5(24):18367–18374
47. Gürgen S, Sofuoğlu MA (2020) Vibration attenuation of sandwich structures filled with shear thickening fluids. Compos Part B Eng 186(October 2019):107831
48. Chen Y, Xu W, Zeng G, Liu W (2015) Shear-thickening behavior of precipitated calcium carbonate particles suspensions in glycerine. Appl Rheol 25(1):1–8
49. Yang W, Wu Y, Pei X, Zhou F, Xue Q (2017) Contribution of surface chemistry to the shear thickening of silica nanoparticle suspensions. Langmuir 33(4):1037–1042
50. Gürgen S, Sofuoğlu MA (2020) Integration of shear thickening fluid into cutting tools for improved turning operations. J Manuf Process 56(May):1146–1154
51. Chen Q, Zhu W, Ye F, Gong X, Jiang W, Xuan S (2014) PH effects on shear thickening behaviors of polystyrene-ethylacrylate colloidal dispersions. Mater Res Express 1(1):015303
52. Comtet J, Chatté G, Niguès A, Bocquet L, Siria A, Colin A (2017) Pairwise frictional profile between particles determines discontinuous shear thickening transition in non-colloidal suspensions. Nat Commun 8(May):1–7

53. Hasanzadeh M, Mottaghitalab V (2016) Tuning of the rheological properties of concentrated silica suspensions using carbon nanotubes. Rheol Acta [Internet]. 55(9):759–766. Available from: https://doi.org/10.1007/s00397-016-0950-7
54. Gürgen S, Li W, Kuşhan MC (2016) The rheology of shear thickening fluids with various ceramic particle additives. Mater Des 104:312–319
55. Islam E, Kaur G, Bhattacharjee D, Singh S, Biswas I, Verma SK (2018) Effect of cellulose beads on shear-thickening behavior in concentrated polymer dispersions. Colloid Polym Sci 296(5):883–893
56. Wei M, Sun L, Zhang C, Qi P, Zhu J (2019) Shear-thickening performance of suspensions of mixed ceria and silica nanoparticles. J Mater Sci [Internet] 54(1):346–355. Available from: https://doi.org/10.1007/s10853-018-2873-4
57. Liu L, Cai M, Liu X, Zhao Z, Chen W (2020) Ballistic impact performance of multi-phase STF-impregnated Kevlar fabrics in aero-engine containment. Thin-Walled Struct [Internet] 157(29):107103. Available from: https://doi.org/10.1016/j.tws.2020.107103
58. Eastwood AR, Barnes HA (1975) The superposition of oscillatory on steady shear for non-Newtonian suspensions. Rheol Acta 14(9):795–800
59. Frith WJ, Lips A (1995) The rheology of concentrated suspensions of deformable particles. Adv Colloid Interf Sci 61(C):161–189
60. Galindo-Rosales FJ, Rubio-Hernández FJ, Velázquez-Navarro JF (2009) Shear-thickening behavior of Aerosil® R816 nanoparticles suspensions in polar organic liquids. Rheol Acta 48(6):699–708
61. Jiang W, Sun Y, Xu Y, Peng C, Gong X, Zhang Z (2010) Shear-thickening behavior of polymethylmethacrylate particles suspensions in glycerine – water mixtures. Rheol. Acta 49:1157–1163
62. Son HS, Kim KH, Kim JH, Yoon KH, Lee YS, Jong PH (2018) High-performance shear thickening of polystyrene particles with poly(HEMA). Colloid Polym Sci 296(9):1591–1598
63. Cao S, Pang H, Zhao C, Xuan S, Gong X (2020) The CNT/PSt-EA/Kevlar composite with excellent ballistic performance. Compos Part B Eng [Internet]. 185(January):107793. Available from: https://doi.org/10.1016/j.compositesb.2020.107793
64. Hassan TA, Rangari VK, Jeelani S (2010) Sonochemical synthesis and rheological properties of shear thickening silica dispersions. Ultrason Sonochem [Internet] 17(5):947–52. Available from: https://doi.org/10.1016/j.ultsonch.2010.02.001
65. Laha A, Majumdar A (2016) Interactive effects of p-aramid fabric structure and shear thickening fluid on impact resistance performance of soft armor materials. Mater Des [Internet] 89:286–93. Available from. https://doi.org/10.1016/j.matdes.2015.09.077
66. Zhang XZ, Li WH, Gong XL (2008) The rheology of shear thickening fluid (STF) and the dynamic performance of an STF-filled damper. Smart Mater Struct 17(3):035027
67. Fischer C, Bennani A, Michaud V, Jacquelin E, Månson JAE (2010) Structural damping of model sandwich structures using tailored shear thickening fluid compositions. Smart Mater Struct 19(3):035017
68. Sun LL, Xiong DS, Xu CY (2013) Application of shear thickening fluid in ultra high molecular weight polyethylene fabric. J Appl Polym Sci 129(4):1922–1928
69. Tryznowski M, Gołofit T, Gürgen S, Kręcisz P, Chmielewski M (2022) Unexpected method of high-viscosity shear thickening fluids based on polypropylene glycols development via thermal treatment. Materials (Basel) 15(17):5818
70. Güler ES (2018) Rheological behaviours of silica/water, silica/PEG systems and mechanical properties of shear thickening fluid impregnated Kevlar composites. Bull Mater Sci 41(4):112
71. Katiyar A, Nandi T, Katiyar P (2021) Energy absorption of graphene and CNT infused hybrid shear thickening fluid embedded textile fabrics. J Polym Res [Internet] 28(9):1–13. Available from: https://doi.org/10.1007/s10965-021-02697-6
72. Huang C-H, Chien C-H, Shiu B-C, Chen Y-S, Lin J-H, Lou C-W (2022) Reinforcement effects of shear thickening Fluid over mechanical properties of nonwoven fabrics. Polymers (Basel) 14(22):4816

73. Chatterjee VA, Dey P, Verma SK, Bhattacharjee D, Biswas I, Neogi S (2019) Probing the intensity of dilatancy of high performance shear-thickening fluids comprising silica in polyethylene glycol. Mater Res Express 6(7): 075702
74. Gürgen S, Sert A (2019) Polishing operation of a steel bar in a shear thickening fluid medium. Compos Part B Eng [Internet] 175(June):107127. Available from: https://doi.org/10.1016/j.compositesb.2019.107127
75. Grover G, Verma SK, Thakur A, Biswas I, Bhatacharjee D (2020) The effect of particle size and concentration on the ballistic resistance of different shear thickening fluids. Mater Today Proc [Internet] 28:1472–6. Available from: https://doi.org/10.1016/j.matpr.2020.04.823
76. Sharma S, Kumar Walia Y, Grover G, Sanjeev VK (2022) Effect of surface modification of silica nanoparticles with thiol group on the shear thickening behaviors of the suspensions of silica nanoparticles in polyethylene glycol (PEG). IOP Conf Ser Mater Sci Eng 1225(1):012053
77. Otsubo Y, Fujiwara M, Kouno M, Edamura K (2007) Shear-thickening flow of suspensions of carbon nanofibers in aqueous PVA solutions. Rheol Acta 46(7):905–912
78. Yang B, Wang S, Xu G, Xin F (2012) Preparation of SiO 2/PEG shear thickening system by centrifugal dispersion. Adv Mater Res 560–561:586–590
79. Xu Y, Gong X, Peng C, Sun Y, Jiang W, Zhang Z (2010) Shear thickening fluids based on additives with different concentrations and molecular chain lengths. Chinese J Chem Phys 23(3):342–346
80. Yu K, Cao H, Qian K, Sha X, Chen Y (2012) Shear-thickening behavior of modified silica nanoparticles in polyethylene glycol. J Nanoparticle Res 14(3):747
81. Zheng S-B, Xuan S-H, Jiang W-Q, Gong X-L (2015) High performance shear thickening fluid based on calcinated colloidal silica microspheres. Smart Mater Struct [Internet]. 2015 Aug 1 [cited 2017 May 29];24(8):085033. Available from: http://stacks.iop.org/0964-1726/24/i=8/a=085033?key=crossref.7cdafc27407ce3ed5c78cc0006f00c99
82. Ge J, Tan Z, Li W, Zhang H (2017) The rheological properties of shear thickening fluid reinforced with SiC nanowires. Results Phys [Internet] 7:3369–3372. Available from: https://doi.org/10.1016/j.rinp.2017.08.065
83. Pirvu C, Deleanu L, Lazaroaie C (2016) Ballistic tests on packs made of stratified aramid fabrics LFT SB1. IOP Conf Ser Mater Sci Eng 147(1):012099
84. De Oliveira BF, Lima ÉP, De Sousa LE, Monteiro SN (2017) The effect of thickness on aramid fabric laminates subjected to 7.62 MM ammunition ballistic impact. Mater Res 20:676–680
85. Ohta Y, Kajiwara K (2009) High performance fibers: structure, characteristics and identification. In: Identif text fibers, pp 88–110
86. Bilisik K, Korkmaz M (2010) Multilayered and multidirectionally-stitched aramid woven fabric structures: experimental characterization of ballistic performance by considering the yarn pull-out test. Text Res J 80(16):1697–1720
87. Dwivedi AK, Dalzell MW, Fossey SA, Slusarski KA, Long LR, Wetzel ED (2016) Low velocity ballistic behavior of continuous filament knit aramid. Int J Impact Eng [Internet] 96:23–34. Available from: https://doi.org/10.1016/j.ijimpeng.2016.05.009
88. Nilakantan G, Horner S, Halls V, Zheng J (2018) Virtual ballistic impact testing of Kevlar soft armor: predictive and validated finite element modeling of the V0-V100 probabilistic penetration response. Def Technol [Internet] 14(3):213–25. Available from: https://doi.org/10.1016/j.dt.2018.03.001
89. Stopforth R, Adali S (2019) Experimental study of bullet-proofing capabilities of Kevlar, of different weights and number of layers, with 9 mm projectiles. Def Technol [Internet] 15(2):186–92. Available from: https://doi.org/10.1016/j.dt.2018.08.006
90. Mao N (2014) High performance textiles for protective clothing [Internet]. High Performance Textiles and Their Applications. Woodhead Publishing Limited. 91–143 p. Available from: https://doi.org/10.1533/9780857099075.91
91. Afshari M, Sikkema DJ, Lee K, Bogle M (2008) High performance fibers based on rigid and flexible polymers. Polym Rev 48(2):230–274

92. Barhoumi H, Bhouri N, Feki I, Baffoun A, Hamdaoui M, Ben Abdessalem S (2022) Review of ballistic protection materials: properties and performances. J Reinf Plast Compos 073168442211379
93. Information T. Toyobo Co., Ltd. 2005
94. Golovin K, Phoenix SL (2016) Effects of extreme transverse deformation on the strength of UHMWPE single filaments for ballistic applications. J Mater Sci 51(17):8075–8086
95. Van Der Werff H, Heisserer U (2016) High-performance ballistic fibers: Ultra-high molecular weight polyethylene (UHMWPE) [Internet]. Advanced Fibrous Composite Materials for Ballistic Protection. Elsevier Ltd; 71–107 p. Available from: https://doi.org/10.1016/B978-1-78242-461-1.00003-0
96. Zhang H, Zhao S, Xin Z, Ye C, Li Z, Xia J (2019) Wear resistance mechanism of ultrahigh-molecular-weight polyethylene determined from its structure-property relationships. Ind Eng Chem Res 58(42):19519–19530
97. Gürgen S (2019) Wear performance of UHMWPE based composites including nano-sized fumed silica. Compos Part B Eng [Internet] 173(May):106967. Available from: https://doi.org/10.1016/j.compositesb.2019.106967
98. Tian L, Shi J, Chen H, Huang X, Cao H (2022) Cut-resistant performance of Kevlar and UHMWPE covered yarn fabrics with different structures. J Text Inst [Internet] 113(7):1457–63. Available from: https://doi.org/10.1080/00405000.2021.1933327
99. Li CS, Huang XC, Li Y, Yang N, Shen Z, Fan XH (2014) Stab resistance of UHMWPE fiber composites impregnated with thermoplastics. Polym Adv Technol 25(9):1014–1019
100. Deitzel JM, McDaniel P, Gillespie JW (2017) High performance polyethylene fibers. Struct Prop High-Performance Fibers. (October):167–85
101. Cunniff PM, Committee TIB (1999) The performance of poly(para-phenylene benzobizoxazole) (Pbo) fabric for fragmentation protective body armor. 18th Int Symp Ballist. 2(January 1999):837–44
102. Jeffrey W, Chin J, Byrd E, Clerici C, Oudina M, Sung L, et al. NISTIR 7373 chemical and physical characterization of poly(p-phenylene-2,6-benzobisoxazole) fibers used in body armor: temperature and humidity aging. 2006.; Available from: https://ws680.nist.gov/publication/get_pdf.cfm?pub_id=860679
103. Rimdusit S, Pathomsap S, Kasemsiri P, Jubsilp C, Tiptipakorn S (2011) Kevlar TM fiber-reinforced polybenzoxazine alloys for ballistic impact applications. Eng J 15(4):23–39
104. Bandaru AK, Chavan VV, Ahmad S, Alagirusamy R, Bhatnagar N (2016) Ballistic impact response of Kevlar® reinforced thermoplastic composite armors. Int J Impact Eng [Internet] 89:1–13. Available from: https://doi.org/10.1016/j.ijimpeng.2015.10.014
105. Pekbey Y, Aslantaş K, Yumak N (2017) Ballistic impact response of Kevlar composites with filled epoxy matrix. Steel Compos Struct 24(2):191–200
106. Wu KK, Chen YL, Yeh JN, Chen WL, Lin CS (2020) Ballistic impact performance of SiC ceramic-Dyneema fiber composite materials. Adv Mater Sci Eng 2020
107. Demircioglu TK, Balikoglu F, Beyaz S, Bülbül B (2021) Effect of lead metaborate as novel nanofiller on the ballistic impact behavior of Twaron® /epoxy composites. Compos Commun [Internet] 27(March):100832. Available from: https://doi.org/10.1016/j.coco.2021.100832
108. Fan X, Zhu L, Fu X, Chen Y, Huang Z, Zhao C (2022) Pipeline processing via the combination of heat and corona treatments for improving the poly(p-phenylene benzobisoxazole) fiber surface and anti-aging performances. ACS Omega
109. Reddy PRS, Reddy TS, Mogulanna K, Srikanth I, Madhu V, Rao KV (2017) Ballistic impact studies on carbon and E-glass fibre based hybrid composite laminates. Procedia Eng 173:293–298
110. Jr RGE, Decker MJ, Halbach CJ, Lee YS, Kirkwood JE, Kirkwood KM, et al. Stab resistance of shear thickening Fluid (Stf)– Kevlar composites for body armor applications. 2003
111. Park Y, Kim Y, Baluch AH, Kim C-G (2014) Empirical study of the high velocity impact energy absorption characteristics of shear thickening fluid (STF) impregnated Kevlar fabric. Int J Impact Eng [Internet] 72:67–74. Available from: http://linkinghub.elsevier.com/

retrieve/pii/S0734743X14001146%5Cn http://www.sciencedirect.com/science/article/pii/S0734743X14001146
112. Haris A, Lee HP, Tay TE, Tan VBC (2015) Shear thickening fluid impregnated ballistic fabric composites for shock wave mitigation. Int J Impact Eng [Internet] 80:143–51. Available from: https://doi.org/10.1016/j.ijimpeng.2015.02.008
113. Wang FF, Zhang Y, Zhang H, Xu L, Wang P, Guo C (2018) Bin. The influence of graphene nanoplatelets (GNPs) on the semi-blunt puncture behavior of woven fabrics impregnated with shear thickening fluid (STF). RSC Adv 8(10):5268–5279
114. Kang TJ, Hong KH, Yoo MR (2010) Preparation and properties of fumed silica/Kevlar composite fabrics for application of stab resistant material. Fibers Polym 11(5):719–724
115. Kordani N, Vanini AS (2014) Optimizing the ethanol content of shear thickening fluid/fabric composites under impact loading. J Mech Sci Technol 28(2):663–667
116. Xu Y, Chen X, Wang Y, Yuan Z (2017) Stabbing resistance of body armour panels impregnated with shear thickening fluid. Compos Struct [Internet] 163:465–73. Available from: https://doi.org/10.1016/j.compstruct.2016.12.056
117. Kim YH, Park Y, Cha JH, Ankem VA, Kim CG (2018) Behavior of shear thickening fluid (STF) impregnated fabric composite rear wall under hypervelocity impact. Compos Struct [Internet] 204(June):52–62. Available from: https://doi.org/10.1016/j.compstruct.2018.07.064
118. Khodadadi A, Liaghat G, Vahid S, Sabet AR, Hadavinia H (2019) Ballistic performance of Kevlar fabric impregnated with nanosilica/PEG shear thickening fluid. Compos Part B 162(March 2018):643–652
119. Liu L, Yang Z, Zhao Z, Liu X, Chen W (2020) The influences of rheological property on the impact performance of Kevlar fabrics impregnated with SiO2/PEG shear thickening fluid. Thin-Walled Struct [Internet] 151(29):106717. Available from: https://doi.org/10.1016/j.tws.2020.106717
120. Majumdar A, Butola BS, Srivastava A (2013) Optimal designing of soft body armour materials using shear thickening fluid. Mater Des [Internet] 46:191–8. Available from: https://doi.org/10.1016/j.matdes.2012.10.018
121. Srivastava A, Majumdar A, Butola BS (2011) Improving the impact resistance performance of Kevlar fabrics using silica based shear thickening fluid. Mater Sci Eng A [Internet] 529(1):224–9. Available from: https://doi.org/10.1016/j.msea.2011.09.021
122. Feng X, Li S, Wang Y, Wang Y, Liu J (2014) Effects of different silica particles on quasi-static stab resistant properties of fabrics impregnated with shear thickening fluids. Mater Des [Internet] 64:456–61. Available from: https://doi.org/10.1016/j.matdes.2014.06.060
123. Alikarami S, Kordani N, Sadough Vanini A, Amiri H (2016) Effect of the yarn pull-out velocity of shear thickening fluid-impregnated Kevlar fabric on the coefficient of friction. J Mech Sci Technol 30(8):3559–3565
124. Bai R, Ma Y, Lei Z, Feng Y, Liu C (2019) Energy analysis of fabric impregnated by shear thickening fluid in yarn pullout test. Compos Part B Eng 174(June)
125. He Q, Cao S, Wang Y, Xuan S, Wang P, Gong X (2018) Impact resistance of shear thickening fluid/Kevlar composite treated with shear-stiffening gel. Compos Part A Appl Sci Manuf [Internet] 106:82–90. Available from: https://doi.org/10.1016/j.compositesa.2017.12.019
126. Wang Q, Sun R, Yao M, Chen M, Feng Y (2019) The influence of temperature on inter-yarns fictional properties of shear thickening fluids treated Kevlar fabrics. Compos Part A Appl Sci Manuf 116(October 2018):46–53
127. Bajya M, Majumdar A, Butola BS, Verma SK, Bhattacharjee D (2020) Design strategy for optimising weight and ballistic performance of soft body armour reinforced with shear thickening fluid. Compos Part B Eng [Internet] 183(August 2019):107721. Available from: https://doi.org/10.1016/j.compositesb.2019.107721
128. Qin J, Guo B, Zhang L, Wang T, Zhang G, Shi X (2020) Soft armor materials constructed with Kevlar fabric and a novel shear thickening fluid. Compos Part B Eng [Internet] 183(November 2019):107686. Available from: https://doi.org/10.1016/j.compositesb.2019.107686

129. Decker MJ, Halbach CJ, Nam CH, Wagner NJ, Wetzel ED (2007) Stab resistance of shear thickening fluid (STF)-treated fabrics. Compos Sci Technol 67(3–4):565–578
130. Mahfuz H, Clements F, Rangari V, Dhanak V, Beamson G (2009) Enhanced stab resistance of armor composites with functionalized silica nanoparticles. J Appl Phys 105(6):064307
131. Majumdar A, Butola BS, Srivastava A (2013) An analysis of deformation and energy absorption modes of shear thickening fluid treated Kevlar fabrics as soft body armour materials. Mater Des [Internet] 51:148–53. Available from: https://doi.org/10.1016/j.matdes.2013.04.016
132. Office J (2012) Stab resistance of personal body armor: NIJ standard-0115.00. Body Armor Ballist Stab Resist Stand with a Guid to Sel 63–100
133. Laha A, Majumdar A (2016) Shear thickening fluids using silica-halloysite nanotubes to improve the impact resistance of p-aramid fabrics. Appl Clay Sci [Internet] 132–133:468–74. Available from: https://doi.org/10.1016/j.clay.2016.07.017
134. Hasanzadeh M, Mottaghitalab V, Babaei H, Rezaei M (2016) The influence of carbon nanotubes on quasi-static puncture resistance and yarn pull-out behavior of shear-thickening fluids (STFs) impregnated woven fabrics. Compos Part A Appl Sci Manuf [Internet] 88:263–71. Available from: https://doi.org/10.1016/j.compositesa.2016.06.006
135. Santos TF, Santos CM, Fonseca RT, Melo KM, Aquino MS, Oliveira FR et al (2020) Experimental analysis of the impact protection properties for Kevlar® fabrics under different orientation layers and non-Newtonian fluid compositions. J Compos Mater 54(24):3515–3526
136. Gürgen S, Yıldız T (2020) Stab resistance of smart polymer coated textiles reinforced with particle additives. Compos Struct 235(October 2019)
137. Briscoe BJ, Motamedi F (1992) The ballistic impact characteristics of aramid fabrics: the influence of interface friction. Wear 158(1–2):229–247
138. Carr DJ (1999) Failure mechanisms of yarns subjected to ballistic impact. J Mater Sci Lett 18(7):585–588
139. Rao MP, Duan Y, Keefe M, Powers BM, Bogetti TA (2009) Modeling the effects of yarn material properties and friction on the ballistic impact of a plain-weave fabric. Compos Struct [internet] 89(4):556–66. Available from: https://doi.org/10.1016/j.compstruct.2008.11.012
140. Chu TL, Ha-Minh C, Imad A (2016) A numerical investigation of the influence of yarn mechanical and physical properties on the ballistic impact behavior of a Kevlar KM2® woven fabric. Compos part B Eng [internet] 95:144–54. Available from: https://doi.org/10.1016/j.compositesb.2016.03.018
141. Wang Y, Rong Z, Wang Y, Qu J (2016) Ruthenium nanoparticles loaded on functionalized graphene for liquid-phase hydrogenation of fine chemicals: comparison with carbon nanotube. J Catal [internet] 333:8–16. Available from: https://doi.org/10.1016/j.jcat.2015.10.021
142. Chu Y, Min S, Chen X (2017) Numerical study of inter-yarn friction on the failure of fabrics upon ballistic impacts. Mater Des [Internet] 115:299–316. Available from: https://doi.org/10.1016/j.matdes.2016.11.013
143. Ingle S, Yerramalli CS, Guha A, Mishra S (2021) Effect of material properties on ballistic energy absorption of woven fabrics subjected to different levels of inter-yarn friction. Compos Struct [Internet] 266(March):113824. Available from: https://doi.org/10.1016/j.compstruct.2021.113824
144. Ulven C, Vaidya UK, Hosur MV (2003) Effect of projectile shape during ballistic perforation of VARTM carbon/epoxy composite panels. Compos Struct 61(1–2):143–150
145. Gupta NK, Iqbal MA, Sekhon GS (2007) Effect of projectile nose shape, impact velocity and target thickness on deformation behavior of aluminum plates. Int J Solids Struct 44(10):3411–3439
146. Sasikumar M, Sundareswaran V (2011) Influence of projectile nose shape on ballistic limit and damage to glass/vinyl ester composite plates. Adv Compos Lett 20(5):126–133
147. Salhan P, Rashid FM (2022) Effect of shape and obliquity of projectiles on the ballistic response of sandwich structures with carbon/epoxy face sheet subjected to low-velocity impact. Mater Today Proc 62(P12):6780–6787

148. Zeng XS, Shim VPW, Tan VBC (2005) Influence of boundary conditions on the ballistic performance of high-strength fabric targets. Int J Impact Eng 32(1–4):631–642
149. Nilakantan G, Gillespie JW (2012) Ballistic impact modeling of woven fabrics considering yarn strength, friction, projectile impact location, and fabric boundary condition effects. Compos Struct [Internet] 94(12):3624–34. Available from. https://doi.org/10.1016/j.compstruct.2012.05.030
150. Duan Y, Keefe M, Bogetti TA, Cheeseman BA (2005) Modeling friction effects on the ballistic impact behavior of a single-ply high-strength fabric. Int J Impact Eng. 31(8):996–1012
151. Zhou Y, Chen X, Wells G (2014) Influence of yarn gripping on the ballistic performance of woven fabrics from ultra-high molecular weight polyethylene fibre. Compos Part B Eng [Internet] 62:198–204. Available from: https://doi.org/10.1016/j.compositesb.2014.02.022
152. Talreja K, Chauhan I, Ghosh A, Majumdar A, Butola BS (2017) Functionalization of silica particles to tune the impact resistance of shear thickening fluid treated aramid fabrics. RSC Adv 7(78):49787–49794
153. Arora S, Majumdar A, Butola BS (2019) Structure induced effectiveness of shear thickening fluid for modulating impact resistance of UHMWPE fabrics. Compos Struct [Internet] 210(October 2018):41–8. Available from: https://doi.org/10.1016/j.compstruct.2018.11.028
154. Lee YS, Wetzel ED, Wagner NJ (2003) The ballistic impact characteristics of Kevlar?? Woven fabrics impregnated with a colloidal shear thickening fluid. J Mater Sci 38(13):2825–2833
155. Park JL, Yoon B IL, Paik JG, Kang TJ. Ballistic performance of p-aramid fabrics impregnated with shear thickening fluid; Part I – Effect of laminating sequence. Text Res J 2012;82(6):527–541
156. Afeshejani SHA, Sabet SAR, Zeynali ME, Atai M (2014) Energy absorption in a shear-thickening fluid. J Mater Eng Perform 23(12):4289–4297
157. Na W, Ahn H, Han S, Harrison P, Park JK, Jeong E, et al (2016) Shear behavior of a shear thickening fluid-impregnated aramid fabrics at high shear rate. Compos Part B Eng [Internet] 97:162–75. Available from: https://doi.org/10.1016/j.compositesb.2016.05.017
158. Fahool M, Sabet AR (2015) UV-visible assessment of hydrocluster formation and rheological behaviour in bimodal and mono-disperse shear thickening fluids. Rheol Acta 54(1):77–83
159. Haro EE, Odeshi AG, Szpunar JA (2016) The energy absorption behavior of hybrid composite laminates containing nano-fillers under ballistic impact. Int J Impact Eng [Internet] 96:11–22. Available from: https://doi.org/10.1016/j.ijimpeng.2016.05.012
160. Gürgen S, Kuşhan MC (2017) High performance fabrics in body protective systems. Mater Sci Forum 880:132–135
161. Zhang J, Wang Y, Zhou J, Zhao C, Wu Y, Liu S, et al (2021) Intralayer interfacial sliding effect on the anti-impact performance of STF/Kevlar composite fabric. Compos Part A Appl Sci Manuf [Internet] 145(March):106401. Available from: https://doi.org/10.1016/j.compositesa.2021.106401
162. Ávila AF, de Oliveira AM, Leão SG, Martins MG (2018) Aramid fabric/nano-size dual phase shear thickening fluid composites response to ballistic impact. Compos Part A Appl Sci Manuf [Internet] 112(January):468–74. Available from: https://doi.org/10.1016/j.compositesa.2018.07.006
163. Wang X, Zhang J, Bao L, Yang W, Zhou F, Liu W (2020) Enhancement of the ballistic performance of aramid fabric with polyurethane and shear thickening fluid. Mater Des [Internet] 196:109015. Available from: https://doi.org/10.1016/j.matdes.2020.109015
164. Fluid T, Paper STF, Panels H, Chang C, Shih C, You J, et al (2021) Preparation and ballistic performance of a multi-layer armor system composed of Kevlar/Polyurea composites and shear
165. S. E. Holt MPP (2014) Impact resistant, torsion-reducing protective athletic gear using shearthickening fluid. Vol. 2
166. Shepherd RF, Green T (2011) Higher performance golf club and attachment for golf club, golf ball, athletic shoes, andathletic shn guards using shear-thckening fluids, vol 1

167. Hayes WC, Robinovitch SN, McMahon TA (1997) Bone fracture prevention garment and method. United States Patent. https://patentimages.storage.googleapis.com/49/c5/2e/7e9d4f13ec9ce6/US5599290.pdf
168. Cwalina CD, Dombrowski RD, McCutcheon CJ, Christiansen EL, Wagner NJ (2015) MMOD puncture resistance of EVA suits with shear thickening fluid (STF) – Armortm absorber layers. Procedia Eng [internet] 103:97–104. Available from: https://doi.org/10.1016/j.proeng.2015.04.014
169. Cwalina CD, McCutcheon CM, Dombrowski RD, Wagner NJ (2016) Engineering enhanced cut and puncture resistance into the thermal micrometeoroid garment (TMG) using shear thickening fluid (STF) - ArmorTM absorber layers. Compos Sci Technol [Internet] 131:61–6. Available from: https://doi.org/10.1016/j.compscitech.2016.06.001

Chapter 6
High-Velocity Impact Applications with Shear-Thickening Fluid

Prince Kumar Singh and Neelanchali Asija Bhalla

6.1 Introduction

Shear-thickening fluid (STF) is a type of non-Newtonian fluid that exhibits an increase in its viscosity with the applied shear rate [1]. By virtue of this property, STF shows a hardening texture when subjected to shear loading. STFs are made up of suspended particles in a liquid medium. When the fluid is at rest, the particles are distributed randomly in the liquid, and the suspension has a low viscosity causing it to flow easily. However, when the fluid is subjected to a high shear rate, such as when it is squeezed or stirred vigorously, the particles get disordered, thereby causing an increase in its viscosity. This property can be used for protection against impact and penetration [2], as the thickened fluid can absorb more energy than a low-viscosity fluid. The unique properties of STFs make them an attractive choice for various applications such as protective wear, medical devices, and industrial coatings [3].

There are various types of STFs, each with its own unique characteristics. The most common types include suspensions, gels, and colloids. A liquid with suspended solid particles is known as suspension. When the suspension is subjected to a shearing deformation, the solid particles interact with each other and with the surrounding liquid, causing the viscosity to increase abruptly. These types of STFs are generally used in industrial applications, for instance, drilling muds and hydraulic fluids. Gels are another type of STF, which are made up of a network of polymer chains that are dispersed in a liquid. Lotions and gels for personal care and cosmetics generally contain this group. Colloids are a type of STF that are made up of

P. K. Singh · N. A. Bhalla (✉)
Mechanical Engineering Department, Bennett University, Greater Noida, Uttar Pradesh, India

Center for Nanosensors and Nanomedicine, Bennett University,
Greater Noida, Uttar Pradesh, India
e-mail: neelanchali.bhalla@bennett.edu.in

S. Gürgen (ed.), *Shear Thickening Fluids in Protective Applications*,
https://doi.org/10.1007/978-3-031-42951-4_6

particles that are suspended in a liquid but are much smaller in size than the particles found in the suspensions. When a colloid is subjected to high shear rates, the particles become disordered, causing the viscosity to increase abruptly. Common industrial applications for colloids include paints and adhesives.

Highly concentrated granular suspensions often display a noticeable shear-thickening phenomenon. This effect causes a significant rise in fluid viscosity, leading to a phase transition into a solid-like texture, making it perfect for applications requiring personal protection. As a result, the fluid has gained popularity as the most common STF [4, 5]. In granular suspensions, the dispersed phase typically comprises of submicron sized gel particles consisting of organic polymers such as Polystyrene (PS) and Polymethyl Methacrylate (PMMA) [6, 7], or inorganic compounds such as Silicon Dioxide (SiO_2), Calcium Carbonate ($CaCO_3$), and various metal oxides [8–10]. On the other hand, a cross-linked polymer is a three-dimensional arrangement of polymer chains that are chemically bonded to each other. The process of cross-linking involves the formation of covalent bonds linking numerous polymer chains, which increases the strength, stiffness, and thermal stability of the material such as Sodium Polystyrene Sulfonate dispersed in water [11, 12] and cross-linked polyethylene (PEX). Since the polymer cross-linking time is shorter at certain shear rates in comparison to their relaxation time, these cross-linked polymer dispersions exhibit the shear-thickening effect. Moreover, the polymers are capable of being cross-linked to create a network arrangement that exhibits shear-thickening behavior [13]. Cross-linked polymer suspensions have attracted wide attention from researchers, since it is crucial to understand the shear-thickening effect for industrial sectors such as coatings, papermaking, and oil transportation [14]. A micelle system is created by dispersing cationic and anionic surfactants in deionized water in a specific ratio, for example, a solution containing 0.1 wt.% Cetyltrimethylammonium Benzoate (CTAB) and Sodium Salicylate [15, 16]. The micellar rods readily scatter in aqueous solution at rest. Since the micelle rods are layered in the direction of flow, micelle dispersion exhibits shear-thinning behavior at low shear rates. When the applied shear rate surpasses a critical value, the micelle rods join to form a bigger micelle network in the dispersion, consequently resulting in the shear-thickening behavior. Except for the fact that rod micelles are made up of minute molecules and have restricted strength, the severity of shear thickening in micelle dispersions is comparable to that of granular suspensions. This makes it suitable for vibration mitigation applications. Alternatively, a suspension prepared by scattering Polystyrene (PS) and Polyethylene Oxide (PEO) in Ethanol is an example of an insoluble polymer system [12, 17]. Insoluble polymer systems are suspensions made by dispersing high-molecular weight polymers into a solvent. When the polymer in the suspension aggregates and forms a polymer-rich phase under the influence of an externally imposed shear rate, it leads to a dispersion gel with shear-thickening characteristics. The gel network has a relatively high strength due to the polymer's strength, which also contributes to the strong shear-thickening effect. Understanding the shear-thickening effect of this system, which is often employed in the coatings industry, is crucial for coating industry especially in spray-coating procedures [18].

6.2 Shear-Thickening Mechanism

After the identification of shear-thickening behavior, scientists proposed several consistent mechanical explanations such as the order–disorder transition, hydro-clustering, jamming, and friction contact theory to explain the shear-thickening behavior, based upon the interactions between the dispersed phase and dispersion medium.

Hoffman et al. [19] studied colloidal dispersions, wherein the diffraction pattern changed from regular hexagonal to irregular as the viscosity increased. This led to the development of the order–disorder transition theory, which explains how the ordered arrangement of particles in the structure prevents shear-thickening behavior at lower shear rates. However, the ordered structure is destroyed at higher shear rates, resulting in increased viscosity due to the onset of shear-thickening. Further experiments confirmed the continuation of ordered structures in the system before and after the shear-thickening phenomenon. Repulsive forces between the particles were found to maintain the stability of the colloidal system [19, 20], while the fluid lubrication forces caused the destruction of the layered structure, thereby leading to the formation of particle clusters [21]. Although the order–disorder transition was not a necessary condition for the shear-thickening behavior to occur, it contributed significantly to the understanding of the phenomenon in colloidal concentrated suspension systems. Figure 6.1 shows a schematic for order–disorder transition mechanism.

Wagner and Brady [22] proposed the hydro-clustering theory, which explains the process of cluster formation and dissipation under the influence of applied shear stress. At low shear rates, the intermolecular repulsive forces and solvation forces dominate, resulting in a stable, low viscosity colloidal dispersion. As the shear rate increases, the stress between the dispersed particles tends to increase. Eventually, at the critical shear rate, the hydrodynamic forces become significantly greater than

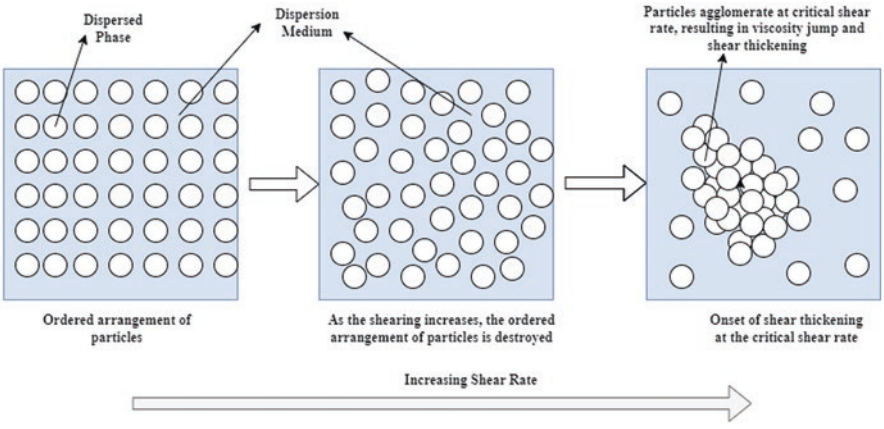

Fig. 6.1 Schematic illustration of order–disorder transition

the intermolecular repulsive forces, causing the dispersed particle to form stress bearing particle clusters, called as hydroclusters, resulting in an abrupt increase in viscosity and the onset of shear-thickening phenomenon, although, the clustered structure is unsteady and collapses when the external shear stress is reduced, causing a rapid decrease in viscosity. Hence, shear thickening is a reversible phenomenon.

When the particle size of the dispersed phase exceeds 4 μm, the Brownian forces get weaker, and inter-particle contacts increase. This process leads to a discontinuous shear-thickening (DST) behavior in the suspension [23]. DST causes a sharp increase in viscosity, and the suspension may transform from a fluid to a solid-like phase abruptly. DST is explained by the jamming theory, wherein the particles aggregate to form blockages, which prevent flow under applied shear stress. Researchers have identified a critical value of volume fraction for the transition from continuous shear-thickening (CST) to DST, with DST only occurring at higher volume fractions of dispersed phase. Peters et al. [24] reported that there is no effect of volume fraction on DST, while a higher volume fraction is required for shear jamming to occur.

Shear-thickening behavior is generally classified as CST and DST. The connection between the CST and DST is explained by the frictional contact theory [25]. The frictional contact forces become important under the influence of dominating normal contact forces amongst particles, causing the destruction of fluid film between them, thereby increasing the contact and frictional forces. Recent studies [25, 26] have demonstrated that the frictional contact between the particles is the underlying cause behind the shear-thickening phenomena in dense particle suspensions.

6.3 Engineering Applications with STF

As the interest in STF increases, it is crucial to comprehend their characteristics and behavior, to enhance their applications through appropriate material selection and synthesis methods. The exceptional characteristics of STF offer considerable potential for use in a wide range of applications. To get over the limitations of conventional materials, it is imperative to create new STFs that incorporate superior particles, additives, and carrier fluids. Engineered and smart material technologies have both used STFs in their processes and procedures. There are numerous patents for the use of STFs in science and engineering, ranging from body armor to medical instruments. An illustration of various applications with STFs is shown in Fig. 6.2.

STFs have an extensive range of applications in various industries, including the medical field, food industry, and even the manufacture of personal protective equipments such as body armor and sportswear. In the medical sector, these fluids have been used as an alternative to traditional lubricants, such as saline or silicone, for medical procedures that require low friction and high resistance to movement. In the food industry, STFs are used as thickeners in sauces and other food products, as well as in the synthesis of non-drip paint.

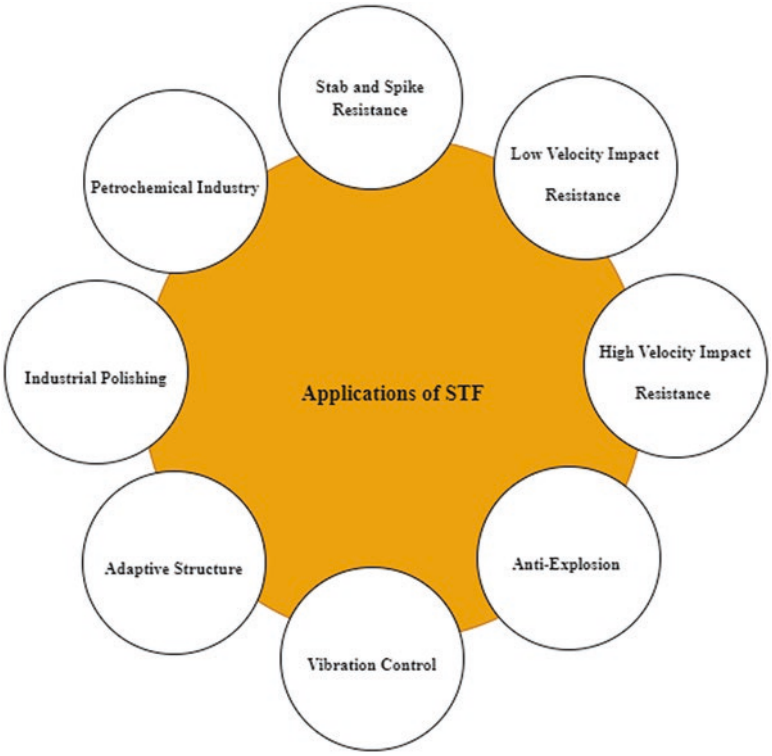

Fig. 6.2 Engineering applications with STF

One of the most notable applications with STFs is in the development of protective gear, such as body armor, helmets, hip protection pads and sportswear [10]. Body armor comprising of these fluids is designed to be lightweight and flexible, yet provide maximum protection against impacts. The shear-thickening properties provide an additional protection as the fluid instantly solidifies upon impact, thereby preventing further penetration in the armor. Similarly, sportswear made with these fluids is designed to provide improved shock and vibration resistance, thereby reducing the risk of injury or blunt trauma. Engineering and robotics are the two key fields, where STFs are extensively used. These fluids are used as hydraulic fluids in robotic systems, as their unique properties enable robots to perform complex movements with improved precision and accuracy. In engineering, these fluids have been used as damping fluids in shock absorbers and vibration dampers to control the motion of the mechanical systems and reduce the transmission of the vibrations and shocks [27].

In this chapter, the focus is on the capabilities of STFs to resist high-velocity impacts. The characterization of impacts is a crucial aspect of understanding the energy exchange phenomenon between the target and projectile. The mechanism of energy dissipation varies greatly with the projectile velocity, making impact

characterization extremely important. Impacts can be broadly classified into four categories based upon projectile velocity. These are - low-velocity impacts, intermediate-velocity impacts, high-velocity impacts, and hyper-velocity impacts. By characterizing the impacts in each of these categories, we can gain a more comprehensive understanding of the variables involved in energy transfer and develop effective strategies for resisting the impacts. Different ranges of velocities for different types of impacts are shown in Fig. 6.3. High-velocity impact resistance can be classified as the impact with a range of velocities between 50 and 1000 m/s [28]. The unique viscosity characteristics of STFs, which become stiffer under applied shear forces, make them suitable candidates for high-velocity impact-resistant applications. High-velocity impact resistance is an inherent property of STF that refers to their ability to withstand the impacts without breaking or cracking. This key feature makes STFs useful in protective equipment such as body armor, helmets, and other protective wear as well as in vibration and shock mitigation applications. STFs are extensively used in the development of fabrics, sports equipment, medical equipment, protective wear for space, and mechanical platforms. Figure 6.4 shows a schematic of various high-velocity impact resistance applications for STFs.

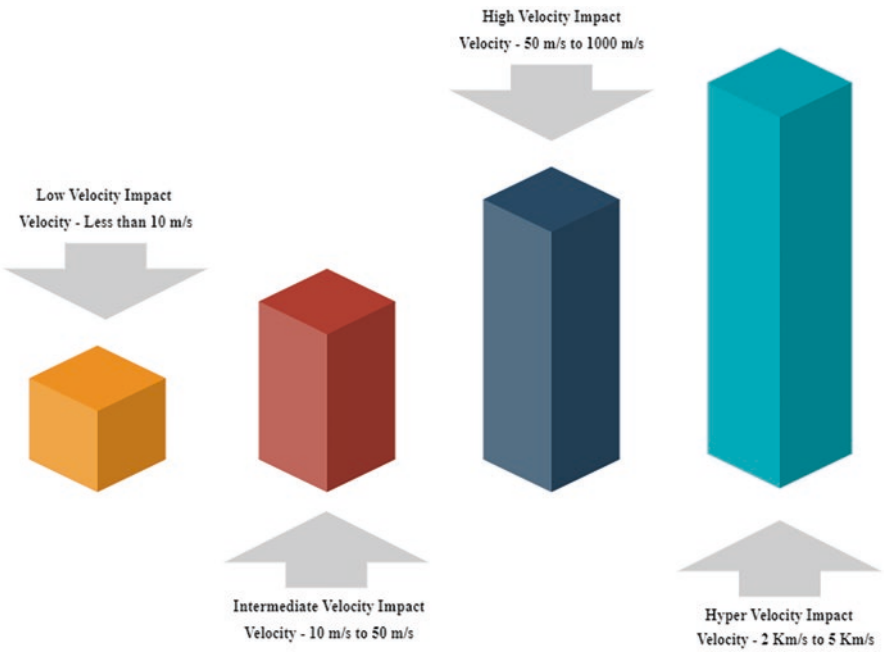

Fig. 6.3 Impact classification based on impact velocity

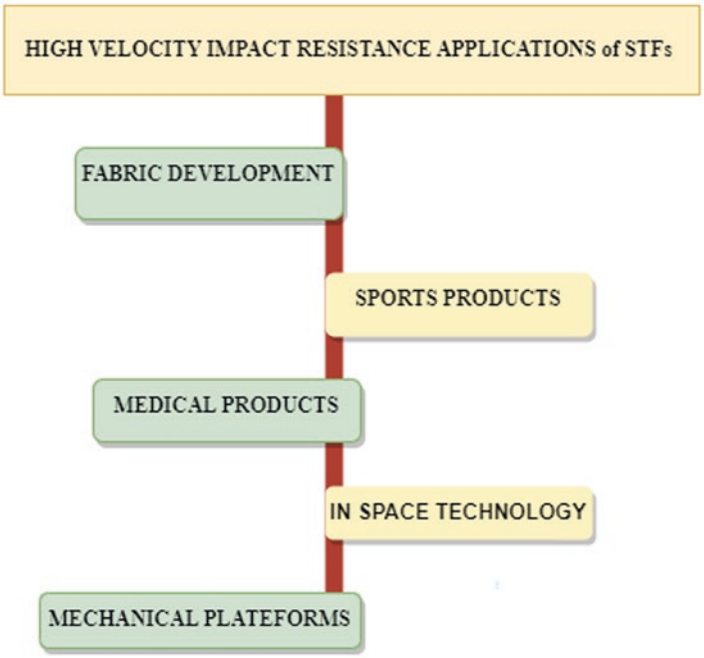

Fig. 6.4 High Velocity Impact Resistant Applications of STF

6.3.1 Fabric Development

In the textile industry, STFs can be integrated into fabrics to achieve enhanced protective properties. One of the main applications of STF in fabric development is in the creation of protective wear for athletes and elderly people. STFs can be incorporated into the fabrics to create a protective layer that stiffens upon impact, providing better protection against injuries. For example, STF can be used in the development of protective gloves for rock climbing, wherein the STF layer stiffens upon the impact to reduce the impact force and prevent hand injuries. STF can also be used in the development of ballistic fabrics. These fabrics are used to make bulletproof vests and other protective wear for military and law enforcement personnel. The incorporation of STF into these fabrics enhances the inter-yarn friction, thereby preventing the penetration of projectiles.

The development of smart textiles is another application of STFs in fabric development. Smart textiles are materials that can alter their characteristics in response to changes in environmental factors such as moisture, temperature, and light. STFs can be incorporated into these fabrics to create a self-stiffening effect that can change the texture of the fabric. This can be useful in the development of fabrics that can adjust their insulation properties based on the temperature or fabrics that can change their stiffness to provide better support during physical activity.

Multiple layers of specialized fabrics such as Ultrahigh Molecular Weight Polyethylene (UHMWPE), Aramid, and Polybenzobisoxazole (PBO) are typically used in conventional body armor fabrics. However, these produce a bulky structure which limits the maneuverability of the wearer and causes discomfort. . Several new materials are used to overcome these limitations. In the initial studies, STF impregnation into Kevlar fabrics was used to enhance the flexibility of conventional body armor, while also improving its ballistic resistance against high-velocity impacts. The findings recommended that STF treatments improved the fabric's hypodermic needle puncture resistance while preserving the natural flexibility in the fabrics [29].

The primary yarns in untreated Kevlar fabrics take part in impact load sharing and energy absorption. Under impact, the STF in fabrics turns into a solid-like material. STF is employed as a bridging matrix in this fabric to produce a single structure that permits load carrying, energy absorption, and impact distribution across the entire fabric as opposed to just the core yarns. The fabric's yarn is made up of several filaments, and the STF and shear-thickening gel (STG) are spread between the filaments. Figure 6.5 shows the magnified cross-section of Kevlar/STF/STG yarn [30].

As per the findings [31], STF-treated fabric composites outperformed the untreated fabrics and Polyethylene Glycol (PEG)-impregnated fabrics in terms of shock wave protection. The normalized average peak pressure amplification was decreased from 2.46 to 1.49 by the STF treatment as shown in Fig. 6.6. The normalized maximum rate of pressure rise was also attenuated from 2.3 to 0.76 as shown in Fig. 6.7. According to this study, STF-treated fabrics can also be employed for shock wave attenuation in addition to ballistic protection.

Na et al. [32] developed STF-impregnated aramid fabrics with increased resistance to stab and ballistic impacts. The rate-sensitive shear stiffness of these fabrics could be attributed to increased resistance to stab and ballistic impacts. Multi-phase STFs (mSTFs) are reported to exhibit an improved ballistic performance of developed fabrics in comparison to single-phase STFs. This study demonstrated that the presence of STFs enhanced fabric inter-yarn friction. However, rheological measurements revealed that there is no direct relationship between the protective capabilities of STF/fabrics and shear-thickening behavior. Despite this fact, the thickening characteristics are pronounced in single-phase STFs than multi-phase

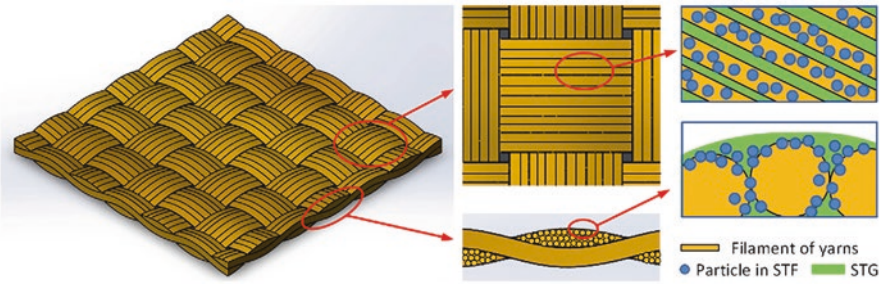

Fig. 6.5 An illustration of Kevlar fabrics with STF and STG [30]

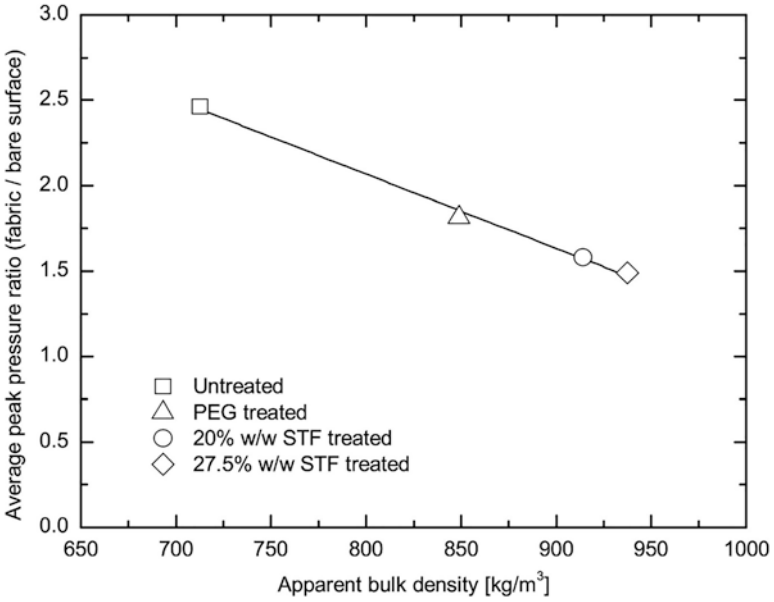

Fig. 6.6 The effect of apparent bulk density on average peak pressure amplification [31]

STFs, whereas the ballistic performance of fabrics impregnated with multi-phase STFs was found to be better. Cao et al. [33] developed a ballistic composite by combining a CNT/polystyrene ethyl acrylate (CNT/PSt-EA)-based STF with Kevlar fabrics. According to the ballistic results, CNT/PSt-EA-based STF application in the fabrics led to an increase in the ballistic limit velocity from 84.6 to 96.5 m/s. Ballistic limit (BL) velocity refers to the minimum velocity required for a projectile to penetrate a specific target material. The BL velocity increased from 92.9 to 99.5 m/s by increasing the volume percentage of dispersed phase in STF from 53.5 to 58.5% . The addition of STF in Kevlar fabrics improves the ballistic performance by enhancing the friction coefficient between the yarns and expanding the fabric's bearing area. Figure 6.8 shows different types of body armors with various components.

6.3.2 Sports Products

The application of STF in sports products is mainly driven by its ability to enhance the overall performance and safety of athletes. STF is known for its exceptional shock-absorbing properties, which are particularly important in sports that involve high impacts such as football, basketball, and skiing. The use of STF in protective wear such as helmets, shoulder pads, and knee pads can provide superior impact resistance and reduce injuries. One of the most significant benefits of STF in sports

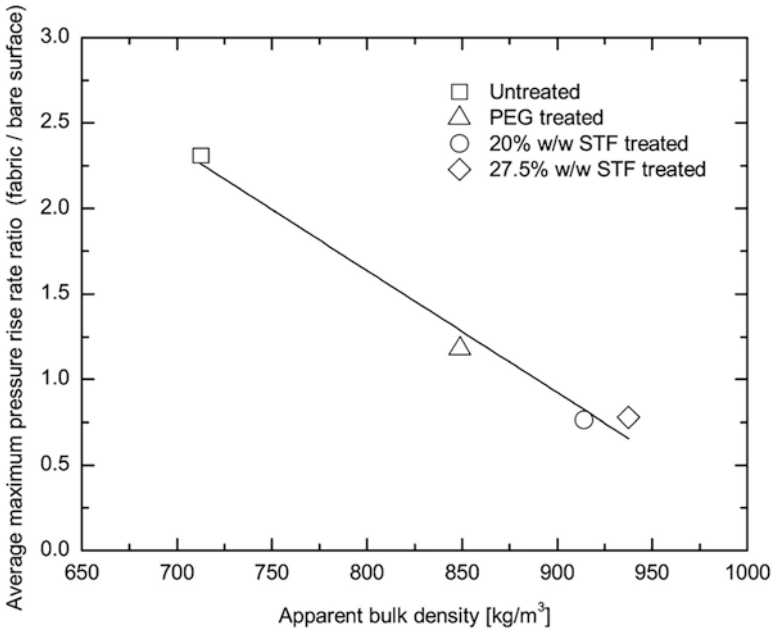

Fig. 6.7 Amplification of average maximum pressure rise rate by material apparent bulk density [31]

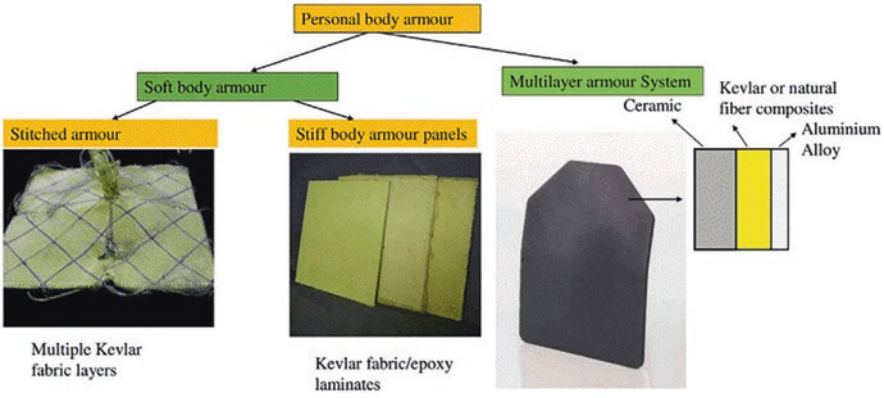

Fig. 6.8 Body armors with various components [34]

products is its ability to provide enhanced comfort and flexibility. For instance, the use of STF in athletic shoes can help to reduce the pressure points and impact forces that an athlete experiences during high-intensity activities. This, in turn, can improve the athlete's performance, reduce the risk of injury, and provide a more comfortable experience.

Between 2011 and 2014, around 8.6 million sports-related injuries occurred per year, as per the Centers for Disease Control and Prevention (CDC) in USA [35]. Roughly one-third of all sports-related and recreation-related injuries occurred on athletic fields, sports facilities, and playgrounds, amounting to approximately 2.9 million injuries per year. Many studies have been carried out to create high-quality sporting goods that offer the best protection to their users, including snowboards, rackets, footwear, and other items. Lammer et al. [36] incorporated STF into a tennis racket. A racket comprises of five subparts, namely head, neck, strings, shaft, and handle as shown in Fig. 6.9. They included STF into several components of a racket, which boosted its performance in several ways. STF impregnation enhanced ball control at the point of ball impact. Shear-thickening materials were added to the racket construction, which changed the head's stiffness and flexibility. As the ball strikes the racket, it gets stiffer thereby increasing the power of strike. Since the STF returned to a flowable state, the modified racket maintained its normal flexibility. One advantage of adopting STF in rackets was energy absorption during collisions and strikes against the wall, ground, or any hard object. STF also provided vibration dampening in the racket during the strike of the ball. STF in rackets also had the benefit of versatility, which offered variable levels of racket flexibility for various user preferences. The advantages of stiffness and flexibility can be obtained simultaneously by adding shear-thickening materials at various locations in the racket.

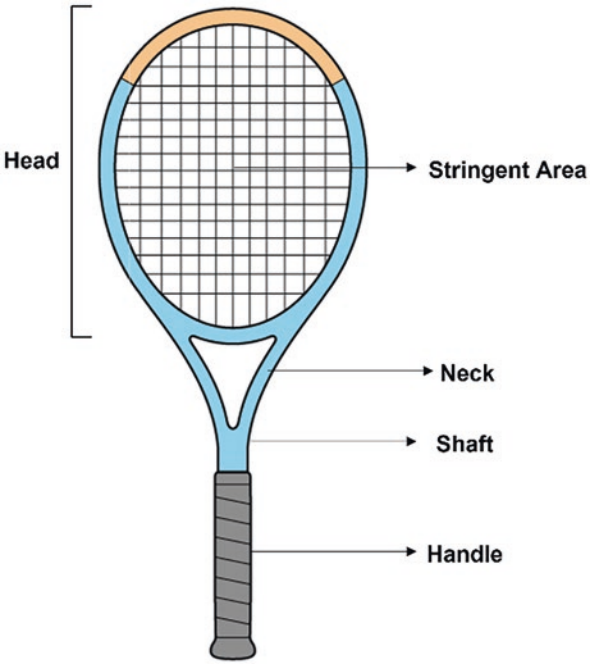

Fig. 6.9 Schematic illustration of a tennis racket

Shear-thickening materials are also reported to enhance the user's performance in other sports equipment. For instance, shear thickening in footwear may help with impact absorption between the user's shoes and the ground. When STF-impregnated shoes are worn on the ground, any contact with hard surfaces or sharp objects leads to the triggering of shear thickening phenomenon, thereby preventing injuries in the foot. Furthermore, STF increases the life span of shoes and attenuates vibrations, thereby enhancing the player's performance. Shear-thickening material is excellent for skies and snowboards because it suppresses the vibration and impact damages [36]. Nylon, polyester, cotton, rayon, synthetic foams, and other fabrics, where STF may fill holes and opacities within the fabric matrix, are a few materials where STF is used. Soft tissues are protected by the application of STF from abrupt twisting, internal joint stress, and external strong blows. The risk of injuries brought on by instability in the knee, ankle, and elbow is lowered by the inclusion of STF in sports equipment that are close to the joints. The STF-modified sports equipment was found to be flexible during regular user exercises, but instantly became rigid when subjected to a force or impact to prevent joint torsional damage. The carrier liquid could be PEG, polypropylene glycol (PPG), or polyethylene oxide (PEO), while silica or oxides of other transition metals such as copper, gold, titanium, iron, and silver in a colloidal/spherical form could be used as the solid phase for the STFs used in sports applications [37]. Moreover, an STF composite can be utilized in golf sticks to increase the magnitude of striking force, causing the ball to travel further.

Despite the numerous benefits of STF in sports, there are still some challenges that need to be addressed. One of the major challenges is the high cost of manufacturing STF-based products. The complex manufacturing process of STF makes it more expensive than traditional materials used in sports products. This, in turn, can limit its application in some sports products, particularly those that are not considered essential ones. For example, a tennis ball is a sports product that requires a soft outer layer to achieve optimal bounce and playability. While STF could potentially be used in the manufacturing of tennis balls to provide additional shock absorption and reduce the risk of injury, the cost of incorporating STF may not be justifiable, given the relatively low cost of tennis balls and the large volumes in which they are produced. Therefore, it is unlikely that STF would be used in the production of tennis balls.

In conclusion, the application of STF in sports products is an area that has the probability to transform the sports industry. STF can provide superior impact resistance, enhanced comfort, and flexibility, making it an ideal material for sports products such as protective wear, athletic shoes, and gloves. However, further research is required to overcome the challenges associated with manufacturing STF-based products and make them more accessible to the wider sports industry.

6.3.3 Medical Products

The production of efficient medical items for both professional and everyday use has made use of STF-related materials. For instance, Williams et al. [38] developed a surgical ensemble comprising an STF-impregnated surgical gown, glove, and mask. Both the internal and external sides of the garment were lined with STF. The use of STF caused the surgical garment's viscosity to increase, making it more difficult for sharp objects such as surgical blades or needles to pierce through it. STF can also be used to enhance the puncture resistance of surgical gloves and other wound care supplies. The general flexibility of the garment remained unchanged, preserving the user's freedom of movement and tactile sense because of the flowable state of the STF at low shear rate, which is a considerable advantage. Moreover, because STF is lightweight, there was little change in the fabric's or garment's weight. The materials designed using STF can also be used to make bandages and other wound care items, adding a further layer of defense against any injury. Bandages can also contain STF to lessen detrimental organ movement, in the wake of any muscular or ligament injury. STFs in the bandages were initially less viscous, but body movement increased their viscosity, thereby making the bandages stiffer. STF-integrated bandages provide both functional support and protection against excessive displacement, thereby enhancing the healing rate.

6.3.4 Space Technology

In space technology, STFs could be used in several ways. For example, they could be included in the design of spacecraft to protect against micrometeoroid impacts, which can cause significant damage to spacecraft and their occupants. STFs could be used as a lining material for the spacecraft's outer shell, or they could be included in the design of internal compartments to provide additional protection for sensitive equipment and instruments. Another potential application of STFs in space technology is in the design of space suits. STFs could be used to create flexible and lightweight materials that offer greater protection against impact and penetration than traditional materials such as Kevlar, Zylon, or other high-strength ballistic fabrics. This could enhance the safety of astronauts during spacewalks and other activities when they step out of the protective shell of spacecraft.

STFs could also be used in the development of robotic systems for space exploration. These systems use STFs to protect against impact and vibration, as well as to enhance grip and traction. This could enable robots to operate more effectively in the challenging conditions of space, where gravity is low or absent, and surfaces may be uneven or slippery. The astronauts' extra-vehicular activities (EVAs) in low earth orbit (LEO) are influenced by the direct threat of micrometeoroids and orbital debris (MMOD) hyper-velocity impacts. Micrometeoroids arise from comets and asteroidal debris in the solar system. In addition, many kinds of titanium and

aluminum orbital debris are created during spacecraft, shuttle, and satellite operations. The velocities of micrometeoroids range from 11 to 72 km/s, whereas the velocities of orbital debris in LEO ranges from 1 to 15 km/s, with an average velocity of 9 km/s. Due to this, MMODs present a main threat to astronauts and mechanical components of spacecraft [39]. STF-intercalated Kevlar (STF-Armor™) was developed for EVA suits by Cwalina et al. [39] against the hyper-velocity impacts of MMOD. They studied the efficacy of STF-Armor™ in EVA suits under MMOD-impact conditions compared to the preexisting neoprene-coated nylon absorber layers. The findings demonstrated that the STF-Armor™-equipped EVA suit lay-ups were more resistant to cutting and puncture damages than the conventional neoprene-coated nylons. Moreover, the STF-Armor™-included EVA suit outperformed the conventional EVA suit in the hyper-velocity impact tests, despite its thinner and lighter structure. Conventional EVA suits have textile layers known as the thermal micrometeoroid garment (TMG), which shields the outside of the pressurized air bladder, to help counteract the treatment of MMOD. The STF-Armor™ enhanced the cut and puncture resistance of TMG according to Cwalina et al. [40]. An impact case of hypervelocity MMOD on the International Space Station (ISS) were modeled using hypodermic needles to replicate the cutting and piercing risks. Impact test findings showed that adding colloidal STF in the STF-Armor™ boosted the energy absorption of TMG by 117% and 99% for 18 and 21 gauge needles, respectively. The STF-Armor™ also increased the TMG puncture resistance without reducing the density or flexibility of the material. An STF-impregnated fabric was developed by Kim et al. [41] to enhance the back wall of the space shields. The impact resistance of neat multilayer Heracron fabric and STF-treated Heracron fabric was investigated at high-impact velocities (3.6–4.0 km/s). The high-velocity impact to the AA 6061-T6 frontal bumper did not entirely pierce the Heracron fabric rear wall. Heracron fabric layers were swapped out with STF-impregnated layers to enhance the number of layers that were still intact. According to this study, STF-impregnated layers are beneficial to enhance space shielding systems against high-velocity impacts.

6.3.5 Mechanical Platforms

Mechanical platforms are the systems that involve motion or motion control such as robotics, prosthetics, and vehicles. These systems often require fluids that can provide high stability and control to ensure optimal performance. STFs have unique rheological properties that make them ideal for use in these systems [42, 43]. One of the most significant advantages of STFs is their capability to provide increased stability and control. This property can be leveraged in mechanical platforms, especially in situations where there is a risk of impact or sudden changes in velocity. STFs can be used in rotational brakes [44] and various damper systems due to their increased energy absorption capabilities. Fig. 6.10 illustrates the application of STF in rotational brake systems.

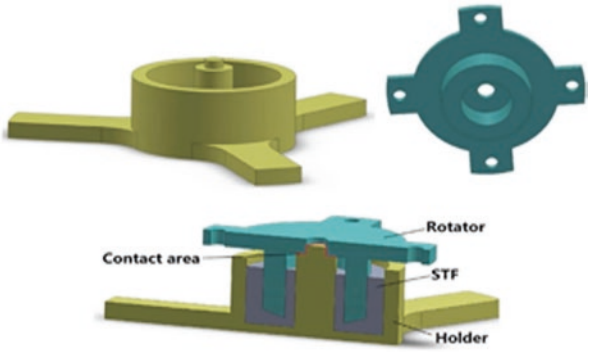

Fig. 6.10 The structure of the rotational STF brake [44]

With dampers, kinetic energy is transformed into thermal energy that may be released through the fluid. Dampers typically consist of a piston and a tube filled with a fluid. In automobiles, mounts serve as a streamlined version of dampers. Engine vibrations have been suppressed by damping technologies. The majority of suspension systems use rubber blocks, passive hydraulic suspensions, or passive vibration systems [45]. Damping characteristics in passive suspension systems are fixed and immutable. The engine or vehicle's overall performance is impacted by the inability to adjust. Traditional passive suspension systems, therefore, had a limited ability to isolate engine vibrations. Moreover, dampers used in buildings and bridges are made specifically for these types of constructions. The tunable damping platforms such as electro-rheological and magneto-rheological dampers require an external power source, making their durability questionable. Magneto-rheological (MR) fluids are suspensions of micron-sized magnetic particles, typically iron or iron oxide, in a carrier fluid, oil, or water. When a magnetic field is applied, the magnetic particles align with the field, causing the fluid to increase in viscosity and become stiffer. When the magnetic field is removed, the MR fluid turns to its original low-viscosity state. Electrorheological (ER) fluids, on the other hand, are suspensions of micron-sized particles, typically made of materials such as silica, in a carrier fluid, oil, or water. When an electric field is applied, the particles in this fluid align with the field, causing the fluid to undergo a rapid increase in viscosity. When the electric field is removed, the fluid turns to the initial low-viscosity state. STFs are advantageous in this situation since they change their rheology without the need for an external stimulus. Yeh et al. [46] investigated the rheology and operation of an STF-filled viscous damper. STFs were produced using nanoscale fumed silica powder in PPG liquid. The STF was poured into the hydraulic tube to create a damper device. The study demonstrated that the STF-filled dampers effectively reduced the vibrations. By applying different vibration frequencies, this ingenious viscous damper could enhance the damping coefficient and energy dissipation behavior. The shear-thickening and shear-thinning rheologies can also be used to alter the performance of an STF damper. Chen et al. [47] applied STFs to a

traditional viscous damper device for a performance that was at par with a magneto-rheological damper. They used nanoparticles of fumed silica to produce STFs in PPG. This work showed that STF could be used to act as a viscous damper in an efficient manner. Fischer et al. [48] studied the various usages of STFs as tunable dampening components for dynamically exposed structures to flexural loads. The first resonance frequency was dampened by a factor of two and even up to nine when silica suspension layers were used. Moreover, the increasing viscosity in the structure enhanced the flexural rigidity, which improved stress transfer between the rigid polyvinyl chloride layers. In addition to particle concentration, its morphology could also be used to regulate the extent to which the structure is stiffened and dampened. In a different study, Tian et al. [49] developed STFs and investigated their rheological characteristics for application in rotational brakes. The results showed that the rotational STF brake had long-term stability. Compared to the magneto-rheological fluids braking systems, the rotational STF brake had several advantages such as non-necessity of an external power supply to trigger shear-thickening phenomenon, a simpler structure, no requirement of a magnetic system or a controller, and steadiness due to fewer components. Another STF based on silica nanoparticles in Ethylene Glycol (EG) was developed by Zhang et al. [44] for a smart damper system. When integrated with the damper, STF with a "speed-activated" behavior led to instantaneous changes in damping and stiffness as the frequency was altered. Shear-thickening effect made the damper stiffer with enhanced energy-absorbing properties.

6.4 Conclusions

STF is a unique class of non-Newtonian fluids that offers an attractive alternative to traditional materials for high-velocity impact applications. The increase in viscosity under high shear rates makes STF effective in impact energy absorbing applications, thereby reducing the developed forces in the target. STF can be applied in various ways, such as coatings, fabrics, and composites, making it a versatile material for high-velocity impact applications. Despite several advantages, there are some limitations of STF, which restrict the path of large-scale utilization. For example, the temperature sensitivity of STF is a major drawback in applications. STF packaging is another limitation in bulk-use applications. Moreover, exposure to environmental factors such as humidity and ultraviolet radiations drastically effect the rheological properties of the system. On the other hand, characterization of STF is a complex process that requires cautious control of experimental parameters, advanced measurement techniques, meticulous analysis, and in-depth interpretation of rheological data as well as a good understanding of the underlying physics. Hence, thorough characterization of STF, both in the low as well as high strain rate domain, is crucial to develop STF-based impact and shock resistant structures, while preserving the efficacy of STF against detrimental effects of the environment.

References

1. Barnes HA (1989) Shear-thickening ('Dilatancy') in suspensions of nonaggregating solid particles dispersed in Newtonian liquids. J Rheol (N Y N Y) 33(2):329–366. https://doi.org/10.1122/1.550017
2. Asija N, Chouhan H, Amare Gebremeskel S, Bhatnagar N (2018) Impact response of Shear Thickening Fluid (STF) treated ultra high molecular weight poly ethylene composites – study of the effect of STF treatment method. Thin-Walled Struct 126(April):16–25. https://doi.org/10.1016/j.tws.2017.04.025
3. Gürgen S, Sofuoğlu MA (2020) Integration of shear thickening fluid into cutting tools for improved turning operations. J Manuf Process 56(June):1146–1154. https://doi.org/10.1016/j.jmapro.2020.06.012
4. Lim AS, Lopatnikov SL, Wagner NJ, Gillespie JW (2010) Investigating the transient response of a shear thickening fluid using the split Hopkinson pressure bar technique. Rheol Acta 49(8):879–890. https://doi.org/10.1007/s00397-010-0463-8
5. Park JL, Il Yoon B, Paik JG, Kang TJ (2012) Ballistic performance of p-aramid fabrics impregnated with shear thickening fluid; part II – effect of fabric count and shot location. Text Res J 82(6):542–557. https://doi.org/10.1177/0040517511420765
6. Jiang W, Sun Y, Xu Y, Peng C, Gong X, Zhang Z (2010) Shear-thickening behavior of polymethylmethacrylate particles suspensions in glycerine-water mixtures. Rheol Acta 49(11):1157–1163. https://doi.org/10.1007/s00397-010-0486-1
7. Zhou Z et al (2014) Effects of particle softness on shear thickening of microgel suspensions. Soft Matter 10(33):6286–6293. https://doi.org/10.1039/c4sm01181c
8. Fahool M, Sabet AR (2016) Parametric study of energy absorption mechanism in Twaron fabric impregnated with a shear thickening fluid. Int J Impact Eng 90:61–71. https://doi.org/10.1016/j.ijimpeng.2015.11.016
9. Yang HL, Ruan JM, Zou JP, Wu QM, Zhou ZC, Xie YY (2009) Non-linear viscoelastic rheological properties of PCC/PEG suspensions. Chinese J Chem Phys 22(1):46–50. https://doi.org/10.1088/1674-0068/22/01/46-50
10. Asija N, Chouhan H, Bhatnagar N (2017) Synthesis of shear thickening fluids for liquid armour applications. ISME J Manuf Sci 06(1):9–17
11. Weiss RA, Zhao H (2009) Rheological behavior of oligomeric ionomers. J Rheol (NY NY) 53(1):191–213. https://doi.org/10.1122/1.3003570
12. Van Egmond JW (1998) Shear-thickening in suspensions, associating polymers, worm-like micelles, and poor polymer solutions. Curr Opin Colloid Interface Sci 3(4):385–390. https://doi.org/10.1016/S1359-0294(98)80054-X
13. Wang SQ (1992) Transient network theory for shear-thickening fluids and physically cross-linked networks. Macromolecules 25(25):7003–7010. https://doi.org/10.1021/ma00051a043
14. Ma SX, Cooper SL (2001) Shear thickening in aqueous solutions of hydrocarbon end-capped poly(ethylene oxide). Macromolecules 34(10):3294–3301. https://doi.org/10.1021/ma001772i
15. Bautista F et al (2015) A master dynamic flow diagram for the shear thickening transition in micellar solutions. Soft Matter 12(1):165–170. https://doi.org/10.1039/c5sm01625h
16. Kim WJ, Yang SM (2000) Microstructures and rheological responses of aqueous CTAB solutions in the presence of benzyl additives. Langmuir 16(15):6084–6093. https://doi.org/10.1021/la991086g
17. Van Egmond JW (1997) Effect of stress-structure coupling on the rheology of complex fluids: poor polymer solutions. Macromolecules 30(25):8045–8057. https://doi.org/10.1021/ma9706891
18. Elliott PT, Mahli DM, Glass JE (2007) Spray applications: part IV. Compositional influences of HEUR thickeners on the spray and velocity profiles of waterborne latex coatings. J Coatings Technol Res 4(4):351–374. https://doi.org/10.1007/s11998-007-9051-y
19. Hoffman RL (1974) Discontinuous and dilatant viscosity behavior in concentrated suspensions. II. Theory and experimental tests. J Colloid Interface Sci 46(3):491–506. https://doi.org/10.1016/0021-9797(74)90059-9

20. Chow MK, Zukoski CF (1995) Nonequilibrium behavior of dense suspensions of uniform particles: volume fraction and size dependence of rheology and microstructure. J Rheol (NY NY) 39(1):33–59. https://doi.org/10.1122/1.550687
21. Chen LB, Chow MK, Ackerson BJ, Zukoski CF (1994) Rheological and microstructural transitions in colloidal crystals. Langmuir 10(8):2817–2829. https://doi.org/10.1021/la00020a052
22. Bender JW, Wagner NJ (1995) Bender & Wagner. J Colloid Interface Sci 172(1):171–184
23. Jiang W, Xuan S, Gong X (2015) The role of shear in the transition from continuous shear thickening to discontinuous shear thickening. Appl Phys Lett 106(15). https://doi.org/10.1063/1.4918344
24. Olsson P, Teitel S (2007) Critical scaling of shear viscosity at the jamming transition. Phys Rev Lett 99(17):1–4. https://doi.org/10.1103/PhysRevLett.99.178001
25. Mari R, Seto R, Morris JF, Denn MM (2014) Shear thickening, frictionless and frictional rheologies in non-Brownian suspensions. J Rheol (NY NY) 58(6):1693–1724. https://doi.org/10.1122/1.4890747
26. Clavauda C, Be-ruta A, Metzgera B, Forterrea Y (2017) Revealing the frictional transition in shear-thickening suspensions. Proc Natl Acad Sci U S A 114(20):5147–5152. https://doi.org/10.1073/pnas.1703926114
27. Gürgen S, de Sousa RJA (2020) Rheological and deformation behavior of natural smart suspensions exhibiting shear thickening properties. Arch Civ Mech Eng 20(4):110. https://doi.org/10.1007/s43452-020-00111-4
28. Safri SNA, Sultan MTH, Yidris N, Mustapha F (2014) Low velocity and high velocity impact test on composite materials – a review. Int J Eng Sci 3(9):50–60. https://doi.org/10.1177/1464420711409985
29. Wagner NJ (2014) Hypodermic needle puncture of shear thickening fluid (STF) -treated fabrics. October, 2014
30. He Q, Cao S, Wang Y, Xuan S, Wang P, Gong X (2018) Impact resistance of shear thickening fluid/Kevlar composite treated with shear-stiffening gel. Compos Part A Appl Sci Manuf 106:82–90. https://doi.org/10.1016/j.compositesa.2017.12.019
31. Haris A, Lee HP, Tay TE, Tan VBC (2015) Shear thickening fluid impregnated ballistic fabric composites for shock wave mitigation. Int J Impact Eng 80:143–151. https://doi.org/10.1016/j.ijimpeng.2015.02.008
32. Na W et al (2016) Shear behavior of a shear thickening fluid-impregnated aramid fabrics at high shear rate. Compos Part B Eng 97:162–175. https://doi.org/10.1016/j.compositesb.2016.05.017
33. Cao S, Pang H, Zhao C, Xuan S, Gong X (2020) The CNT/PSt-EA/Kevlar composite with excellent ballistic performance. Elsevier. https://doi.org/10.1016/j.compositesb.2020.107793
34. Naveen J, Jayakrishna K, Sultan MTBH, Amir SMM (2020) Ballistic performance of natural fiber based soft and hard body armour – a mini review. Front Mater 7(December):1–6. https://doi.org/10.3389/fmats.2020.608139
35. United States (2016) National health statistics reports, number 99, November 18, 2016. Centers Dis Control Prev 99:2011–2014
36. Rosenkranz H, At L (2012) (12) United States Patent 2 no. 12
37. Majeed et al (2010) United States patent: 3871965 United States patent: 3871965. Yeast 2(19):4–6
38. Utriainen M, Application F, Data P, Oy E (2009) (12) Patent Application Publication (10) Pub. No.: US 2009/0312954 A1 D Patent Application Publication. 1(19), 1–6
39. Cwalina CD, Dombrowski RD, McCutcheon CJ, Christiansen EL, Wagner NJ (2015) MMOD puncture resistance of EVA suits with shear thickening fluid (STF) – armortm absorber layers. Procedia Eng 103:97–104. https://doi.org/10.1016/j.proeng.2015.04.014
40. Cwalina CD, McCutcheon CM, Dombrowski RD, Wagner NJ (2016) Engineering enhanced cut and puncture resistance into the thermal micrometeoroid garment (TMG) using shear thickening fluid (STF) – armor™ absorber layers. Compos Sci Technol 131:61–66. https://doi.org/10.1016/j.compscitech.2016.06.001

41. Kim YH, Park Y, Cha JH, Ankem VA, Kim CG (2018) Behavior of shear thickening fluid (STF) impregnated fabric composite rear wall under hypervelocity impact. Compos Struct 204(June):52–62. https://doi.org/10.1016/j.compstruct.2018.07.064
42. Gürgen S, Sofuoğlu MA (2021) Smart polymer integrated cork composites for enhanced vibration damping properties. Compos Struct 258:113200. https://doi.org/10.1016/j.compstruct.2020.113200
43. Gürgen S, Sofuoğlu MA (2019) Experimental investigation on vibration characteristics of shear thickening fluid filled CFRP tubes. Compos Struct 226:111236. https://doi.org/10.1016/j.compstruct.2019.111236
44. Zhang XZ, Li WH, Gong XL (2008) The rheology of shear thickening fluid (STF) and the dynamic performance of anSTF-filled damper. Smart Mater Struct 17(3). https://doi.org/10.1088/0964-1726/17/3/035027
45. Yeh F, Chang K, Chen T (2008) Smart viscous dampers utilizing shear thickening fluids with silica nanoparticles, no. 2006
46. Taylor P, Yeh F, Chang K, Chen T, Yu C (2014) The dynamic performance of a shear thickening fluid viscous damper. J Chin Inst Eng 37(August):983. https://doi.org/10.1080/02533839.2014.912775
47. Yeh S et al (2018) High-velocity impact performance of shear-thickening fluid/kevlar composites made by the padding process. 1–10. https://doi.org/10.1002/pc.25147
48. Fischer C, Bennani A, Michaud V, Jacquelin E, Månson JAE (2010) Structural damping of model sandwich structures using tailored shear thickening fluid compositions. Smart Mater Struct 19(3). https://doi.org/10.1088/0964-1726/19/3/035017
49. Tian T, Nakano M (2017) Design and testing of a rotational brake with shear thickening fluids. Smart Mater Struct 26(3). https://doi.org/10.1088/1361-665X/aa5a2c

Chapter 7
Blast Protection with Shear-Thickening Fluid-Integrated Composites

Mohammad Rauf Sheikhi and Mahdi Hasanzadeh

7.1 Introduction

Shear-thickening fluids (STFs) belong to the category of non-Newtonian fluids, which exhibit an intriguing behavior of increasing viscosity when subjected to shear loading. Indeed, they have a liquid-like viscosity at low shear rates, allowing easy flow and flexibility. However, when subjected to high shear rates, such as those experienced during a shock wave impact, STFs rapidly increase in viscosity and become stiffer, almost solid-like. This property known as shear thickening provides enhanced protection against impact and deformation. STFs consist of a liquid medium, such as water or oil, containing a suspension of solid particles. The defining characteristic of STFs lies in the interactions between these particles, which give rise to the observed shear-thickening phenomenon. Under low shear stress conditions, the particles within the fluid are relatively distant from each other and move independently, allowing the fluid to flow easily. However, under high shear rates, such as when the fluid is rapidly stirred or subjected to impact forces, the particles begin to interact and form temporary particle networks, namely hydroclusters. These particle networks impede the flow of the fluid, causing a substantial increase in viscosity. As more shear stress is applied, the particle interactions become stronger, resulting in greater resistance to flow. This behavior is commonly referred to as "jamming," as the particles effectively interlock, hindering the fluid's motion.

M. R. Sheikhi
Key Laboratory of Traffic Safety on Track of Ministry of Education, School of Traffic & Transportation Engineering, Central South University, Changsha, Hunan, China

M. Hasanzadeh (✉)
Department of Textile Engineering, Yazd University, Yazd, Iran
e-mail: m.hasanzadeh@yazd.ac.ir

S. Gürgen (ed.), *Shear Thickening Fluids in Protective Applications*,
https://doi.org/10.1007/978-3-031-42951-4_7

STFs find practical applications in various areas, particularly in the development of protective wear and impact-resistant materials. By incorporating STFs into fabrics or coatings, it becomes possible to produce flexible and comfortable materials under normal conditions, but they become rigid upon impact. This property enables them to absorb and distribute the force of impacts, providing enhanced protection. STFs also hold potential for applications in other fields such as robotics, automotive, aerospace, machinery, manufacturing, and buildings. They can be utilized in damping systems, where their increased viscosity under impact contributes to the vibration and shock absorption. Additionally, STFs can be employed in advanced lubricants, drilling fluids, and even in the development of flexible electronics.

The use of STF in body armor has garnered significant attention. Specifically, STF has been combined with high-performance fabrics to improve their stab, puncture, and ballistic resistance properties without significantly increasing the thickness or stiffness of the fabrics. Early advancements in this area were made by Wagner's group and the US Army Research Laboratory, who developed soft-body armors using STF in conjunction with Kevlar fabric [1]. Their experimental findings demonstrate that impregnating Kevlar fabric with an STF, which consists of silica particles dispersed in ethylene glycol, enhances its resistance to ballistic penetration. Compared to Kevlar fabrics of the same weight but without STF treatment, the STF-treated Kevlar fabric provides nearly identical ballistic protection while being thinner and more flexible. It is important to note that the improved ballistic performance is not solely due to the effects of the carrier liquid, as Kevlar treated with ethylene glycol alone, without any particles, exhibits relatively poor ballistic performance compared to both STF-treated Kevlar and untreated Kevlar fabric.

When STFs are incorporated into textiles, such as fabrics used in protective clothing or armor, they impart several beneficial properties in the context of shock wave mitigation. STF-treated textiles exhibit excellent energy absorption capabilities. The sudden increase in viscosity upon impact enables the material to absorb and disperse the incoming energy from the shock wave, reducing its damaging effects on the wearer or underlying structures. Moreover, STFs can enhance the resistance of textiles to penetration by high-velocity projectiles associated with blast events. The shear-thickening behavior creates a stiff barrier upon impact, preventing the penetration of fragments or debris that may accompany a blast wave. This property is particularly valuable in military applications and personal protective equipment (PPE). Another advantage of STF-treated textiles is their ability to dampen shock waves. The increased viscosity of the STF absorbs and dissipates the energy of the shock wave, reducing its magnitude and duration. This damping effect can help protect against traumatic injuries and structural damage. Growing research in recent years has been observed. Figure 7.1 depicts the rise of publications related to the blast wave and STF during the past 10 years. In this chapter, the blast wave properties of STF-treated textiles are discussed.

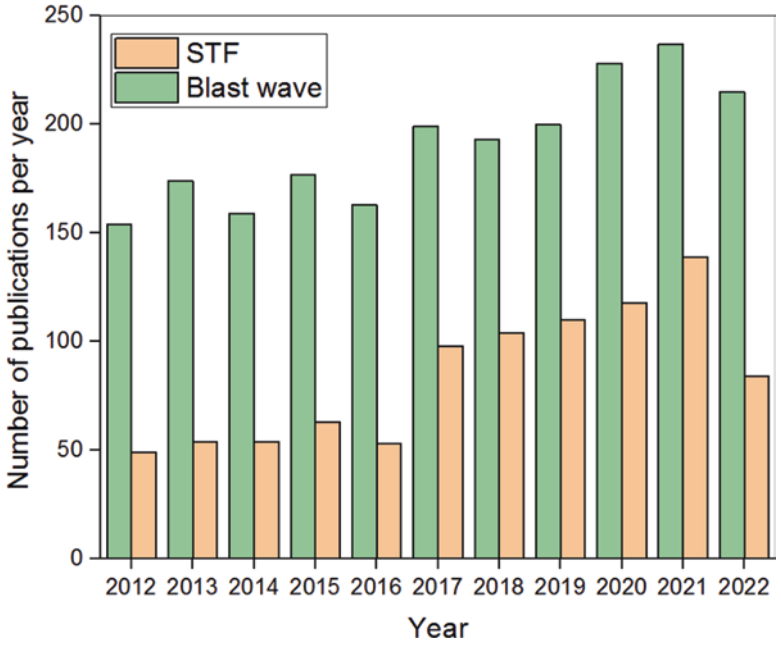

Fig. 7.1 The number of publications related to STF and blast based on the Scopus database

7.2 Shear-Thickening Rheology

Shear thickening is a fascinating phenomenon observed in certain fluids known as STFs, where the viscosity of the fluid increases significantly under applied shear stress. While the exact mechanisms behind shear thickening are still being studied, several theories have been proposed to explain this behavior. It is believed that a combination of these mechanisms contributes to the overall behavior of STFs. One prominent theory is the particle-jamming mechanism. STFs often consist of a suspension of solid particles in a liquid medium. At low shear rates, these particles can move relatively freely, allowing the fluid to flow easily. However, as the shear rate increases, the particles can become jammed together, forming temporary structures or networks that hinder the flow. This jamming leads to an abrupt increase in viscosity and results in shear-thickening behavior [2]. Another proposed mechanism is based on hydrodynamic lubrication. At low shear rates, the fluid acts as a lubricant between the particles, reducing inter-particle friction and allowing them to move more freely. However, at high shear rates, the lubricating film between the particles is squeezed out, leading to increased friction and aggregation. This aggregation results in the formation of particle clusters or chains, which contribute to shear thickening [3].

Hoffman [4] investigated concentrated monodisperse suspensions. Monodisperse suspensions exhibit in-situ light diffraction patterns that undergo changes upon the

onset of a shear-thickening region. He proposed that under low shear rates, the interplay of attractive and repulsive forces between particles with the shear field forces leads to the formation of two-dimensional hexagonally packed layers. These layers are primarily oriented parallel to the constant shear surfaces, with one axis aligned in the direction of flow. As the applied stress increases, the excess stress is transmitted from one particle to its neighboring particles. Eventually, a critical stress level is reached, triggering flow instability. The shear stress acting on the layers becomes sufficient to overcome the interparticle forces that hold them together. Consequently, the ordered layers of particles break down and interlock, resulting in a sudden increase in the viscosity of the fluid. The stability of the system is determined by a delicate balance between the repulsive forces that stabilize the particles and the hydrodynamic forces in concentrated colloidal dispersions. The transition from ordered layers to disrupted particles is referred to as the "order–disorder transition" (ODT) [4, 5].

Hydrocluster formation is another suggested mechanism. Under low shear rates, hydroclusters – regions of locally ordered particle arrangements surrounded by liquid – are relatively small and easily broken apart, allowing the fluid to flow smoothly. However, at high shear rates, the hydroclusters grow and become more interconnected, causing an increase in viscosity and shear thickening. This theory focuses on the interplay between inter-particle interactions and hydrodynamic forces between the solid particles (dispersing phase) and the continuous phase of the STFs. The equilibrium structure of the STF is primarily influenced by stochastic forces such as electrostatic and Brownian interactions between particles. However, at low shear rates that gradually increase, both inter-particle and hydrodynamic forces become significant. Remarkably, despite the presence of hydrodynamic forces, the inter-particle interactions facilitate easy particle passage under these conditions. As the applied stress intensifies, the hydrodynamic lubrication forces surpass all other forces in magnitude. At the point where hydrodynamic and inter-particle forces are comparable, the particles within the STF form "hydroclusters," which are stress-bearing clusters resulting from particle jamming. The difficulty of particles flowing past one another in this state leads to a pronounced elevation in viscosity and a higher rate of energy dissipation [6–8]. Figure 7.2 provides a visual depiction of the formation of hydroclusters under escalating shear stress or shear rates.

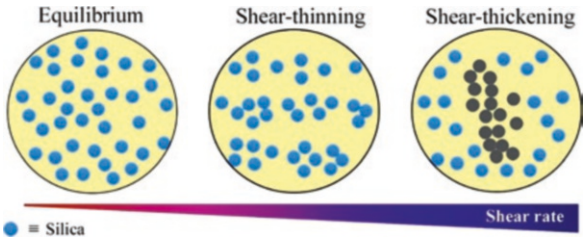

Fig. 7.2 Schematic representation of shear thinning and shear thickening

7.3 Fabrication of STF-Treated Textiles

Several studies have been carried out on the treatment of high-performance fabrics such as ultrahigh-molecular weight polyethylene (UHMWPE), Kevlar, and high-modulus polypropylene (HMPP) with different STF systems. In recent years, various techniques have been introduced by researchers to prepare the STF/textile composites with enhanced impact and blast properties. The most common approach is based on the impregnation process, in which the STF with suitable rheological properties impregnate the textiles. Generally, STF-treated textiles were prepared through the following procedure (Fig. 7.3): (i) dilution of STF with appropriate alcohols, such as methanol and ethanol, for more efficient impregnation of fabric with STF by reducing the surface tension and viscosity of STF; (ii) cleaning the surface of fabric to impregnate evenly with STF; (iii) immersion of fabric in the diluted STF solution; (iv) complete evaporation of alcohol from textile in a convection oven and drying the STF-treated textile. For instance, Hasanzadeh et al. [9] diluted the multiphase STF (silica-multiwalled carbon nanotubes (MWCNT)/polyethylene glycol (PEG)) with ethanol (1:3) to facilitate the impregnating process. Then, the HMPP fabric was immersed in the STF/ethanol solution followed by padding with a specific pressure and wet pickups. Finally, the STF-treated HMPP fabrics were dried at 80 °C for 20 min for complete ethanol evaporation. This procedure has been widely used by researchers with slight modifications to fabricate the STF-treated textile for impact resistance and blast wave mitigation applications. For instance, the diluted STF was rubbed into the Twaron fabric and hung freely to remove excess diluted STF [10]. However, it is found that the padding is more suitable for impregnation of textiles with STF, as it can provide a more uniform distribution of STF within the fabrics by applying padding pressure [11].

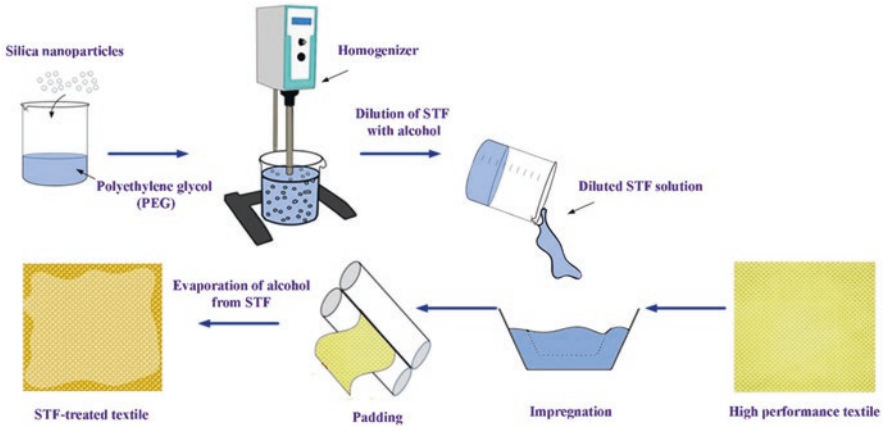

Fig. 7.3 Schematic representation of fabrication of STF-treated textiles

7.4 Blast Properties of STF-Treated Textiles

7.4.1 Significant Parameters Affecting the Energy Absorption of STF-Treated Textiles

Most of the studies report the fabrication and utilization of STF-treated textiles in impact resistance applications. However, a few studies focused on the blast properties of STF-treated textiles. Several significant parameters have been introduced by researchers to achieve the STF-treated textiles with enhanced impact and blast properties. Figure 7.4 summarizes the different parameters affecting the impact and blast properties of STF-treated textiles. The impact and blast properties of STF-treated textiles can be divided into three categories, namely (i) rheological behavior of STF, (ii) fabric structure, and (iii) impregnation process.

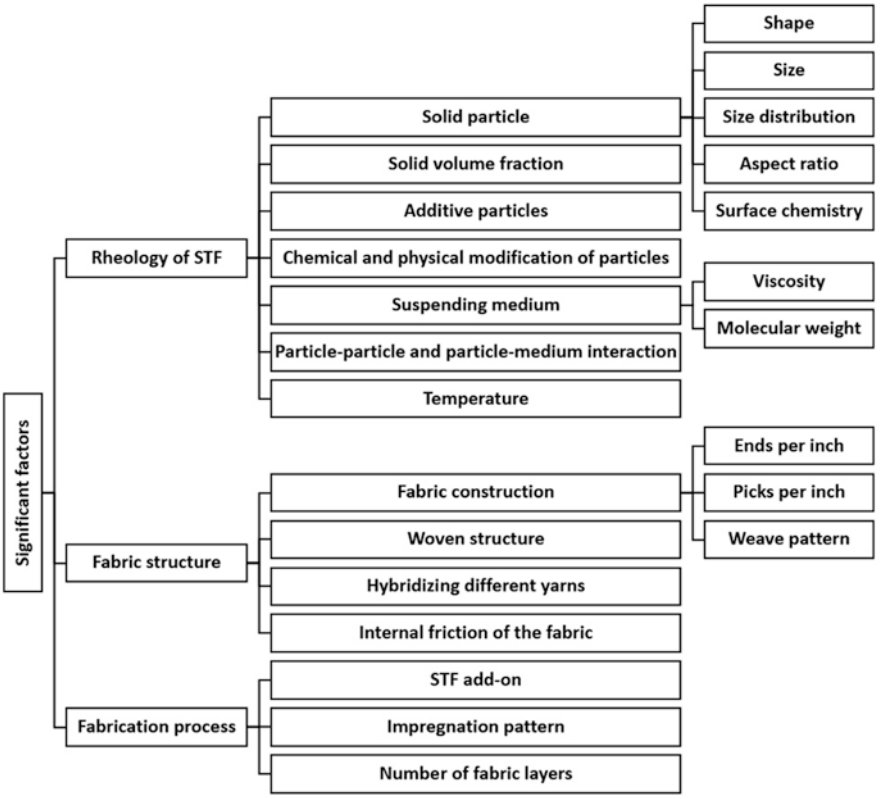

Fig. 7.4 The most influencing factors on the energy absorption of STF-treated textiles

7.4.1.1 Rheological Behavior of STF

It is reported that the rheological properties of STFs can be tuned by appropriate selection of particle type, its size and size distribution, volume fraction and aspect ratio of particles, two or more solid particles, surface chemistry, suspending medium characteristics, etc. For instance, it is shown that the rheological behavior of STF changes dramatically with shear rate, when the particle volume fraction is above 50% [12]. Barnes [12] found that the shear rate at which shear thickening begins (critical shear rate) has an inverse relationship with volume fraction of the particles. Similarly, the effect of silica concentration on the shear-thickening behavior STF was investigated by Kang et al. [13]. They found that the critical shear rates of STFs decreases with increasing silica particle concentrations. Tan et al. [14] conducted a study on the ballistic behavior of Twaron fabrics treated with a water suspension of silica colloidal particles at varying concentrations. Their results showed that systems with a particle concentration of 40% w/w demonstrated the highest ballistic limits for single, double, and quadruple ply systems, with the double ply system exhibiting the greatest improvement. In another study, it is found that increasing the aspect ratio of particles leads to decreases in required particle volume fraction to reach the critical shear rate [15]. Investigating the effect of particle size by Maranzano et al. [16] also showed significant effect on the shear-thickening behavior in dense colloidal suspensions. They showed that the rheology curves systematically shift to lower shear stresses as particle size increases. Similar behavior was also observed by Lee et al. [17]. Kang et al. [13] also studied the effect of temperature on the rheological properties of STFs. They found that the hydrodynamic interactions inducing the shear-thickening phenomenon get larger at higher temperatures. This phenomenon is likely attributed to the increased thermal Brownian motion of solid particles in carrier liquid, which leads the critical shear rate to appear at higher shear rates. Moreover, incorporation of particular additives can also enhance the rheological properties of STFs. In this regard, several microadditives and nanoadditives, including carbon-based structure, metal oxides, and inorganic materials, have been utilized for tuning the rheological behavior of STFs. For instance, Hasanzadeh et al. [18] studied the possibility of using multiwalled carbon nanotubes (MWCNTs) fillers to adjust the rheological behavior of fumed silica/PEG-based STFs. Rheological analysis confirmed the significant role of MWCNTs on the tuning rheological behavior of silica-based STF. Even at low amounts of MWCNT fillers (0.4 wt.%), the critical viscosity in the STF decreased with the fillers. Moreover, shear-thickening properties appeared at higher shear rates in the multiphase STF suspension. They suggested that the increased interactions between the fumed silica nanoparticles, PEG as a carrier fluid, and MWCNT fillers are responsible for changing the shear-thickening behavior. It is shown that the incorporation of additives to STF and fabrication of multiphase STFs with unique rheological and microstructural properties provide new possibilities into the design and development of efficient STF-based systems for different kinds of applications [19]. In the most recent investigation, Sheikhi et al. [20] studied the effect of conductive fillers, including MWCNT, carbon nanofiber (CNF), and mixtures of MWCNT/CNF on the

rheological and conductive behavior of high-performance STFs. The multiphase STF systems containing different types of fillers and filler concentrations (0.44, 0.88, 1.32, 1.76, and 2.2 wt.%) were prepared. A systematic investigation has been performed using response surface methodology to figure out the individual and combined effects of filler content, temperature, and type of fillers on the electrical resistance and rheological behavior of multiphase-STFs. The obtained results revealed the significant role of conductive fillers not only on the rheological properties but also on the electrical conductivity of multiphase STFs. The multiphase STFs exhibits higher initial viscosity and electrical conductivity than the pure STFs. Moreover, they found that the multiphase STFs containing CNF exhibit higher electrical conductivity and lower percolation threshold than MWCNT and their mixture.

The effect of suspending medium, as another factor for tuning the rheology of STFs, has been carefully reviewed by Gürgen et al. [3] and Mawkhlieng et al. [21]. It is reported that the suspending medium not only carries the solid particles but also has an interactive effect on the rheological properties of the STF. It is shown that [1] that suspending medium with low viscosity and low molecular weight is preferred to form the STF. This is attributed to the fact that the trigger time for the STF to shear thicken is longer in the lower molecular weight medium. On the other hand, the impregnation of STF to textile and distribution of the solid particles are expected to be enhanced in the low viscous suspending medium. Hence, a balance should be carried out between suspending medium with low viscosity for ease of fabrication and suspending medium with high viscosity for stronger shear-thickening behavior.

Although several kinds of studies have been carried out to figure out the rheological behavior of STFs, there are some challenging issues that make some features of the STFs unprecedented. For instance, different microparticles and nanoparticles exhibit different shear-thickening behavior due to differences in shape, size, size distribution, surface chemistry, and interactions with other particles and suspending medium. Hence, the prediction of the rheological behavior of STFs is a challenging issue. Furthermore, finding a controlling factor to obtain STF with a specific critical shear rate and peak viscosity is rather questionable. Developing a simple and systematic method for presenting the combined effects of significant factors is also challenging. Hence, more experimental and theoretical investigation should be carried out for better understanding of the rheological behavior of STFs.

7.4.1.2 Fabric Structure

The structure of fabric is another major parameter affecting the impact and blast properties of STF-treated textiles. Changing the parameters of the fabric construction such as ends per inch, picks per inch, and weave pattern can improve the blast properties by altering the areal density and porosity of fabric. On the other hand, utilization of unidirectional (UD), double, and three-dimensional (3D) fabrics, as well as hybridizing different yarns can also enhance the blast properties and energy absorption of STF-treated textiles. Chemical and/or physical modification of fabric surface, such as the growth of nanoparticles and plasma treatment, which lead to the

increasing surface roughness and consequently internal friction of the fabric, is another approach for improving the impact and blast properties of STF-treated textiles [22].

The investigation of the effect of fabric structure on energy absorption by Arora et al. [23] revealed the interactive effect of STF with UHMWPE fabric structure. They found that the positive effect of STF is more pronounced when the fabric structure is neither too tight nor too loose. Losing the effectiveness of STF on fabric with jam structure was reported by Laha et al. [24]. Similarly, energy-absorbing capabilities in STF-treated fabrics were investigated for low-sett and high sett Kevlar fabrics [25, 26]. The results showed the effective role of STF on low-sett Kevlar fabric. The fabric weave is another important parameter on energy absorption of STF-treated textile, as it alters the openness or looseness of the fabric structure. According to the literature, the plain weave, due to an optimized balance between the isotropic nature and firmness of the structure, exhibits superior performance than the other weaves. However, it should be noted that the fabric structure should be designed based on the type of impact, yarn count, and number of layers in the final product. Although a tight plain woven structure is expected to be more suitable for low-velocity impact conditions to resist the impacting object from windowing through the structure, in the case of multilayer panel against higher velocity impact, a balance should be assessed between tight weaves and low yarn crimp. While the tight plain weaves ensure structural integrity, the low yarn crimp ensures quick wave propagations from the impact area. For instance, Shimek et al. [27] found the superior impact resistance behavior of a four-weave harness satin than the plain weave.

Investigating the effect of UD, 2D, and 3D fabric structures on energy absorption revealed the superiority of UD than the others. However, due to the high stiffness and low flexibility of such fabrics, they suggested UD to be used in the high-velocity impact application especially at the front and back of an assembled panel. Indeed the absence of interlacement in UD fabrics not only provides maximum accommodation of fibers or filaments in a given area but also eliminates the interstices that can work as weak spots [22]. In the most relevant investigation, Mishra et al. [28] studied the high-velocity impact resistance of STF-treated UD UHMWPE fabric. Impact tests were conducted on various thicknesses of STF-treated fabric panels, and their ballistic limit (V50) and energy absorption were compared to panels made of untreated fabric. The results indicated that STF treatment improved the ballistic limit by up to 5% and energy absorption by up to 13%. The enhanced energy absorption was attributed to increased friction between fabric layers and shear-thickening effect. The study also examined the failure mechanisms and backface signature of the treated panels, highlighting localized damage, tensile fracture, and fibrillation phenomena. An energy enhancement ratio (EER) was introduced to assess impact resistance, revealing that the weight penalty restricted further energy absorption improvement beyond 20 layers. The study concluded that STF impregnation can enhance the ballistic resistance of UHMWP fabric without compromising flexibility or significantly increasing weight.

The presence of interlacements in woven structures enables the STF to act as a friction enhancer in textile composites. The deposition of STF on the interstices and surface of the fabric leads to achieving a certain level of firmness, generating increased friction upon pulling out the yarns in the textiles. The two-dimensional (2D)-woven fabric also exhibits superior energy absorption properties at least against low-velocity impact. Although the angle interlocks of 3D-woven fabric enhance energy absorption, their loose structure cannot withstand yarn pullout during impact [22]. Although several studies have analyzed the effect of fabric structure on impact energy absorption, to the best of our knowledge, there is no report on the effect of fabric structure on blast properties of STF-treated textiles. Hence, further research in this direction is required.

Increasing the fabric friction is another approach to enhance the energy absorption of STF-treated textiles as confirmed by yarn pullout test results. Although the STF treatment increases the fabric friction by itself, other techniques such as the growth of nanoparticles and plasma treatment were also reported to enhance the fabric friction. However, more research should be conducted in this area to explore the significant parameters and their effect on the energy absorption of STF-treated textiles [22].

7.4.1.3 Fabrication Process

The impregnation process parameters such as STF add-on (peak up), level of penetration, pattern of STF impregnation, and number of fabric layers can also significantly improve the blast properties of STF-treated textiles. The impregnation of STF to textiles is naturally a challenge. Due to the high viscosity of STFs, it is difficult to simply soak the fabrics uniformly in the STF solution and remove excess STF. The uniform treatment of STF on textile in all direction is necessary to achieve desirable energy absorption properties. In the most relevant research in this area, Majumdar et al. [29] employed a Box–Behnken design of experiment to find out the optimum fabrication process condition, including padding pressure, silica loading, and diluent to STF ratio, to achieve high-energy absorbing properties in STF-treated Kevlar fabric. Bajya et al. [30] also conducted the same study on the STF-treated UHMWPE fabric. Surprisingly, the results revealed that the higher STF add-on is not beneficial to higher energy absorption. In other words, the excessive values of STF on fabrics and extra weight addition are not useful and hinder the practical applicability of STF-treated textiles. Park et al. [31] also investigated the energy absorption capabilities of a silica/PEG-based STF-treated Kevlar fabric under high-velocity impact conditions. They achieved projectile velocities above 1 km/s using a two-stage light gas gun in the experiments. Their findings indicate that STF impregnation significantly enhances energy absorption performance at lower areal density and material cost. A thinner configuration of STF exhibits almost identical energy absorption properties as a thicker configuration of neat fabric. The researchers concluded that further exploration of the effect of STF application on the energy absorption behavior of Kevlar fabric could lead to an effective design of a ballistic

resistance configuration for high-velocity impact applications, reducing volume and mass while maintaining or improving the structure's impact resistance.

7.4.2 STF-Treated Textiles Against Blast Wave

Blast waves, also known as shock waves, are high-pressure waves that propagate rapidly through a medium, typically air, when an explosive or sudden release of energy occurs. These waves can cause significant damage to structures and pose a threat to human safety. However, recent advancements in materials science have led to the development of innovative solutions, such as STF-treated textiles, which can enhance the protective properties of materials against blast waves. There are several studies discussing STF-treated textiles that benefit from the shear-thickening behavior rheology and enhanced impact resistance properties. However, to the best of our knowledge, there is rarely a study on the protective performance of STF-treated textiles against blast wave. In the most related investigation in this area, the effect of STF application on the blast wave properties of multiple layers of Twaron fabric was studied by Haris et al. [10]. They prepared STF by mixing fumed silica nanoparticles in liquid PEG polymer. Rheological analysis revealed that the STF exhibited shear-thinning behavior at low shear rates while showing shear-thickening phenomenon at high shear rates. The blast wave properties of untreated and STF-treated fabrics were evaluated in terms of two blast wave parameters, including peak pressure and rate of pressure rise. The obtained results revealed that STF-treated fabrics have superior properties not only for impact protection but also for blast wave mitigation. They designed a gas-driven blast tube to generate blast wave loading on the STF-treated textile. They found a correlation between apparent density of STF-treated textile and average peak pressure and maximum pressure rise rate, indicating that increased density prevented the formation of shock waves in the fabric. The STF-treated fabrics exhibit lower peak pressure and lower maximum rate of pressure rise than the untreated fabric and PEG-treated fabric. Consequently, the STF-treated textiles displayed the best blast wave protection properties. Their study suggested that STF-treated fabrics have potential applications in both ballistic protection and shock wave mitigation.

In another study, Haris et al. [32] conducted an experimental study to investigate the effectiveness of suspension pads made from polyurea and STF in mitigating shock waves. The study aimed to compare the performance of these pads with conventional foam pads. The results demonstrated that replacing foam pads with STF and STF-integrated foam pads significantly reduced peak pressure, although it increased impulse. Intriguingly, even a 4-mm thick polyurea pad exhibited substantial shock wave mitigation capabilities. Among the tested pads, the polyurea pad exhibited the best performance, indicating its potential for use in personal protective equipment (PPE) requiring shock wave mitigation, such as fabric-based ballistic vests, combat helmets, and bomb suits. Their study emphasized the importance of

further research to enhance the shock wave protection of existing PPE, emphasizing the need for experimental validation in conjunction with computational studies.

Elden [33] also conducted a study focusing on the preparation, characterization, and numerical modeling of STFs for blast wave mitigation applications. The study involved dispersing fumed silica (FS) particles in polyethylene glycol (PEG) through mechanical mixing to create STF. The average particle size of the dispersion was determined using dynamic light scattering (DLS). Comprehensive rheological tests were conducted, and the viscosity behavior within the thickening range was described using the non-Newtonian power law model. The blast wave threat was evaluated using the AUTODYN software and scaled for a better understanding of equivalent threats. Numerical simulations using FLUENT were performed to assess the blast-loading attenuation capabilities of STF samples. The results indicated that higher loaded samples (10% and 15%) exhibited superior mitigation abilities and could potentially be integrated into composite systems to further enhance their performance.

Another study was conducted by Younghun et al. [34] to explore the blast effects of an STF-based stemming material. The objective of their investigation was to assess the impact of stemming on blast holes, utilizing both the Trauzl lead block test and the high-speed 3D digital image correlation (3D-DIC) system. The experiments were carried out using emulsion explosives, and the stemming materials employed consisted of sand, aggregate, and STF-based materials. The outcomes revealed that the expansion rate of the lead block was predominantly influenced by the presence of STF-based materials, followed by aggregates and sand stemming. The STF-based stemming material exhibited greater displacement and surface strain on the block. Consequently, the study inferred that the use of STF-based stemming material could enhance the efficiency of rock fragmentation, diminish blasting vibrations, and improve sealing capacity, thus rendering it suitable for diverse blasting constructions. The results of numerical analyses substantiated the experimental findings, further affirming the superior performance of STF-based stemming materials.

7.5 Summary

In this chapter, the significant role of STF-treated textiles for blast wave mitigation has been reviewed. The rheology of STF and the mechanism of shear-thickening behavior have been introduced. The fabrication of STF-treated textiles approaches exploring various methods and techniques employed to achieve effective impregnation has been described. The role of significant parameters such as rheological behavior of STF, fabric structure, and impregnation process on blast properties of STF-treated textiles has been critically discussed. Tuning the rheological properties of STFs with particle type, its size and size distribution, volume fraction and aspect ratio of particles, surface chemistry, suspending medium characteristics, and etc. can favor an effective STF for blast wave resistance. The fabric structures with

parameters including ends per inch, picks per inch, and weave pattern can affect the blast properties by altering the areal density and porosity of fabric. Furthermore, the impregnation process parameters such as STF add-on (peak up), level of penetration, pattern of STF impregnation, and number of fabric layers are important aspects to consider for achieving STF-treated textiles with enhanced blast properties. Finally, the protective performance of STF-treated textiles against blast wave has been discussed.

References

1. Lee YS, Wetzel ED, Wagner NJ (2003) The ballistic impact characteristics of Kevlar® woven fabrics impregnated with a colloidal shear thickening fluid. J Mater Sci 38:2825–2833
2. Olsson P, Teitel S (2007) Critical scaling of shear viscosity at the jamming transition. Phys Rev Lett 99(17):178001
3. Gürgen S, Kuşhan MC, Li W (2017) Shear thickening fluids in protective applications: a review. Prog Polym Sci 75:48–72
4. Hoffman R (1972) Discontinuous and dilatant viscosity behavior in concentrated suspensions. I. Observation of a flow instability. Trans Soc Rheol 16(1):155–173
5. Hoffman RL (1998) Explanations for the cause of shear thickening in concentrated colloidal suspensions. J Rheol 42(1):111–123
6. Bossis G, Brady J (1989) The rheology of Brownian suspensions. J Chem Phys 91(3):1866–1874
7. Bender J, Wagner NJ (1996) Reversible shear thickening in monodisperse and bidisperse colloidal dispersions. J Rheol 40(5):899–916
8. Wagner NJ, Brady JF (2009) Shear thickening in colloidal dispersions. Phys Today 62(10):27–32
9. Hasanzadeh M et al (2016) The influence of carbon nanotubes on quasi-static puncture resistance and yarn pull-out behavior of shear-thickening fluids (STFs) impregnated woven fabrics. Compos A: Appl Sci Manuf 88:263–271
10. Haris A et al (2015) Shear thickening fluid impregnated ballistic fabric composites for shock wave mitigation. Int J Impact Eng 80:143–151
11. Majumdar A, Butola BS, Srivastava A (2013) Optimal designing of soft body armour materials using shear thickening fluid. Mater Des 46:191–198
12. Barnes H (1989) Shear-thickening ("Dilatancy") in suspensions of nonaggregating solid particles dispersed in Newtonian liquids. J Rheol 33(2):329–366
13. Kang TJ, Kim CY, Hong KH (2012) Rheological behavior of concentrated silica suspension and its application to soft armor. J Appl Polym Sci 124(2):1534–1541
14. Tan V, Tay T, Teo W (2005) Strengthening fabric armour with silica colloidal suspensions. Int J Solids Struct 42(5–6):1561–1576
15. Wetzel ED et al (2004) The effect of rheological parameters on the ballistic properties of shear thickening fluid (STF)-kevlar composites. In: AIP conference proceedings. American Institute of Physics
16. Maranzano BJ, Wagner NJ (2001) The effects of particle size on reversible shear thickening of concentrated colloidal dispersions. J Chem Phys 114(23):10514–10527
17. Lee B-W, Kim I-J, Kim C-G (2009) The influence of the particle size of silica on the ballistic performance of fabrics impregnated with silica colloidal suspension. J Compos Mater 43(23):2679–2698
18. Hasanzadeh M, Mottaghitalab V (2016) Tuning of the rheological properties of concentrated silica suspensions using carbon nanotubes. Rheol Acta 55:759–766

19. Sheikhi MR, Hasanzadeh M (2023) Multi-phase shear thickening fluid. In: Shear thickening fluid: theory and applications. Springer, pp 33–51
20. Sheikhi MR, Hasanzadeh M, Gürgen S (2023) The role of conductive fillers on the rheological behavior and electrical conductivity of multi-functional shear thickening fluids (M-STFs). Adv Powder Technol 34(8):104086
21. Mawkhlieng U, Majumdar A (2019) Soft body armour. Text Prog 51(2):139–224
22. Mawkhlieng U, Bajya M, Majumdar A (2023) Shear thickening fluid–based protective structures against low velocity impacts. In: Shear thickening fluid: theory and applications. Springer, pp 115–138
23. Arora S, Majumdar A, Butola BS (2019) Structure induced effectiveness of shear thickening fluid for modulating impact resistance of UHMWPE fabrics. Compos Struct 210:41–48
24. Laha A, Majumdar A (2016) Interactive effects of p-aramid fabric structure and shear thickening fluid on impact resistance performance of soft armor materials. Mater Des 89:286–293
25. Mawkhlieng U, Majumdar A (2019) Deconstructing the role of shear thickening fluid in enhancing the impact resistance of high-performance fabrics. Compos Part B 175:107167
26. Bajya M et al (2020) Design strategy for optimising weight and ballistic performance of soft body armour reinforced with shear thickening fluid. Compos Part B 183:107721
27. Shimek M, Fahrenthold E (2012). Effects of weave type on ballistic performance for aramid, UHMWPE, and hybrid fabrics. In: 53rd AIAA/ASME/ASCE/AHS/ASC structures, structural dynamics and materials conference 20th AIAA/ASME/AHS adaptive structures conference 14th AIAA
28. Mishra VD et al (2022) Ballistic impact performance of UHMWP fabric impregnated with shear thickening fluid nanocomposite. Compos Struct 281:114991
29. Majumdar A et al (2016) Improving the impact resistance of p-aramid fabrics by sequential impregnation with shear thickening fluid. Fibers Polym 17:199–204
30. Bajya M et al (2022) Efficacy of various structural forms of disentangled polyethylene laminates against low velocity impact. J Thermoplast Compos Mater:08927057221115713
31. Park Y et al (2014) Empirical study of the high velocity impact energy absorption characteristics of shear thickening fluid (STF) impregnated Kevlar fabric. Int J Impact Eng 72:67–74
32. Haris A, Lee HP, Tan VBC (2018) An experimental study on shock wave mitigation capability of polyurea and shear thickening fluid based suspension pads. Def Technol 14(1):12–18
33. Gamal Elden AE, Wafy TZ, Tantawy HR (2021) Shear thickening fluids for blast wave mitigation applications: preparation, characterization and Nu-merical modeling. In: The international undergraduate research conference. The Military Technical College
34. Ko Y, Kwak K (2022) Blast effects of a shear thickening fluid-based stemming material. Mining 2(2):330–349

Index

B
Blast, 1, 3, 89–101

C
Carbon nanotubes (CNTs), 5–8, 11–13, 18, 19, 21, 23, 30–32, 34, 36, 44, 45, 53, 58, 78, 93, 95
CNT filler, 7, 12, 13, 18, 21, 23, 33, 34, 36–37, 44

D
Deceleration, 1, 17–23, 30

H
High-performance textile, 1, 3–13, 18
High strain rate, 29, 52
High-velocity impact, 1, 29, 48, 51, 55–57, 69–84, 97–99

I
Impact properties, 39–59

L
Low-velocity impact, 5, 13, 17–23, 28, 53, 74, 97, 98

N
Non-Newtonian fluid, 4, 69, 89
Non-Newtonian material, 84
Non-Newtonian rheology, 100

P
Protection, 3, 5, 13, 17, 18, 27, 31, 47, 51, 53, 56, 58, 59, 69, 70, 73, 75, 76, 79, 81, 89–101
Protective applications, 1, 2, 5, 17, 18, 23
Protective structures, 1, 2, 11, 29, 39

S
Shear thickening fluid (STF), 1–13, 17–23, 27–37, 39, 41, 43–46, 50–59, 69–84, 89–101
Shock absorbing, 1, 18, 23, 27–37, 78
Smart foam, 18–23
Stab resistance, 4, 7, 49, 53–55

T
Textile composites, 93, 98
3D Printing, 27, 28, 31

V
Viscosity, 1, 3–7, 10–13, 17, 21–23, 27, 29, 30, 33–35, 39, 41–44, 46, 48, 50, 52, 69–72, 74, 81, 83, 84, 89–93, 95, 96, 98, 100

S. Gürgen (ed.), *Shear Thickening Fluids in Protective Applications*,
https://doi.org/10.1007/978-3-031-42951-4